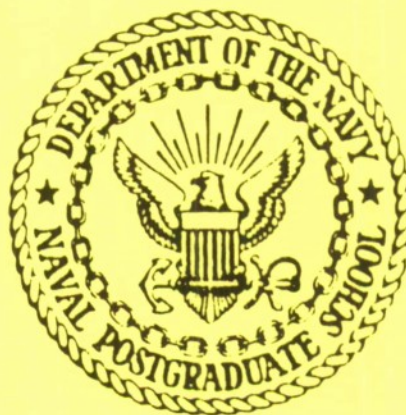


NPS67-84-022

NAVAL POSTGRADUATE SCHOOL

Monterey, California



TECHNICAL REPORT

COMPUTATIONAL MODELS FOR TURBOMACHINERY FLOWS

CHARLES HIRSCH
//

DECEMBER 1984

FINAL REPORT: OCTOBER 1983 - JULY 1984

Approved for public release; distribution unlimited.

Prepared for:
Naval Postgraduate School
Monterey, CA 93943

TJ
267
H57
1984
c.2

20091105014

TJ
267
H57
1984
C.2

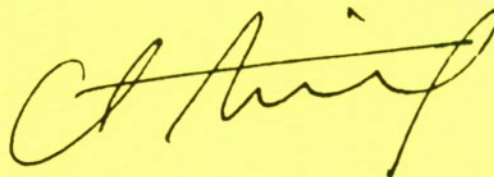
NAVAL POSTGRADUATE SCHOOL
Monterey, California

Rear Admiral R. H. Shumaker
Superintendent

D. A. Schraday
Provost

The present report resulted from the author's appointment as the Naval Air Systems Command Research Professor in Aeronautics at the Naval Postgraduate School during FY84. Professor Hirsch's participation in several research programs at the Turbopropulsion Laboratory was supported by the Air-Breathing Propulsion Research Program of Naval Air Systems Command, under the cognizance of G. Derderian (Propulsion Manager) and Dr. G. Heiche (Chief Scientist).

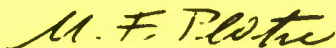
This report was prepared by:



Charles Hirsch, Adjunct Professor
Department of Aeronautics
Professor & Head
Dept. of Fluid Mechanics
Vrije Universiteit
Brussels, Belgium

Reviewed by:

Released by:



MAX F. PLATZER, Chairman
Department of Aeronautics

JOHN N. DYER
Dean of Science and Engineering

UNCLASSIFIED

SECURITY CLASSIFICATION OF THIS PAGE

REPORT DOCUMENTATION PAGE

1a REPORT SECURITY CLASSIFICATION UNCLASSIFIED			1b RESTRICTIVE MARKINGS		
2a SECURITY CLASSIFICATION AUTHORITY			3 DISTRIBUTION / AVAILABILITY OF REPORT APPROVED FOR PUBLIC RELEASE; DISTRIBUTION UNLIMITED		
2b DECLASSIFICATION / DOWNGRADING SCHEDULE					
4 PERFORMING ORGANIZATION REPORT NUMBER(S) NPS67-84-022			5. MONITORING ORGANIZATION REPORT NUMBER(S) NPS67-84-022		
6a. NAME OF PERFORMING ORGANIZATION NAVAL POSTGRADUATE SCHOOL		6b OFFICE SYMBOL (If applicable)		7a. NAME OF MONITORING ORGANIZATION NAVAL POSTGRADUATE SCHOOL	
6c. ADDRESS (City, State, and ZIP Code) MONTEREY, CA 93943-5100				7b. ADDRESS (City, State, and ZIP Code) MONTEREY, CA 93943-5100	
8a. NAME OF FUNDING / SPONSORING ORGANIZATION NAVAL AIR SYSTEMS COMMAND		8b OFFICE SYMBOL (If applicable) AIR931E		9. PROCUREMENT INSTRUMENT IDENTIFICATION NUMBER 61153N; N00019-84-WR-41099	
8c. ADDRESS (City, State, and ZIP Code) WASHINGTON, DC 20361				10 SOURCE OF FUNDING NUMBERS	
				PROGRAM ELEMENT NO. WR024	PROJECT NO 03
11 TITLE (Include Security Classification) COMPUTATIONAL MODELS FOR TURBOMACHINERY FLOWS (UNCLASSIFIED)					
12 PERSONAL AUTHOR(S) CHARLES HIRSCH					
13a. TYPE OF REPORT FINAL		13b TIME COVERED FROM 10/83 TO 7/84		14. DATE OF REPORT (Year, Month, Day) 12/84	
15. PAGE COUNT					
16 SUPPLEMENTARY NOTATION					
17 COSATI CODES			18 SUBJECT TERMS (Continue on reverse if necessary and identify by block number) TURBOMACHINERY FLOW ANALYSIS COMPUTATIONAL MODELS STREAMLINE CURVATURE METHOD		
FIELD	GROUP	SUB-GROUP			
19 ABSTRACT (Continue on reverse if necessary and identify by block number) The analytical modeling of flow through turbomachines is developed from fundamental principles. In Part 1, the levels of approximation involved in Wu's stream-surface method, and in the use of averaging in axi-symmetric quasi-3D models are defined and discussed in detail. In Part 2, computational methods based on both stream surface and passage-averaged quasi-3D models are developed. Streamline curvature and stream function approaches to the solution of the axisymmetric through-flow equations are described and finite difference and finite element solutions methods are detailed.					
20 DISTRIBUTION / AVAILABILITY OF ABSTRACT <input checked="" type="checkbox"/> UNCLASSIFIED/UNLIMITED <input type="checkbox"/> SAME AS RPT. <input type="checkbox"/> DTIC USERS				21. ABSTRACT SECURITY CLASSIFICATION UNCLASSIFIED	
22a NAME OF RESPONSIBLE INDIVIDUAL R. P. SHREEVE				22b TELEPHONE (Include Area Code) (408) 646-2593	
				22c OFFICE SYMBOL 67Sf	

TABLE OF CONTENTS

List of Figures

	PAGE
INTRODUCTION	1
1. PART 1: THE SPATIAL LEVEL OF APPROXIMATION.	2
1.1 THE QUASI-THREE-DIMENSIONAL REPRESENTATION (Q3D) FOR INTERNAL FLOWS: C.H. WU'S STREAMSURFACE METHOD	5
1.1.1 Streamsurface Variations.	7
1.1.2 Streamsurface Formulation of the Mass Conservation Equation	10
1.1.3 Definition of the Streamsheet Thickness	14
1.1.4 Streamsurface Formulation for the Momentum Conservation Equation	19
1.1.5 Streamsurface Formulation for the Energy Conservation Law.	22
1.1.6 Quasi-Three Dimensional Interaction Procedure	24
1.2 THE QUASI-THREE-DIMENSIONAL REPRESENTATION (Q3D) FOR INTERNAL FLOWS: THE AVERAGING PROCEDURE.	26
1.2.1 The Averaged Form of the Continuity Equation.	30
1.2.2 The Averaged Momentum Conservation Equation	32
1.2.3 The Averaged Energy Conservation Equation	34
1.2.4 Crocco's Form for the Averaged Momentum Equation.	38
SUMMARY.	39
REFERENCES	40
FIGURES.	41
2. PART 2: THE COMPUTATION OF TURBOMACHINERY FLOWS	46
2.1 THE DISTRIBUTED LOSS MODEL.	49
2.2 QUASI-THREE-DIMENSIONAL APPROXIMATION FOR TURBOMACHINERY FLOWS: THE STREAMSURFACE MODEL	55
2.2.1 Equations for Hub-to-Shroud S2 Surfaces - Through-Flow Equations.	57

	PAGE
2.2.2 Principles of Through-Flow Computations.	64
2.2.3 Alternative Forms of Through-Flow Equations.	68
2.2.4 Properties of the Through-Flow Equations	70
2.2.5 Flow Equations along Blade-to-Blade Sl Surfaces. . . .	74
2.2.6 The Streamsurface Quasi-Three-Dimensional Interaction.	80
2.3 THE PASSAGE-AVERAGED QUASI-THREE DIMENSIONAL APPROXIMATION .	83
2.3.1 Passage Averaged Continuity Equation	85
2.3.2 Passage Averaged Momentum Equation	85
2.3.3 Passage Averaged Energy Equation	90
2.3.4 Crocco's Form for the Averaged Momentum Equations. . .	92
2.3.5 Blade-to-Blade Flow Equations in the Averaged Flow Model	95
2.3.6 Quasi-Three Dimensional Interaction for the Averaged Flow Model.	95
2.4 THROUGH-FLOW COMPUTATIONAL METHODS	98
2.4.1 Axisymmetric Through-Flow Equations.	98
2.4.2 The Streamline Curvature Method.	101
2.4.3 Numerical Techniques for Streamline Curvature Methods.	112
2.4.4 Streamfunction Methods	121
2.4.5 Finite Difference Solutions of the Streamfunction Equation	129
2.4.6 Finite Element Solutions of the Streamfunction Equation	130
REFERENCES.	132
FIGURES	136
DISTRIBUTION.	149

List of Figures

	Page
Figure 1.1.1.: General configuration of a channel flow.	41
Figure 1.1.2.: Turbomachinery blade passage	41
Figure 1.1.3.: S surface generated by ξ^1 and ξ^2 lines and defined by $\xi^3 = \text{constant}$	42
Figure 1.1.4.: Elementary volume of a streamsheet of thickness B. . . .	43
Figure 1.1.5.: Divergence of streamsheet and relation to thickness variation.	44
Figure 1.2.1.: General configuration of a channel passage	45
Figure 2.1.1.: Complex Flow Phenomena in compressor rotor blade row .	136
Figure 2.1.2.: Flow visualization of horseshoe vortex in the leading edge region of a turbine cascade. Courtesy, C. Sieverding, Von Karman Institute, Belgium	136
Figure 2.1.3.: Transonic pressure field in a compressor cascade from AGARD LS 83.	137
Figure 2.1.4.: Transonic flow shock model associated to figure 2.3. From AGARD LS 83	137
Figure 2.1.5.: Stagnation pressure distribution at outlet of the stator of the second stage of an axial compressor. Courtesy R. Dring, United Technology Research Center, USA	138
Figure 2.2.1.: Angles of S2 surface with cylindrical coordinates (r, θ, z).	139
Figure 2.2.2.: Definition of flow angles and velocity components. . .	139
Figure 2.2.3.: Cross section of a blade row by an axisymmetric surface.	140
Figure 2.2.4.: Through flow interaction with blade to blade flow for choked compressor and turbine configurations	140
Figure 2.2.6.: Scheme of three dimensional flow computation with the streamsurface formulation, from Adler and Krimmerman (1978)	141
Figure 2.2.7.: Comparison of $\psi = 0.5$, mean streamline angles with mean camberline angles, from Novak and Hearsey (1977) . . .	142

List of Figures

	Page
Figure 2.2.8.: Meridional and blade to blade cross section of cross section of contoured turbine nozzle, from Novak and Hearsey (1977).142
Figure 2.2.9.: Radial static pressure variation for leaned and unleaned annular turbine nozzle, from Novak and Hearsey (1977) .	.143
Figure 2.2.10.: Meridional distribution of B_2 or spacific mass flow ratio distribution for turbine nozzle, from Novak and Hearsey (1977).143
Figure 2.3.1.: Meridional and blade to blade sections of a multistage axial flow turbomachine144
Figure 2.4.1.: Meridional cross section of multibladed turbomachine. .	.145
Figure 2.4.2.: Layout of meridional section with arbitrary calculation stations.145
Figure 2.4.3.: Typical lay-out for streamline curvature methods I indicates the station number, j the streamline number .	.146
Figure 2.4.4.: Influence of curvature estimation on meridional velocity distribution in Denton's model problem, from AGARD AR175 (1981).146
Figure 2.4.5.: Relation between density and streamfunction gradients .	.147
Figure 2.4.6.: Iterative solution procedure for the density equation (2.4.118), in function of streamfunction gradients. . .	.147
Figure 2.4.7.: Meridional section of mixed flow machine and gird layout.148

NOMENCLATURE

B	streamsheet thickness in normal direction	p^*	rotary stagnation pressure
E	total energy	r	radius
\vec{F}	force vector	r	gas constant
\vec{F}_f	distributed friction force vector	s	entropy
H	total enthalpy	t	time
I	rothalpy	\vec{u}	x-velocity vector
J	jacobian	\vec{v}	y-velocity vector
M	Mach number	\vec{w}	relative velocity vector
Q	heat sources	β	relative flow angle
Q_B	additional heat source	β'	blade angle
S	stream surface	γ	specific heat ratio
T	temperature	γ	station angle
\vec{V}	average absolute velocity vector	ϵ'	blade lean angle
W	average relative velocity vector	\vec{e}^α	contravariant base vector
a	speed of sound	\vec{e}_α	covariant base vector
b	streamsheet thickness in ξ^3 -direction	ζ	vorticity vector
b	channel width	θ	angular coordinate
d	blade thickness	ξ^α	curvilinear coordinate, $\alpha = 1, 2, 3$
\vec{e}_i	unit base vector, $i = 1, 2, 3$	ρ	density
\vec{f}_e	external force	σ	meridional flow angle
\vec{f}_B	body force	$\bar{\sigma}$	stress tensor
h	static enthalpy	τ	shear stress tensor
h_i	metric coefficients, $i = 1, 2, 3$	$\bar{\tau}$	secondary stress tensor
k	thermal conductivity	ψ	stream function
k	averaged kinetic energy	Ω	volume
m	meridional distance	ω	angular velocity
\vec{n}	normal to streamsurface	ω	pressure loss coefficient
p	pressure	$\vec{\nabla}$	streamwise gradient operator
		$\bar{\nabla}$	gradient operator

Superscripts

- \bar{A} averaged quantity A
 \tilde{A} density averaged quantity A
 A' fluctuating quantity with respect to \bar{A}
 A'' fluctuating quantity with respect to \tilde{A}
- T_o' relation stagnation quantity

Subscripts

- r cylindrical coordinate components
 θ cylindrical coordinate components
z cylindrical coordinate components
m stagnation quantities
p pressure side
s suction side

INTRODUCTION

The computation of turbomachinery flows, particularly in the multistage configuration, is based on a complex set of approximations and interaction with empirical data. It combines an approximate space description with a representation of the shear stresses, which reduces to their effect on the stagnation pressure losses, or entropy production, provided by empirical information.

In this report a rigorous derivation of these components is presented.

Part 1 contains a systematic derivation of the conservation laws for the two quasi three dimensional space approximations, namely the streamsurface approach, initially introduced by C.H.Wu, and the averaging procedure.

Part 2 describes the formulation of the Through-flow models and their coupling with the blade to blade flows, including a discussion of their numerical discretization. In particular, the derivation of the streamline curvature method is presented in details and its implementation can be compared with the streamfunction approach. In both cases the limitations of the methods, in presence of supersonic flows, are discussed and their origin are pointed out.

This work has been performed while the author was holding the NAVAIR Research Chair at the Naval Postgraduate School. The stimulating atmosphere, and discussions with Professor R. Shreeve have greatly contributed to the realisation of this work.

PART 1 : THE SPATIAL LEVEL OF APPROXIMATION

The most general representation of a fluid flow is obviously the fully three-dimensional one, since it corresponds to the dimensionality of the real world. But needless to say, this representation puts in general very strong requirements on computer storage and computational times and, although three-dimensional computations are to be applied in increasing measure in the coming years, many physical situations can still be described with reasonable accuracy by an approach with a reduced number of space variables.

Many configurations are indeed developed which, although not strictly two-dimensional in nature, can be considered as not "strongly" three-dimensional in the sense that one can expect that the variation, or the magnitude, of one velocity component is less important than the variations of the other two. A typical example of such a situation is the wing of a modern airplane with varying chord length and spanwise varying profile shape. Within a certain approximation which excludes in particular the wing-body junction and the tip regions, the flow along the wing could be approached two-dimensionally. Alternatively, a cylindrical airfoil under a sweep angle with respect to the upstream flow will present limited three-dimensional effects for relatively small values of the sweep angle.

Axisymmetric configurations are similarly suitable for descriptions with a reduced number of space variables.

It is clear that, neither for the spatial level of approximation nor for the other levels, is it possible to put forward general conditions of validity for a given set of assumptions. Depending on the initial flow conditions, the geometrical configurations and the required level of accuracy for any system of approximations, one will have to check the calculated flow behaviour against either experimental data or results from computations at a higher level of approximation.

Hence, a fully three-dimensional computation will allow to check by comparison, the limits of validity of a two-dimensional approach, in the same way as experimental data or a reliable viscous calculation will allow to ascertain the limits of validity of an inviscid approach.

For example, it is well known that for flow incidences along an airfoil lower than certain values, the boundary layers will not separate and an inviscid two-dimensional approach might be of sufficient validity to predict the lift coefficients with acceptable accuracy; while for higher incidences the occurrence of large separated regions might require a three-dimensional viscous computation in order to maintain the same level of accuracy.

In the field of internal flows, such as channels and turbomachinery passages, three-dimensional effects are induced by the presence of material walls and the geometrical configuration will lead to three-dimensional flow components, even with a two-dimensional inlet flow.

In order to treat these situations an intermediate description between the fully three-dimensional and the two-dimensional can be introduced. This intermediate level of approximation which can be called Quasi-Three-Dimensional, approximates the flow as a succession of interacting families of two-dimensional flows along intersecting surfaces. Appropriate families of surfaces are defined, which can be treated as streamsurfaces, along which a two-dimensional velocity field projection is determined. Obviously a fully three-dimensional time-dependent flow field will require three families of intersecting surfaces in order to be determined completely. This corresponds to requiring three inter-dependent scalar functions of three coordinates in order to describe the three component velocity field restricted by the continuity equation. But only two families of surfaces are required for steady flows, see Section 2-8. Such a representation is equivalent to a complete three-dimensional description and no spatial approximations are involved. The Quasi-Three-Dimensional approximation comes in when the number of surfaces is reduced; that is, when it is considered that a valid description of the flow behaviour is obtained by neglecting the flow contributions along either certain families of surfaces or along certain members of a given family of surfaces.

Actually, one could visualize these families of surfaces as generating a system of coordinate surfaces, such as the $\xi^1 = \xi$, $\xi^2 = \eta$, $\xi^3 = \zeta$ families of figure 1.1.1. The projections of the velocity vectors in these surfaces are computed on a two-dimensional basis, and the Quasi-3D approximation is contained in the assumption that either the projection of the velocity field in one set of surfaces is independent of the third coordinate, with the consequence that the flow in one of the members of the family is representative of all of them, (for instance, the flow in a (ξ, ζ) surface being independent of η), or eventually that the velocity field in one family is of negligible magnitude with respect to the others, (for instance the velocity projection in the (ζ, η) surfaces).

An alternative to the stream- or pseudo stream-surface method for obtaining a quasi-three-dimensional approximation is offered by the Averaging Method. This approach consists in averaging out the conservation equations with respect to a chosen coordinate, for instance the ξ^3 direction, obtaining equations with the remaining coordinates as independent variables.

Two-dimensional equations are obtained in this way, representative of the average flow with respect to the ξ^3 coordinate, but containing geometrical terms function of the averaged space direction. Clearly, limits of integration have to be defined and hence this procedure is best suited for internal flows with streamwise varying cross-sections.

This procedure can also be extended to an averaging over a two-dimensional region such as the cross-section of the channel, leading to a quasi-two dimensional flow description in the direction perpendicular to this section involving terms which are functions of the varying cross-section.

Although both approaches lead to equivalent representations in Quasi-3D approximations, with differences only in the way the interaction between the various families of surfaces are defined, the streamsurface approach can be used to define a description of a fully three-dimensional flow

whereas the averaging procedure can not.

The two models are presented and discussed in the following sections. It is also clear from the preceding considerations that the interest of this quasi three-dimensional approach lies mainly in the field of bounded or internal flows. Therefore we will present this approach in view of its original development in the field of turbomachinery and channel flows.

1.1. THE QUASI-THREE-DIMENSIONAL REPRESENTATION (Q3D) FOR INTERNAL FLOWS :
C.H. WU'S STREAMSURFACE METHOD Wu (1952), Wu (1976)

The streamsurface method described in this section has been introduced by C.H. Wu (1952) in order to approximate the internal flow in a turbomachinery blade passage.

We will consider an arbitrary channel bounded by an inlet and an outlet surface, for instance a duct or the passage between two blades in a turbomachine, or the part of a river between two cross sections. A typical configuration is represented schematically in figure 1.1.1. An arbitrary curvilinear coordinate system ξ^1, ξ^2, ξ^3 (or ξ, η, ζ) is shown with ξ^1 taken approximately in the mainstream direction and ξ^2, ξ^3 defining roughly transverse directions. The inlet and outlet sections may be defined by constant ξ^1 surfaces. A typical representation for a turbomachine passage is shown in figure 1.1.2.

In this figure the direction of the axis of rotation of the machine z may be identified with ξ^1 , while the cylindrical coordinates θ and r are respectively to be considered as ξ^2 and ξ^3 coordinates.

Representative streamsurfaces, such as the S_1 or S_2 surfaces in the above figures are obtained by following the paths of the fluid particles lying along selected lines in the inlet section. For instance, the fluid particles along the line A_1B_1 of figure 1.1.1 will generate a ξ^3 type of surface, or S_1 surface, and the particles along A_2B_2 will generate a ξ^2 type of surface (S_2 surface)

More generally, the considered surface S is described by a time dependent equation

$$S(\xi^1, \xi^2, \xi^3, t) = 0 \quad (1.1.1)$$

obtained by following the paths of the fluid particles emanating from an initial line. In a general time dependent flow, S will not be a strict streamsurface, in the sense of the velocity vector being normal to the surface. This will however be the case when the flow is steady.

The surface (1.1.1) can be written explicitly in terms of the reference coordinate ξ^3 as follows,

$$\xi^3 = \xi^3(\xi^1, \xi^2, t) \quad (1.1.2)$$

where the direction ξ^3 can be visualized as being roughly in the direction of the normal to S , and where ξ^1 and ξ^2 are coordinates defining the surfaces. In the following, we will restrict ourselves to time independent surfaces ; since S is then a streamsurface, one has at each point of the surface S , with \vec{n} being defined as normal to S

$$\frac{dS}{dt} = \vec{v} \cdot \vec{\nabla} S = \vec{v} \cdot \vec{n} = 0 \quad (1.1.3)$$

for \vec{n} defined by

$$\vec{n} = \vec{\nabla} S \quad (1.1.4)$$

Two possibilities are open in order to describe the family of surfaces with respect to the arbitrary curvilinear system of coordinates, figure 1.1.3.

1) The surface S does not contain the ξ^1 and ξ^2 lines and is situated arbitrarily with respect to the local coordinate system ξ^α , ($\alpha=1,2,3$).

In this case, the surface can be represented by equation (1.1.2) and the normal to the surface is proportional to the vector \vec{n} , defined by its covariant components $n_\alpha (-\partial_1 \xi^3, -\partial_2 \xi^3, 1)$. Indeed, from equation (1.1.4) with $S = \xi^3 - \xi^3(\xi^1, \xi^2)$,

$$\vec{n} = - \left(\frac{\partial \xi^3}{\partial \xi^1} \right) \cdot \vec{\epsilon}^1 - \left(\frac{\partial \xi^3}{\partial \xi^2} \right) \cdot \vec{\epsilon}^2 + 1 \cdot \vec{\epsilon}^3 \quad (1.1.5)$$

where $\vec{\epsilon}^1, \vec{\epsilon}^2, \vec{\epsilon}^3$ are the contravariant base vectors of the coordinate system. Note that the components of \vec{n} as defined by equation (1.1.5) are not projected along unit vectors, since the base vectors are not of unit length. For instance, in an orthogonal curvilinear system with metric coefficients h_1, h_2, h_3 , the length of the contravariant basis vector $\vec{\epsilon}^\alpha$ is equal to $1/h_\alpha$.

Hence, one would have, with \vec{e}^α denoting the unit base vectors

$$\vec{n} = \frac{-1}{h_1} \frac{\partial \xi^3}{\partial \xi^1} \vec{e}^1 - \frac{1}{h_2} \frac{\partial \xi^3}{\partial \xi^2} \vec{e}^2 + \frac{1}{h_3} \vec{e}^3 = \tilde{n}_\alpha \vec{e}^\alpha \quad (1.1.6)$$

defining hereby components \tilde{n}_α as the projections of the normal \vec{n} along the unit vectors \vec{e}^α .

It is to be remembered that the covariant base vectors $\vec{\epsilon}_\alpha$ are tangent to the ξ^α -coordinate lines, while the contravariant base vectors $\vec{\epsilon}^\alpha$ are normal to the surface $\xi^\alpha = \text{constant}$. These two sets of base vectors are aligned in the same directions when the coordinate system is orthogonal.

11) The surface S is defined by the coordinate lines ξ^1 and ξ^2 ; that is, S is a $\xi^3 = \text{constant}$ surface, and the surface S contains the lines $\xi^1 = \text{constant}$ and $\xi^2 = \text{constant}$. In this case, it is seen from equation (1.1.5) that $\vec{n} = \vec{\epsilon}^3$ and if the coordinate system is orthogonal, the unit vector along the normal direction is given by $\vec{i}_n = h_3 \cdot \vec{n}$.

1.1.1. Streamsurface variations

With the general representation of S by equation (1.1.2), the (covariant) components of the normal vector \vec{n} , are given by

$$\frac{\partial \xi^3}{\partial \xi^1} = \partial_1 \xi^3 = -n_1 \quad (1.1.7)$$

and

$$\frac{\partial \xi^3}{\partial \xi^2} = \partial_2 \xi^3 = -n_2 \quad (1.1.8)$$

with $n_3 = 1$.

This allows us to define the variations of any scalar flow quantity along the streamsurfaces S , as functions of ξ^1 and ξ^2 , by the following relations, where the overbars indicate variations along the surface,

$$\frac{\bar{\partial}}{\partial \xi^1} = \frac{\partial}{\partial \xi^1} + \left(\frac{\partial \xi^3}{\partial \xi^1} \right) \frac{\partial}{\partial \xi^3} \quad (1.1.9a)$$

or in condensed notation

$$\bar{\partial}_1 = \partial_1 + (\partial_1 \xi^3) \cdot \partial_3 = \partial_1 - n_1 \cdot \partial_3 \quad (1.1.9b)$$

Similarly

$$\frac{\bar{\partial}}{\partial \xi^2} = \frac{\partial}{\partial \xi^2} + \left(\frac{\partial \xi^3}{\partial \xi^2} \right) \frac{\partial}{\partial \xi^3} \quad (1.1.10a)$$

or in condensed notation

$$\bar{\partial}_2 = \partial_2 + (\partial_2 \xi^3) \cdot \partial_3 = \partial_2 - n_2 \cdot \partial_3 \quad (1.1.10b)$$

Obviously, the variations $\bar{\partial}_3$ with respect to ξ^3 along the surface are identically equal to zero, for arbitrary functions g

$$\frac{\bar{\partial}}{\partial \xi^3} g = \bar{\partial}_3 g = 0 \quad (1.1.11)$$

Equations (1.1.9) to (1.1.11) can be grouped in the form

$$\bar{\partial}_\alpha g = \partial_\alpha g - n_\alpha \cdot \partial_3 g \quad \alpha = 1, 2, 3 \quad (1.1.12)$$

or in vector notation

$$\vec{\bar{V}}g = \vec{V}g - \vec{n} \cdot \partial_3 g \quad (1.1.13)$$

for any scalar quantity g .

In the particular choice of coordinates where the surface S is the (ξ^1, ξ^2) surface, that is a surface $\xi^3 = \text{constant}$, case ii above, the variations $\bar{\partial}_1$ and $\bar{\partial}_2$ are identical to the ordinary partial derivatives ∂_1 and ∂_2 , since the components n_1 and n_2 of the normal vector are zero according to equation (1.1.5).

The gradient with overbar $\vec{\bar{V}}g$ is the projection of the three-dimensional operator $\vec{V}g$ on the surface S . This can be seen from the definition of the gradient of a scalar in curvilinear coordinates, when the coordinates ξ^1 and ξ^2 are in the surface S ; case ii. With the index γ ranging from one to two, one has

$$\vec{V}g = \vec{\epsilon}^\alpha \cdot \partial_\alpha g = \vec{\epsilon}^\gamma \cdot \partial_\gamma g + \vec{\epsilon}^3 \cdot \partial_3 g \quad \begin{matrix} \alpha = 1,2,3 \\ \gamma = 1,2 \end{matrix} \quad (1.1.14)$$

Since in this case $\vec{\epsilon}^3 = \vec{n}$, this equation is identical to equation (1.1.13) with the definition

$$\vec{\bar{V}}g = \vec{\epsilon}^\gamma \cdot \partial_\gamma g \quad \gamma = 1,2 \quad (1.1.15)$$

when the ξ^1 and ξ^2 lines are in the surface S .

Note that equation (1.1.13) remains valid for any system of coordinates.

This approach can be applied to obtain the streamsurface variations for a vector quantity \vec{F} . from the definition of the divergence of a vector in curvilinear coordinates, one has

$$\begin{aligned} \vec{\bar{V}} \cdot \vec{F} &= \vec{\epsilon}^\alpha \cdot \partial_\alpha \vec{F} = \vec{\epsilon}^\gamma \cdot \partial_\gamma \vec{F} + \vec{\epsilon}^3 \cdot \partial_3 \vec{F} \\ &= \vec{\epsilon}^\gamma \cdot \partial_\gamma \vec{F} + \vec{n} \cdot \partial_3 \vec{F} \end{aligned} \quad (1.1.16)$$

If ξ^1 and ξ^2 are orthogonal coordinates in the streamsurface S , the first term can be worked out explicitly as follows,

$$\begin{aligned}
\vec{\nabla} \cdot \vec{F} &= \vec{\epsilon}^Y \cdot \partial_Y \vec{F} \\
&= \vec{\epsilon}^Y \cdot \partial_Y (F^\alpha \vec{\epsilon}_\alpha) \\
&= \frac{1}{h_1 h_2} [\bar{\partial}_Y (F^Y h_1 h_2) + F^3 \partial_3 (h_1 h_2)] \\
&= \frac{1}{h_1 h_2} \bar{\partial}_Y (F^Y h_1 h_2) + \frac{\vec{n} \cdot \vec{F}}{h_1 h_2} \partial_3 (h_1 h_2)
\end{aligned} \tag{1.1.17}$$

The first term is the two dimensional form of the divergence operator, while the second term represents a contribution to the "streamsurface" divergence operator $\vec{\nabla} \cdot \vec{F}$, arising from the deformation of the surface in the third direction.

This contribution vanishes when the vector \vec{F} lies in the surface ($\vec{F} \cdot \vec{n} = 0$) or when the streamsurface is independent of the third coordinate ξ^3 .

In both these cases the flow can be considered as two-dimensional.

With the definition (1.1.17), equation (1.1.13) can be generalized to vector quantities as

$$\vec{\nabla} \cdot \vec{F} = \vec{\nabla} \cdot \vec{F} - \vec{n} \cdot \partial_3 \vec{F} \tag{1.1.18}$$

There are various ways to obtain the flow equations considered along the streamsurface S. One way can be termed as an "algebraic method" and was originally followed by Wu (1952) with cylindrical coordinates, and further extended to formulations in arbitrary, curvilinear coordinate systems by Wu (1976).

This approach consists in introducing directly the streamsurface derivatives $\bar{\partial}_1$ and $\bar{\partial}_2$ in all the equations of motion written in the ξ^α coordinate system in place of the ordinary derivatives ∂_1 and ∂_2 , obtaining in this way two dimensional equations where all flow variables are considered as functions of ξ^1 and ξ^2 along the selected streamsurface.

The derivatives of the flow variables with respect to ξ^3 appearing in the obtained "streamsurface" equations, are considered as known quantities. This is also the case for the geometry of the streamsurface S, which has to be given through the knowledge of the normals \vec{n} in each point. Since the flow surface will only be known once the whole flow field has been obtained, the present decomposition of the three dimensional flow field is clearly an iterative procedure.

In order to obtain the necessary information about the derivatives of the flow variables in the third direction ξ^3 , the two dimensional flows have to be solved along all the surfaces of the same family $\xi^3 = \xi^3(\xi^1, \xi^2)$. This corresponds to the different surfaces of the type $A_1 B_1 C_1 D_1$ of figure 1.1.1 or to the different surfaces S_1 on figure 1.1.2.

On the other hand, the information which is necessary in order to define the shape of these streamsurfaces can only be obtained through the determination of the flow components along the streamsurfaces of another family, such as the surfaces of the type $A_2 B_2 C_2 D_2$ on figure 1.1.1, or the S_2 family of figure 1.1.2, when the first family is taken to be S_1 surfaces.

Therefore, for time independent flows, the complete three dimensional flow field will be reconstructed through the iterative solution of the two dimensional flows on two families of intersecting streamsurfaces.

In the following we will follow an approach which differs from the "algebraic" method, in order to derive the two dimensional "streamsurface" equations. We will express directly the conservation laws on a finite volume delimited by two neighbouring streamsurfaces, forming a streamsheet of thickness b . This will lead to a formulation which is written in vector form, with gradient operators along the

surface, such as the $\vec{\nabla}$ operator of equation (1.1.17). The obtained formulation will therefore be valid in any system of coordinates and the explicit, algebraic form of the flow equations can be obtained by expressing the gradient operators in function of the selected coordinate system.

1.1.2. Streamsurface Formulation of the Mass Conservation Equation

Referring to figure 1.1.4, we consider the domain enclosed between two streamsurfaces, forming a streamsheet of thickness B . A reference streamsurface is considered as formed by the mid-points of the streamsheet and the obtained differential equations are referred to this surface. In order to define the streamsurfaces, a curvilinear coordinate system is introduced with the direction ξ^3 representing the coordinate which is to be eliminated from the flow equations. The streamsurface will be assumed to contain the ξ^1 and ξ^2 coordinates and is therefore defined as a $\xi^3 = \text{constant}$ surface. We will select ξ^1 and ξ^2 to form an orthogonal system in the streamsurface with metric coefficients h_1 and h_2 .

The unit vectors along the ξ^α axes are defined by \vec{e}_α related to the $\vec{\epsilon}_\alpha$, if the coordinate system is orthogonal, by

$$\vec{e}_\alpha = \frac{1}{h_\alpha} \vec{\epsilon}_\alpha = h_\alpha \vec{\epsilon}^\alpha = \vec{\epsilon}^\alpha \quad \begin{array}{l} \text{no summation on } \alpha \\ \alpha = 1, 2, 3 \end{array}$$

The normal vector \vec{n} is equal to \vec{e}^3 according to equation (1.1.5). The physical streamsheet thickness in the direction of the coordinate ξ^3 , is measured by \bar{B} .

The thickness \bar{B} is also written as $\bar{B} = bh_3$, where h_3 is the metric coefficient associated to ξ^3 , that is the elementary length dl_3 along this axis is $dl_3 = h_3 d\xi^3$. The quantity b is then a thickness measured in units of the variable ξ^3 . For instance, if $\xi^3 = \theta$ the angular variable in cylindrical coordinates, then b is an angular thickness and $\bar{B} = br$ where r is the local radial coordinate.

The volume $d\tau$ formed by variations $d\xi^1$, $d\xi^2$ and $d\xi^3$ along the three ξ^α -axes, is measured by the determinant of the inverse jacobian matrix of the transformation from a cartesian coordinate system to the ξ^α -system, $1/J$. That is $d\tau = \frac{1}{J} d\xi^1 d\xi^2 d\xi^3$ and when the ξ -system is orthogonal, $1/J = h_1 h_2 h_3$.

Therefore, the elementary volume $d\Omega$ formed with the length elements $dl_1 = h_1 d\xi^1$, $dl_2 = h_2 d\xi^2$ on the surface, and b in the direction ξ^3 , see figure 1.1.4, is defined by

$$d\Omega = \frac{b}{J} d\xi^1 d\xi^2 \quad (1.1.19)$$

If the metric coefficients h_1 and h_2 are introduced, we can define the streamsheet thickness B , measured in the direction normal to the surface, by

$$\frac{b}{J} = Bh_1 h_2 \quad (1.1.20)$$

When the coordinate system is orthogonal, $B = \bar{B} = bh_3$, but in general the ratio B/b is equal to the ratio of the elementary distance dn along the normal to the surface, and the variation $d\xi^3$ along the ξ^3 direction. That is

$$\frac{B}{b} = \frac{dn}{d\xi^3} \quad (1.1.21)$$

The general form of a scalar conservation law for a quantity u , is given by

$$\frac{\partial}{\partial t} \int_{\Omega} \rho u d\Omega + \oint_S \vec{F} \cdot d\vec{S} = 0 \quad (1.1.22)$$

For instance for the mass conservation law, $u=1$ and $\vec{F}=\rho\vec{v}$.

This integral formulation is applied to the infinitesimal volume $d\Omega$ of figure 1.1.4. The side faces 1 and 2, formed by the ξ^2 and ξ^3 directions have the surface elements

$$d\vec{S}^{(1)} = \frac{b}{J} d\xi^2 \cdot \vec{e}^1 \quad (1.1.23)$$

If the coordinate system is orthogonal $d\vec{S}^{(1)} = Bh_2 d\xi^2 \cdot \vec{e}^1 = Bh_1 h_2 d\xi^2 \cdot \vec{e}^1$. The balance of fluxes for faces 1 and 2 is given by

$$\begin{aligned} \int_{1+2} \vec{F} \cdot d\vec{S}^{(1)} &= (F^1 b/J d\xi^2)_{\xi^1+d\xi^1} - (F^1 b/J d\xi^2)_{\xi^1} \\ &= \overline{\frac{\partial}{\partial \xi^1}} (bF^1/J) d\xi^1 d\xi^2 \\ &= \overline{\frac{\partial}{\partial \xi^1}} (Bh_1 h_2 F^1) d\xi^1 d\xi^2 \end{aligned} \quad (1.1.24)$$

where F^1 is the projection of the flux vector on the base vector \vec{e}^1 ,

$$F^1 = \vec{F} \cdot \vec{e}^1 \quad (1.1.25)$$

and the overbar on the partial derivative indicates a derivative along the streamsurface. This implies that with another system of coordinates, whereby the ξ^1 , ξ^2 axes are not in the surface, the derivatives will have to be evaluated by relations (1.1.12). A similar contribution is obtained for the balance of fluxes through the faces 3 and 4, with

$$d\vec{S}^{(2)} = \frac{b}{J} d\xi^1 \cdot \vec{e}^2 \quad (1.1.26)$$

leading to

$$\begin{aligned}
\int_{3+4} \vec{F} \cdot d\vec{S}^{(2)} &= (F^2 b / J d\xi^1)_{\xi^2+d\xi^2} - (F^2 b / J d\xi^1)_{\xi^2} \\
&= \overline{\frac{\partial}{\partial \xi^2}} (F^2 b / J) d\xi^1 d\xi^2 \\
&= \overline{\frac{\partial}{\partial \xi^2}} (B h_1 h_2 F^2) d\xi^1 d\xi^2
\end{aligned} \tag{1.1.27}$$

with

$$F^2 = \vec{F} \cdot \vec{e}^2 \tag{1.1.28}$$

If the coordinate system is orthogonal $d\vec{S}^{(2)} = B h_1 d\xi^1 \cdot \vec{e}^2 = B h_1 h_2 d\xi^1 \cdot \vec{e}^2$.
The balance of fluxes for the remaining faces 5 and 6, with surface element

$$d\vec{S}^{(3)} = h_1 h_2 d\xi^1 d\xi^2 \cdot \vec{e}^3 = \frac{\vec{e}^3}{J} d\xi^1 d\xi^2 = \frac{B}{b} h_1 h_2 d\xi^1 d\xi^2 \cdot \vec{e}^3 \tag{1.1.29}$$

is obtained as follows,

$$\begin{aligned}
\int_{5+6} \vec{F} \cdot d\vec{S}^{(3)} &= (F^3 h_1 h_2 d\xi^1 d\xi^2)_{\xi^3+b} - (F^3 h_1 h_2 d\xi^1 d\xi^2)_{\xi^3} \\
&= b \frac{\partial}{\partial \xi^3} (h_1 h_2 F^3) d\xi^1 d\xi^2 \\
&= b \frac{\partial}{\partial \xi^3} \left(\frac{B}{b} h_1 h_2 \vec{F} \cdot \vec{n} \right)
\end{aligned} \tag{1.1.30}$$

since, from equation (1.1.29)

$$\begin{aligned}
F^3 &= \vec{F} \cdot \vec{e}^3 = \vec{F} \cdot \vec{1}_n \\
&= (\vec{F} \cdot \vec{n}) \frac{B}{b} = F^3 \frac{B}{b}
\end{aligned} \tag{1.1.31}$$

Grouping all the terms, one obtains after dividing by $d\xi^1 d\xi^2$, the conservation law for the streamsheet of thickness B

$$\frac{\partial}{\partial t} (\rho u B h_1 h_2) + \overline{\frac{\partial}{\partial \xi^1}} (B h_1 h_2 F^1) + \overline{\frac{\partial}{\partial \xi^2}} (B h_1 h_2 F^2) = -b \frac{\partial}{\partial \xi^3} (\vec{F} \cdot \vec{1}_n h_1 h_2) \tag{1.1.32}$$

In the left hand side one recognizes the expression of the two

dimensional divergence operator in the coordinates ξ^1 and ξ^2 along the surface. The conservation equation becomes, for time independent surfaces, applying the definition (1.1.17)

$$\frac{\partial}{\partial t} (\rho u B) + \vec{\nabla} (B \vec{F}) = -b \partial_3 (\vec{F} \cdot \vec{t}_n) \quad (1.1.33)$$

where the overbar on the gradient operator indicates a "streamsurface " derivative.

The right hand side term is a reminder of the fact that the present description is not strictly two dimensional, but describes a selective sheet out of a general three dimensional flow.

The condition for the considered surface to be a streamsurface is, from equation (1.1.3), $\vec{v} \cdot \vec{n} = 0$. Consequently, the right hand side of equation (1.1.33) vanishes for the mass conservation equation (since $\vec{F} = \rho \vec{v}$) which reduces to the following form

$$\frac{\partial}{\partial t} (\rho B) + \vec{\nabla} (\rho B \vec{v}) = 0 \quad (1.1.34)$$

Considering now equation (1.1.34) as a starting point, one can apply this equation to any system of coordinates, with the definitions (1.1.13) and (1.1.17) of the streamsurface derivatives.

1.1.3. Definition of the Streamsheet Thickness

The above formulation of the continuity equation along the streamsurface has to be identical locally to the full three dimensional form of the mass conservation equation. This condition provides a relation between the streamsheet thickness B and the three dimensional properties of the flow.

Indeed, applying the relations (1.1.13) and (1.1.17) to the general three dimensional form of the continuity equation,

$$\frac{\partial \rho}{\partial t} + \vec{\nabla} (\rho \vec{v}) = 0 \quad (1.1.35)$$

gives

$$\frac{\partial \rho}{\partial t} + \vec{\nabla} (\rho \vec{v}) = -\rho n \cdot \partial_3 \vec{v} \quad (1.1.36)$$

Equation (1.1.36) should be identical to the streamsheet form (1.1.34) of the mass conservation law. Identifying these two equations, leads to a relation defining the streamsheet thickness as a function of the three

dimensionality of the flow, namely

$$\frac{\partial B}{\partial t} + (\vec{v} \cdot \vec{\nabla})B = B \vec{n} \cdot \partial_3 \vec{v} \quad (1.1.37)$$

For time independent flows, the time derivative vanishes and the above relation becomes

$$\frac{1}{B} (\vec{v} \cdot \vec{\nabla})B = \vec{n} \cdot \partial_3 \vec{v} = -\vec{v} \cdot \partial_3 \vec{n} \quad (1.1.38)$$

If the three dimensional flow field is known and the streamsurface normals \vec{n} defined, equation (1.1.38) will determine the evolution of B along the selected streamsurface. Note that the operator on the left hand side is the convective derivative in the streamsurface. This equation expresses that the variation of the streamsheet thickness is defined by the variation of the velocity field in the third direction. Therefore if the flow is independent of this coordinate, the right hand side of equation (1.1.38) will vanish and B may be taken as constant : the flow is then two dimensional.

Geometrical interpretation

The condition (1.1.38) on B can also be written as a purely geometrical relation between the variations of B and the normal to the streamsurface, expressing that a divergence or contraction of the streamsheet necessarily implies that the direction of the normals to the surface change during a displacement accross the streamsheet, as illustrated on figure 1.1.5.

From figure 1.1.5, considering a displacement dl in the streamsheet, it can be seen that the divergence angle α of the streamsheet is given by

$$\tan \alpha = \frac{1}{2} \frac{dB}{dl} \quad (1.1.39)$$

and that the normal unit vectors rotate by the same angle in the displacement from P to Q. Hence

$$\vec{i}_{nQ} - \vec{i}_{nP} = \frac{B}{2} \frac{\partial \vec{i}_n}{\partial n} = -\vec{i}_1 \cdot \alpha \quad (1.1.40)$$

where $\partial/\partial n$ represents the derivative in the normal direction. With the approximation $\tan \alpha \approx \alpha$ one obtains

$$\frac{1}{B} \frac{dB}{dl} \cdot \vec{i}_1 = -\frac{\partial \vec{i}_n}{\partial n} \quad (1.1.41)$$

Since \vec{i}_1 is an arbitrary direction within the streamsurface, the left hand side operator is equal to $\vec{\nabla}B/B$, and equation (1.1.41) becomes with (1.1.21)

$$\frac{1}{B} \vec{\nabla}B = - \frac{\partial \vec{i}_n}{\partial n} = - \frac{b}{B} \frac{\partial \vec{i}_n}{\partial \xi^3} \quad (1.1.42)$$

When ξ^3 is along the normal $dn = h_3 d\xi^3$, $\vec{i}_n = h_3 \vec{n} = h_3 \vec{e}^3$ and

$$\frac{1}{B} \vec{\nabla}B = - \frac{1}{h_3} \partial_3 (h_3 \vec{n}) = - \partial_3 \vec{n} - \frac{\vec{n}}{h_3} \partial_3 h_3 \quad (1.1.43)$$

Introducing $B = \bar{B} b h_3$, in this relation, leads to the following equation for b

$$\frac{1}{b} \vec{\nabla}b = - \partial_3 \vec{n} - \frac{1}{h_3} \vec{\nabla}h_3 \quad (1.1.44)$$

Equation (1.1.44) can also be written in the following form, which is more appropriate for explicit computations,

$$\frac{(\vec{v} \cdot \vec{\nabla})b}{b} = -v^\alpha \cdot \partial_\alpha n_\alpha = n_\alpha \cdot \partial_\alpha v^\alpha \quad (1.1.45)$$

where the orthogonality property (1.1.4) has been introduced under the form

$$v^\alpha \cdot n_\alpha = 0 \quad (1.1.46)$$

Example E.1.1.1. Cartesian coordinates

In cartesian coordinates and a streamsurface defined by $z=z(x,y)$ one can eliminate the z -variations along this streamsurface in the continuity equation (1.1.34). One has

$$\frac{\partial}{\partial t}(\rho B) + \frac{\partial}{\partial x}(\rho B u) + \frac{\partial}{\partial y}(\rho B v) = 0 \quad (E.1.1.1)$$

The streamsurface derivatives are defined by

$$\overline{\frac{\partial}{\partial x}} = \frac{\partial}{\partial x} - n_x \frac{\partial}{\partial z} \quad (\text{E.1.1.2})$$

$$\overline{\frac{\partial}{\partial y}} = \frac{\partial}{\partial y} - n_y \frac{\partial}{\partial z} \quad (\text{E.1.1.3})$$

with the normal vector \vec{n} given by

$$\vec{n} = - \left(\frac{\partial z}{\partial x} \right) \vec{i}_x - \left(\frac{\partial z}{\partial y} \right) \vec{i}_y + \vec{i}_z \quad (\text{E.1.1.4})$$

Equation (1.1.38) becomes

$$\frac{1}{B} \left(u \cdot \overline{\frac{\partial}{\partial x}} B + v \cdot \overline{\frac{\partial}{\partial y}} B \right) = \vec{n} \cdot \frac{\partial \vec{v}}{\partial z} \quad (\text{E.1.1.5})$$

Observe that $B=b$, since all metric coefficients are equal to one.

Example E.1.1.2. Cylindrical coordinates - S1 family

If the streamsurface S1 of figures 1.1.1 or 1.1.2 is considered as a surface defined by $r=r(\theta, z)$, in cylindrical coordinates, one can identify $\xi^1=\theta$, $\xi^2=z$ and $\xi^3=r$. The metric coefficients are $h_1 = r$, $h_2=h_3=1$.

The continuity equation (1.1.34) becomes

$$\frac{\partial}{\partial t} (\rho B) + \frac{1}{r} \overline{\frac{\partial}{\partial \theta}} (\rho B v_\theta) + \frac{1}{r} \overline{\frac{\partial}{\partial z}} (\rho B v_z r) = 0 \quad (\text{E.1.1.6})$$

where the velocity components v_r, v_z, v_θ denote the physical components. The streamsurface derivatives are defined by

$$\overline{\frac{\partial g}{\partial \theta}} = \frac{\partial g}{\partial \theta} - n_\theta \frac{\partial g}{\partial r} \quad (\text{E.1.1.7})$$

$$\overline{\frac{\partial g}{\partial z}} = \frac{\partial g}{\partial z} - n_z \frac{\partial g}{\partial r}$$

where the components of the normal vector $\vec{n} = \vec{\nabla} r(\theta, z)$ are given by

$$\begin{aligned}
n_\theta &= - \frac{\partial r(\theta, z)}{\partial \theta} = r \cdot \tilde{n}_\theta \\
n_z &= \frac{-\partial r(\theta, z)}{\partial z} = \tilde{n}_z \\
n_r &= 1 = \tilde{n}_r
\end{aligned} \tag{E.1.1.8}$$

where \tilde{n} represents the projections of \vec{n} along the corresponding unit vectors.

Equation (1.1.38) for the streamsheet thickness $B=b$ becomes

$$\vec{v} \cdot \vec{\nabla} B = \frac{v_\theta}{r} \frac{\partial B}{\partial \theta} + v_z \frac{\partial B}{\partial z} = B \left[n_\theta \frac{\partial}{\partial r} \left(\frac{v_\theta}{r} \right) + n_r \frac{\partial}{\partial r} v_r + n_z \frac{\partial}{\partial r} v_z \right] \tag{E.1.1.9}$$

Example E.1.1.1. Cylindrical coordinates - S2 family

If the streamsurface S2 of figures 1.1.1 or 1.1.2 is considered as a surface defined by $\theta=\theta(r, z)$ in cylindrical coordinates, one can identify $\xi^1=z$, $\xi^2=r$ and $\xi^3=\theta$. The metric coefficients are $h_1=1$, $h_2=1$, $h_3=r$. The continuity equation (1.1.34) becomes, with $B=b \cdot r$

$$\frac{\partial \rho B}{\partial t} + \frac{\partial}{\partial z} (\rho B v_z) + \frac{\partial}{\partial r} (\rho B v_r) = 0 \tag{E.1.1.10}$$

The streamsurface derivatives are defined by

$$\frac{\partial \bar{g}}{\partial z} = \frac{\partial g}{\partial z} - n_z \frac{\partial g}{\partial \theta} \tag{E.1.1.11}$$

$$\frac{\partial \bar{g}}{\partial r} = \frac{\partial g}{\partial r} - n_r \frac{\partial g}{\partial \theta}$$

where the components of the normal vector $\vec{n} = \vec{\nabla} \theta(z, r)$ are given by

$$\begin{aligned}
n_z &= - \frac{\partial \theta(z, r)}{\partial z} = \tilde{n}_z \\
n_r &= - \frac{\partial \theta(z, r)}{\partial r} = \tilde{n}_r \\
n_\theta &= 1 = r \cdot \tilde{n}_\theta
\end{aligned} \tag{E.1.1.12}$$

Equation (1.1.45) for the streamsheet thickness b becomes,

$$\vec{v} \cdot \vec{\nabla} b = v_z \frac{\partial b}{\partial z} + v_r \frac{\partial b}{\partial r} = b \left[n_z \frac{\partial v_z}{\partial \theta} + n_r \frac{\partial v_r}{\partial \theta} + \frac{n_\theta}{r} \frac{\partial v_\theta}{\partial \theta} \right] \tag{E.1.1.13}$$

1.1.4. Streamsurface Formulation for the Momentum Conservation Equation

The momentum equation is written in integral form in an absolute frame of reference, in presence of external forces \vec{f}_e

$$\frac{\partial}{\partial t} \int_{\Omega} \rho \vec{v} d\Omega + \oint_S \vec{F} \cdot d\vec{S} = \int_{\Omega} \rho \vec{f}_e d\Omega \quad (1.1.47)$$

where

$$\vec{F} = \rho \vec{v} \otimes \vec{v} + p \vec{I} - \vec{\tau} = \rho \vec{v} \otimes \vec{v} - \vec{\sigma} \quad (1.1.48)$$

is the momentum flux tensor.

Following the procedure which led to equation (1.1.32) in the previous section, one obtains,

$$\begin{aligned} \frac{\partial}{\partial t} (\rho \vec{v} B) + \frac{1}{h_1 h_2} [\overline{\partial_1} (\vec{F} \cdot \vec{e}^1 B h_1 h_2) + \overline{\partial_2} (\vec{F} \cdot \vec{e}^2 B h_1 h_2)] \\ = \rho \vec{f}_e \cdot B - \frac{b}{h_1 h_2} \partial_3 (\vec{F} \cdot \vec{I}_n h_1 h_2) \end{aligned} \quad (1.1.49)$$

The product $(\vec{F} \cdot \vec{I}_n)$ reduces to the contributions from the pressure and shear stresses since $\vec{v} \cdot \vec{n} = 0$ expressing the fact that one follows a streamsurface. Hence,

$$-\vec{F} \cdot \vec{I}_n = \vec{\sigma} \cdot \vec{I}_n \quad (1.1.50)$$

The derivative terms on the left hand side, with an overbar to indicate that they are to be considered along the streamsurface, have the form of the divergence of a tensor in the two-dimensional space ξ^1 - ξ^2 . Hence the quasi-three-dimensional momentum equation becomes, applying equation (1.1.17)

$$\frac{1}{B} \left[\frac{\partial}{\partial t} (\rho B \vec{v}) + \vec{\nabla} (\rho B \vec{v} \otimes \vec{v}) \right] + \frac{1}{B} \vec{\nabla} [(p \vec{I} - \vec{\tau}) B] = \rho \vec{f}_e + \frac{b}{B} \partial_3 (\vec{\sigma} \cdot \vec{I}_n) \quad (1.1.51)$$

written completely in the two-dimensional space ξ^1 - ξ^2 .

The additional term in the right hand side appears as an extra force term \vec{f} acting on the "streamsurface" flow and originating from the three dimensionality of the flow.

$$\rho B \vec{f} = -b \partial_3 [(\rho \vec{I} - \vec{\tau}) \cdot \vec{I}_n] = b \partial_3 (\vec{\sigma} \cdot \vec{I}_n) \quad (1.1.52)$$

An alternative expression for the additional force term can be obtained, if the relation (1.1.42) between B and the derivatives of \vec{n} is introduced in equation (1.1.51).

One has

$$\vec{\nabla} (\vec{\sigma} B) = B (\vec{\nabla} \cdot \vec{\sigma}) + (\vec{\sigma} \cdot \vec{\nabla}) B = B (\vec{\nabla} \cdot \vec{\sigma}) - \vec{\sigma} b \partial_3 (\vec{I}_n) \quad (1.1.53)$$

and transferring the second term to the right hand side of equation (1.1.51), leads to the following form of the quasi-three dimensional momentum equation applying $b \vec{I}_n = B \cdot \vec{n}$ as derived from equation (1.1.29)

$$\frac{1}{B} \left[\frac{\partial}{\partial t} (\rho \vec{v} B) + \vec{\nabla} (\rho B \vec{v} \otimes \vec{v}) - \vec{\nabla} \cdot \vec{\sigma} \right] = + \vec{n} \cdot \partial_3 \vec{\sigma} + \rho \vec{f}_e \quad (1.1.54)$$

The first term on the right hand side is the expression of an additional force \vec{f}_B , obtained from the relations

$$\rho \vec{f}_B = \rho \vec{f} + \frac{(\vec{\sigma} \cdot \vec{\nabla}) B}{B} = \vec{n} \cdot \partial_3 \vec{\sigma} \quad (1.1.55a)$$

or applying the relation (1.1.21)

$$\rho \vec{f}_B = \vec{I}_n \cdot \frac{\partial \vec{\sigma}}{\partial n} \quad (1.1.55b)$$

Equation (1.1.54) takes the following form

$$\frac{1}{B} \left[\frac{\partial}{\partial t} (\rho \vec{v} B) + \vec{\nabla} (\rho B \vec{v} \otimes \vec{v}) \right] + \vec{\nabla} (\rho \vec{I} - \vec{\tau}) = \rho \vec{f}_B + \rho \vec{f}_e \quad (1.1.56)$$

Non-conservative formulation

Subtracting the quasi-three dimensional continuity equation (1.1.34) multiplied by \vec{v} , from the momentum equation (1.1.51), one obtains the non conservative formulation for the quasi-three-dimensional momentum equation,

$$\frac{\partial \vec{v}}{\partial t} + (\vec{v} \cdot \vec{\nabla}) \vec{v} = \frac{1}{\rho B} \vec{\nabla} (\vec{\sigma} B) + \vec{f} + \vec{f}_e \quad (1.1.57a)$$

or, from equation (1.1.56)

$$\frac{\partial \vec{v}}{\partial t} + (\vec{v} \cdot \vec{\nabla}) \vec{v} = \frac{1}{\rho} \vec{\nabla} \cdot \vec{\sigma} + \vec{f}_B + \vec{f}_e \quad (1.1.57b)$$

The last equation has the usual form of a two-dimensional momentum equation in the subspace of the streamsurface, with however the addition of the distributed force \vec{f}_B acting on the flow. Hence, the whole effect of the three-dimensionality on the non conservative, two dimensional flow description is contained in the force term \vec{f}_B . This extra force arises from the projection, on the normal direction, of the pressure and shear stress gradients in the third coordinate direction, as shown by equation (1.1.55). Note also, that the conservative formulation (1.1.56) contains also the influence of the variation of the streamtube thickness B.

In absence of shear stresses and in a steady flow configuration, equations (1.1.55) and (1.1.3) show that the additional force \vec{f}_B is orthogonal to the velocity field along the streamsurface S. One has in this case

$$\rho \vec{f}_B = - \vec{n} \frac{\partial p}{\partial \xi^3} = - \vec{i}_n \frac{\partial p}{\partial n} \quad (1.1.58)$$

and

$$\rho \vec{f}_B \cdot \vec{v} = 0 \quad (1.1.59)$$

This is an interesting relation which will be used in conjunction with the distributed loss model in the field of turbomachinery flow models.

The results obtained in this section remain valid for other forms of the momentum equation, in particular for Crocco's form, or for the equations in a relative system.

Crocco's form of the momentum equation becomes, when written along the streamsurface S

$$\frac{\partial \vec{v}}{\partial t} - \vec{v} \times \vec{\zeta} = T \vec{\nabla}_S - \vec{\nabla} H + \frac{1}{\rho} \vec{\nabla} \cdot \vec{\tau} + \vec{f}_B + \vec{f}_e \quad (1.1.60)$$

with the absolute vorticity $\vec{\zeta}$ defined along the streamsurface by

$$\vec{\zeta} = \vec{\nabla} \times \vec{v} \quad (1.1.61)$$

where all the derivatives are streamsurface derivatives. Note that by

application of (1.1.13) to the entropy relation, one can eliminate the pressure from \vec{f}_B , since

$$-\frac{\vec{n}}{\rho} \partial_s p = \vec{n} (T \partial_s s - \partial_s h) \quad (1.1.62)$$

Example E.1.1.4 : Cylindrical coordinates

Take $\xi^1 = \theta$, $\xi^2 = z$, $\xi^3 = r$, for the streamsurface S_1 defined by $r = r(\theta, z)$ with $h_1 = r$, $h_2 = h_3 = 1$.

The additional force term \vec{f}_B , equation (1.1.55), becomes with \vec{n} defined by equation (E.1.1.8)

$$\rho \vec{f}_B = \left[-\frac{\partial p}{\partial r} + \frac{\partial \bar{\tau}}{\partial r} \right] \vec{n} \quad (E.1.1.14)$$

For the S_2 type of surface, figure 1.1.2, $\theta = \theta(z, r)$, one obtains the force term \vec{f}_B , with $h_3 = r$, $h_1 = h_2 = 1$ and \vec{n} defined by equation (E.1.1.12)

$$\rho \vec{f}_B = \left[-\frac{\partial p}{\partial \theta} + \frac{\partial \bar{\tau}}{\partial \theta} \right] \vec{n} \quad (E.1.1.15)$$

The momentum equations are obtained in cylindrical coordinates with the addition of \vec{f}_B and with the derivatives replaced by the streamsurface derivatives $\bar{\partial}$, with $\bar{\partial}/\partial \theta$ set to zero.

For inviscid flows, one obtains for instance

$$\rho \vec{f}_B = -\vec{n} \frac{\partial p}{\partial \theta} \quad (E.1.1.16)$$

and the radial component of the momentum equation becomes

$$\frac{\partial v_r}{\partial t} + v_r \frac{\bar{\partial} v_r}{\partial r} + v_z \frac{\bar{\partial} v_r}{\partial z} = -\frac{1}{\rho} \frac{\bar{\partial} p}{\partial r} + f_{B,r} + f_{e,r} \quad (E.1.1.17)$$

1.1.5. Streamsurface Formulation for the Energy Conservation Law

The energy equation can be treated exactly in the same way as the mass conservation equation. The integral form of the energy equation is

$$\frac{\partial}{\partial t} \int_{\Omega} \rho E \, d\Omega + \oint_S \vec{F} \cdot \vec{dS} = \int_{\Omega} Q \, d\Omega \quad (1.1.63)$$

where Q is a source term and the energy flux is defined by

$$\vec{F} = \rho \vec{v} H - \vec{\tau} \cdot \vec{v} - k \vec{\nabla} T \quad (1.1.64)$$

Following the same steps as in section 1.1.1., equation (1.1.63) becomes

$$\frac{\partial}{\partial t} (\rho B E) + \vec{\nabla} \cdot [(\rho \vec{v} H - \vec{\tau} \cdot \vec{v} - k \vec{\nabla} T) B] = Q B - b \partial_3 (\vec{F} \cdot \vec{1}_n) \quad (1.1.65)$$

where

$$\vec{F} \cdot \vec{1}_n = -(\vec{\tau} \cdot \vec{v} + k \vec{\nabla} T) \cdot \vec{1}_n \quad (1.1.66)$$

since $\vec{v} \cdot \vec{n} = 0$.

Applying the continuity equation leads to the alternative form

$$\rho \left[\frac{\partial H}{\partial t} + (\vec{v} \cdot \vec{\nabla}) H \right] = \frac{\partial p}{\partial t} + \frac{1}{B} \vec{\nabla} \cdot [(\vec{\tau} \cdot \vec{v} + k \vec{\nabla} T) B] + Q - \frac{b}{B} \partial_3 (\vec{F} \cdot \vec{1}_n) \quad (1.1.67)$$

or introducing equation (1.1.42)

$$\rho \left[\frac{\partial H}{\partial t} + (\vec{v} \cdot \vec{\nabla}) H \right] = \frac{\partial p}{\partial t} + \vec{\nabla} \cdot (\vec{\tau} \cdot \vec{v} + k \vec{\nabla} T) + Q - \vec{n} \cdot \partial_3 \vec{F} \quad (1.1.68)$$

Hence, the confinement of the energy balance to the streamsurface S , leads to a conservation equation for the energy fluxes within the streamsheet of thickness $B = b h_3$, whereby an additional heat source term appears, due to the three dimensionality of the flow, given by equation (1.1.69).

$$\begin{aligned} Q_B &= - \vec{n} \cdot \partial_3 \vec{F} = \vec{n} \cdot \partial_3 (k \vec{\nabla} T + \vec{\tau} \cdot \vec{v}) \\ &= - \vec{1}_n \cdot \frac{\partial \vec{F}}{\partial n} \end{aligned} \quad (1.1.69)$$

These additional sources result from the normal components of the gradients, or the normal direction of the heat conduction fluxes and the work of the viscous shear stresses, in the third direction.

In absence of shear stresses and heat conduction effects, the quasi three dimensional form of the energy equation reduces to, with the source term $Q=0$,

$$\frac{dH}{dt} = \frac{1}{\rho} \frac{\partial p}{\partial t} \quad (1.1.70)$$

where

$$\frac{d}{dt} = \frac{\partial}{\partial t} + \vec{v} \cdot \vec{\nabla} \quad (1.1.71)$$

is the total material derivative along the streamsurface, and is identical to its two-dimensional restriction.

1.1.6. Quasi-Three Dimensional Interaction Procedure

Summarizing this approach, we have seen that the flow behaviour can be followed along a streamsurface $\xi^3 = \xi^3(\xi^1, \xi^2)$ and the conservation equations for mass, momentum and energy can be written in a two-dimensional form in function of the space variables ξ^1 and ξ^2 with space derivatives taken along the streamsurface. The influence of the three-dimensionality of the flow appears in all three conservation equations through

- i) a variable streamtube thickness B
- ii) through an additional force term whose non-viscous contribution is the pressure gradient in the ξ^3 direction acting in the direction normal to the surface, in the momentum equation and
- iii) for the energy conservation equation, through an energy source term whose non-viscous contribution is a normal flux arising from the thermal conductivity in the ξ^3 direction.

In order to solve this two-dimensional system of equations, the extra terms just mentioned have to be known, as well as the shape of the streamsurface. These informations, known only if the complete three-dimensional flow description is available, have therefore to be obtained in an iterative procedure.

In practical applications to internal flows, the present approach is best suited for steady state flow situations, since in this case, one can completely define the velocity field through two families of streamfunctions ψ_1 and ψ_2 , Yih (1979).

The steady state continuity equation $\vec{\nabla}(\rho \vec{v}) = 0$ is satisfied by the existence of two functions ψ_1 and ψ_2 such that

$$\rho \vec{v} = \rho_0 (\vec{\nabla} \psi_1 \times \vec{\nabla} \psi_2) \quad (1.1.72)$$

By definition, one has

$$(\vec{v} \cdot \vec{\nabla}) \psi_1 = 0 \quad (1.1.73)$$

$$(\vec{v} \cdot \vec{\nabla}) \psi_2 = 0 \quad (1.1.74)$$

which shows that the velocity vectors are tangent to the surfaces

$\psi_1(\xi^1, \xi^2, \xi^3) = \text{constant}$ and $\psi_2(\xi^1, \xi^2, \xi^3) = \text{constant}$ and hence that the intersection of any of these two surfaces is a streamline. Therefore, these surfaces form two families of streamsurfaces generated by the various streamlines issued from the fluid particles situated in the inlet surface of the flow domain. In figure 1.1.1, the surfaces $A_1B_1C_1D_1$ (or S_1 in figure 1.1.2) and $A_2B_2C_2D_2$ (or S_2 in figure 1.1.2) are typical representations of surfaces of constant ψ_1 and ψ_2 values.

The complete three-dimensional flow description is therefore reconstructed by writing the two-dimensional form of the equations of motion along two families of intersecting surfaces such as ψ_1 and ψ_2 . The information necessary on one family of surfaces is to be obtained from the flow behaviour on the other family. For instance, if the surface S considered above is a member of ψ_1 family, the shape of this surface as well as the streamtube thickness B and the additional terms which are all determined by the variations of certain flow variables in the ξ^3 direction, will be obtained by the solution of the same two-dimensional form of the equations written along the other ψ_2 family of surfaces, which contains, by definition the variations in the ξ^3 direction.

For this latter family of two-dimensional flows, the knowledge of the additional terms can only be obtained from the ψ_1 family of flows and this sets up the iterative procedure.

In practical applications, the computation will start by assuming a reasonable shape for the first family of surfaces (ψ_1) and by neglecting the contributions of the additional terms. After the solutions along this first family are obtained, the flow is calculated along the second (ψ_2) family of surfaces with an input from the first family in order to determine the three-dimensional contributions to the equations of motions. After this step, a new approximation to the ψ_1 flows can be obtained and the whole computation is continued solving alternatively the flow along each set of streamsurfaces until a chosen convergence criterion is satisfied.

This calculation procedure, in a simplified form, is widely used in the field of single and (or) multistage turbomachines and will be described more in details with regard to computational details and additional approximations in part 2 of this report dealing with the internal turbomachinery flows.

1.2. THE QUASI-THREE-DIMENSIONAL REPRESENTATION (Q3D) FOR INTERNAL FLOWS : THE AVERAGING PROCEDURE

As discussed in the introduction, an alternative to the streamsurface approach in reducing the complexity of the three dimensionality of the flow, can be obtained by taking the average of the conservation equations over one of the spatial directions. This procedure will lead to exact equations for the flow conservation laws in the remaining space variables, reducing in this way the flow description to a lower number of space variables.

Since this averaging technique requires limits of integrations for the corresponding variable the method takes its full potentiality within the framework of internal flows, such as channel or turbomachinery flows.

Let us consider therefore a channel limiting the flow region by upper and lower surfaces, as well as side surfaces, these surfaces being either material, solid walls or fluid boundaries, figure 1.2.1. Average values of any flow variable A over say, the ξ^3 direction, can be defined through

$$\bar{A} = \frac{1}{b(\xi^1, \xi^2, t)} \int_{b_0}^{b_1} A(\xi^1, \xi^2, \xi^3, t) d\xi^3 \quad (1.2.1)$$

The quantities $\xi^3 = b_1(\xi^1, \xi^2, t)$ and $\xi^3 = b_0(\xi^1, \xi^2, t)$ define the limits of the integration region corresponding to the surfaces A, A_2, C_2, C_1 and B_1, B_2, D_2, D_1 , with

$$b = b_1 - b_0 \quad (1.2.2)$$

($b = A, B_1$ on figure 1.2.1). These boundary surfaces are, in general, functions of the other coordinates and eventually of time. Note that b is the width of the integration region expressed in units of ξ^3 .

Relations for the averaged derivatives are obtained as follows : from the general properties of the derivative of an integral one has, the subscript α indicating either time t or the coordinates ξ^1 or ξ^2 ,

$$\begin{aligned}
\overline{\partial_{\alpha} A} &= \frac{1}{b} \int_{b_0}^{b_1} \partial_{\alpha} A \, d\xi^3 \\
&= \frac{1}{b} \partial_{\alpha} \int_{b_0}^{b_1} A \, d\xi^3 - \frac{1}{b} [A(\xi^1, \xi^2, b_1, t) \partial_{\alpha} b_1 - A(\xi^1, \xi^2, b_0, t) \partial_{\alpha} b_0] \\
&= \frac{1}{b} \partial_{\alpha} (b\bar{A}) - \frac{1}{b} (A_1 \partial_{\alpha} b_1 - A_0 \partial_{\alpha} b_0)
\end{aligned} \tag{1.2.3}$$

where A_1 and A_0 are the values taken by the variable A on the upper and lower limits of the integration domain.

Similarly, for $\alpha=3$, one obtains

$$\overline{\partial_3 A} = \frac{1}{b} (A_1 - A_0) \tag{1.2.4}$$

On the other hand, the average of a product of two quantities requires the introduction of the deviations from the average value following

$$A = \bar{A} + A' \tag{1.2.5}$$

with, by definition

$$\overline{A'} = 0 \tag{1.2.6}$$

Hence, one obtains for the average of a product of two quantities A and B and for their derivative, the following relations

$$\overline{AB} = \bar{A} \cdot \bar{B} + \overline{A'B'} \tag{1.2.7}$$

$$\overline{\partial_{\alpha} AB} = \frac{1}{b} \partial_{\alpha} (b \cdot \bar{A} \cdot \bar{B}) + \frac{1}{b} \partial_{\alpha} (b \cdot \overline{A'B'}) - \frac{1}{b} (A_1 B_1 \partial_{\alpha} b_1 - A_0 B_0 \partial_{\alpha} b_0) \tag{1.2.8}$$

where α represents the coordinates ξ^1 , ξ^2 or time.

The boundary surfaces of the integration region will be defined by

$$S_1 \equiv \xi^3 - b_1(\xi^1, \xi^2, t) = 0 \tag{1.2.9}$$

and

$$S_0 \equiv \xi^3 - b_0(\xi^1, \xi^2, t) = 0 \tag{1.2.10}$$

for the upper and lower limits respectively.

An important simplification of the averaging process occurs when the boundary surfaces can be assumed to be streamsurfaces, that is surfaces which do not allow any cross-flow. This assumption will be satisfied for the solid surfaces bounding a duct or channel flow, but is also valid in free surface problems where one of the boundaries, represents the time and space dependent free surface of an open channel fluid flow, as occurs in river and sea hydraulics or tidal flows.

Expressing that the velocity vector lies at each instant t in these surfaces, that is

$$\frac{d}{dt} S_0 = \frac{\partial S_0}{\partial t} + (\vec{v} \cdot \vec{\nabla}) S_0 = 0 \quad (1.2.11)$$

along the surface S_0 , one obtains with (1.2.9) and (1.2.10) the relation

$$-\frac{\partial b_0}{\partial t} + \vec{v} \cdot \vec{n}_0 = 0 \quad (1.2.12)$$

where $\vec{n}_0 = \vec{\nabla} S_0$ is the normal to the considered surface.

The components of \vec{n}_0 along the unit vectors of an orthogonal coordinate system are defined by, see equation (1.1.6)

$$\vec{n}_0 = \left(\frac{-1}{h_1} \frac{\partial b_0}{\partial \xi^1}, \frac{-1}{h_2} \frac{\partial b_0}{\partial \xi^2}, \frac{1}{h_3} \right) \quad (1.2.13)$$

Similarly, one has for the second boundary

$$-\frac{\partial b_1}{\partial t} + \vec{v} \cdot \vec{n}_1 = 0 \quad (1.2.14)$$

with

$$\vec{n}_1 = \left(\frac{-1}{h_1} \frac{\partial b_1}{\partial \xi^1}, \frac{-1}{h_2} \frac{\partial b_1}{\partial \xi^2}, \frac{1}{h_3} \right) \quad (1.2.15)$$

With these relations, the averaging rules can be written, grouping (1.2.3) and (1.2.4) as the average of the gradient of a quantity A .

$$\overline{\vec{\nabla} A} = \frac{1}{b} \vec{\nabla} (b \bar{A}) + \frac{1}{b} [A \cdot \vec{n}] \quad (1.2.16)$$

where the square brackets indicate the difference over the two boundaries

$$[\vec{A}\vec{n}] = A_1\vec{n}_1 - A_0\vec{n}_0 \quad (1.2.17)$$

The gradient operator is restricted to the two-dimensional space $\xi^1-\xi^2$, since

$$\frac{\partial}{\partial \xi^3} (b\vec{A}) = 0 \quad (1.2.18)$$

for any averaged quantity \vec{A} .

The same relations apply to the divergence of a vector \vec{F} or a tensor quantity $\vec{\tau}$, that is,

$$\vec{\nabla} \cdot \vec{F} = \frac{1}{b} \vec{\nabla} (\vec{F}b) + \frac{1}{b} [\vec{F} \cdot \vec{n}] \quad (1.2.19)$$

and

$$\vec{\nabla} \cdot \vec{\tau} = \frac{1}{b} \vec{\nabla} (b\vec{\tau}_a) + \frac{1}{b} [\vec{\tau} \cdot \vec{n}] \quad (1.2.20)$$

where $\vec{\tau}_a$ is the averaged value of $\vec{\tau}$. These averaging rules express that the averaged gradients of a flow quantity over a given direction are equal to the gradients in the (two) remaining coordinates of the averaged quantity weighted by the width of the integration region, plus a contribution expressing the balance of the normal components of the considered quantities over the two boundaries.

It is essential to observe that the explicit form of the divergence operator acting on the averaged quantities, has to be written in its three-dimensional form, where all derivatives with respect to ξ^3 are set to zero afterwards.

These two relations, written in operator form, are valid on an arbitrary system of coordinates provided the metric coefficients are independent of the integration variable. When this is not the case, the divergence operators have to be written first in the system of coordinates considered and then integrated over the variable ξ^3 . Averaged values of the metric coefficients will then appear in the explicit formulation. For instance, if the integration variable is the radial coordinate in a cylindrical or spherical coordinate representation, an average radius will appear in the equations.

Hence, in orthogonal curvilinear coordinates one has

$$\vec{\nabla} \cdot (\vec{F}b) = \frac{1}{h_1 h_2 h_3} [\partial_1 (h_1 h_2 h_3 b \vec{F}^1) + \partial_2 (h_1 h_2 h_3 b \vec{F}^2)] \quad (1.2.21)$$

This has to be compared with the streamsurface divergence operator

$\vec{\nabla}$ as defined by equation (1.1.29).

The explicit occurrence of h_s in the above equation, explains why the quantity b appears in the averaged equations while the quantity $B=bh_s$ appears in the streamsurface equations of the previous section.

1.2.1. The averaged form of the continuity equation

Applying the above rules to the continuity equation $\frac{\partial \rho}{\partial t} + \vec{\nabla} \rho \vec{v} = 0$ leads to

$$\frac{\partial}{\partial t} (\bar{\rho} b) + \vec{\nabla} (\bar{\rho} \vec{v} b) + [\rho \vec{v} \cdot \vec{n}] + (\partial_t b_0 - \partial_t b_1) = 0 \quad (1.2.22)$$

Expressing that the two bounding surfaces are streamsurfaces, equations (1.2.12) and (1.2.14), the averaged continuity equation becomes

$$\frac{\partial}{\partial t} (\bar{\rho} b) + \vec{\nabla} (\bar{\rho} \vec{v} b) = 0 \quad (1.2.23)$$

Applying equation (1.2.7) to the averaged product $\overline{\rho \vec{v}}$, leads to

$$\frac{\partial}{\partial t} (\bar{\rho} b) + \vec{\nabla} (\bar{\rho} \vec{v} b) = - \vec{\nabla} (\bar{\rho' \vec{v}' b}) \quad (1.2.24)$$

If an integrating factor μ is defined such that

$$- \vec{\nabla} (\bar{\rho' \vec{v}' b}) = \frac{1}{\mu} \bar{\rho} (\vec{v} \cdot \vec{\nabla}) \mu \quad (1.2.25)$$

equation (1.2.24) becomes

$$\frac{\partial (\bar{\rho} B)}{\partial t} + \vec{\nabla} (\bar{\rho} \vec{v} B) = 0 \quad (1.2.26)$$

where

$$B = b \cdot \mu \quad (1.2.27)$$

Comparing this with equation (1.1.34), a two-dimensional mass conservation equation is obtained where the B -factor represents a varying streamtube thickness which is equal to the product of the geometrical thickness of the fluid layer over which the averaging is performed, multiplied by a correction factor which represents

the effect of the mass flux fluctuations over the flow domain. Hence, this B factor is dependent on the three-dimensional flow properties.

It is to be noticed that for incompressible flow, there are no density fluctuations and hence that $B=b$.

The present space averaging technique has strong resemblances with the time averaging procedure applied in the study of turbulent flows. An elegant way of accounting for the effects of the turbulent density fluctuations on the time averaged flow is to define density averaged quantities instead of the usual time averaged variables. A similar procedure can be applied in the present context where the compressibility effects included in B and described by the terms in equation (1.2.25) can be absorbed through the definition of the following density-average of a variable A, see for instance Hirsch and Warzee (1979)

$$\overline{\rho A} = \frac{1}{b} \int_{b_0}^{b_1} \rho A \, d\xi^3 \quad (1.2.28)$$

Denoting, in the following, the ordinary average as defined by equation (1.2.1) by an overbar and the density averaged values by a tilde, one has

$$\tilde{A} = \frac{\overline{\rho A}}{\bar{\rho}} = \frac{1}{\bar{\rho} b} \int_{b_0}^{b_1} \rho A \, d\xi^3 \quad (1.2.29)$$

The fluctuation of the variable A with respect to its usual average \bar{A} is indicated by A' while A'' will indicate the fluctuations with respect to the density average \tilde{A} . Therefore, the following relations hold,

$$A = \bar{A} + A' = \tilde{A} + A'' \quad (1.2.30)$$

with

$$\begin{aligned} \overline{A'} &= 0 \\ \overline{A''} &\neq 0 \end{aligned}$$

but

$$\overline{\rho A''} = 0 \quad (1.2.31)$$

One has also, from the above definitions

$$(\tilde{A} - \bar{A}) = -\overline{A''} = -\frac{\overline{\rho' A'}}{\bar{\rho}} \quad (1.2.32)$$

and for the product of two quantities A, B

$$\overline{\rho AB} = \bar{\rho} \tilde{A} \tilde{B} + \overline{\rho A'' B''} \quad (1.2.33)$$

while the above relations for the average of a derivative remain unchanged.

Applying these various properties to the averaged mass conservation law, equation (1.2.23) leads to the equation

$$\frac{\partial}{\partial t} (\bar{\rho} b) + \vec{\nabla} \cdot (\bar{\rho} \vec{V} b) = 0 \quad (1.2.34)$$

writing \vec{V} for the averaged velocity vector \vec{v} .

This exact relation has the advantage that the flow dependent streamtube thickness B in equation (1.2.26) reduces here, in all cases, to the geometrical thickness b of the flow region in the ξ^3 direction, since the influence of the density fluctuations are included in the definition of \vec{V} . Therefore, if the surfaces b_0 and b_1 are not flow dependent, the streamtube thickness of the considered fluid layer $b = b_1 - b_0$ is a known, geometrical quantity. This represents an important conceptual simplification of the averaged compressible flow equations compared to the previous form of equation (1.2.26).

Comparing equations (1.2.34) with the form of the continuity equation (1.1.34) obtained following the streamsurface approach, one notices that not with standing the close formal resemblance, the former equation describes the two-dimensional evolution of the averaged flow considered in the ξ^1 - ξ^2 coordinate system while the latter, equation (1.1.34), describes the evolution of the local flow variables followed along a given streamsurface of the three-dimensional flow.

1.2.2. The Averaged Momentum Conservation Equation

Considering the differential form of the momentum equation, in an absolute frame of reference, eventually as a Reynolds averaged equation for turbulent flows

$$\frac{\partial}{\partial t} (\vec{\rho} v) + \vec{\nabla} \cdot (\vec{\rho} v \otimes \vec{v} + \vec{p} I - \vec{\tau}) = \vec{\rho} f_e \quad (1.2.35)$$

the application of the averaged rules (1.2.16) to (1.2.20) leads to the following averaged momentum equation

$$\frac{\partial}{\partial t} (\bar{\rho} \vec{v} b) + \vec{\nabla} \cdot (\bar{\rho} \vec{v} \otimes \vec{v} b + \bar{p} b - \bar{\tau}_a b) = \bar{\rho} f_e \cdot b - [\bar{\rho} \vec{v} \cdot (\vec{v} \cdot \vec{n} - \frac{\partial b}{\partial t})] - [\bar{p} \vec{n}] + [\bar{\tau} \cdot \vec{n}] \quad (1.2.36)$$

writing $\bar{\tau}_a$ for the averaged viscous shear stress tensor, plus

eventually the Reynolds stress tensor.

The first term under brackets in the right hand side vanishes when the streamsurface assumptions equations, (1.2.12) and (1.2.14), are satisfied. Otherwise they contribute to an impulse flux through the boundary surfaces. The last two terms represent the components of an additional force term which appears as an outcome of the averaging procedure in a way that completely parallels the way the additional force appears in equation (1.1.52) derived in the streamsurface approach. The force term, defined by

$$\bar{\rho} \vec{f} = - \frac{1}{b} [\bar{\sigma} \cdot \vec{n}] = - \frac{1}{b} [(\bar{p}\vec{I} - \bar{\tau}) \cdot \vec{n}] \quad (1.2.37)$$

results from the difference in the normal components of the pressure and shear stresses acting on both limiting surfaces b_1 and b_0 .

The close resemblance between the two expressions of the extra force term equation (1.1.52) and (1.2.37) is obvious, so more that they become identical if the averaging is performed over an infinitesimal distance $d\xi^3 = b$, with metric coefficients independent of ξ^3 . Hence, equation (1.2.36) becomes

$$\frac{\partial}{\partial t}(\bar{\rho}\vec{v}b) + \vec{\nabla} \cdot (\bar{\rho}\vec{v} \otimes \vec{v} b) = + \vec{\nabla} \cdot (\bar{\sigma}_a \cdot b) + \bar{\rho} \vec{f}_e b + \bar{\rho} \vec{f} b \quad (1.2.38)$$

writing $\bar{\sigma}_a$ for the averaged shear stress tensor $\bar{\sigma}$.

If the averaging rule of products, equation (1.2.33) is introduced with density weighted averages, one obtains the following equation

for the density averaged velocity vector $\vec{V} = \vec{v}$,

$$\frac{\partial}{\partial t}(\bar{\rho}\vec{V}b) + \vec{\nabla} \cdot (\bar{\rho}b\vec{V} \otimes \vec{V}) = + \vec{\nabla} \cdot (\bar{\sigma}_a \cdot b) + \bar{\rho} \vec{f}_e b + \bar{\rho} \vec{f} b - \vec{\nabla} \cdot (\bar{\rho}\vec{v}'' \otimes \vec{v}'' b) \quad (1.2.39)$$

or alternatively, taking into account the averaged continuity equation (1.2.34),

$$\frac{\partial}{\partial t} \vec{V} + (\vec{V} \cdot \vec{\nabla}) \vec{V} = - \frac{1}{b\bar{\rho}} \vec{\nabla} \cdot (\bar{\sigma}_a \cdot b) + \vec{f}_e + \vec{f} - \frac{1}{b\bar{\rho}} \vec{\nabla} \cdot (\bar{\rho}\vec{v}'' \otimes \vec{v}'' b) \quad (1.2.40)$$

This last equation can be made formally identical to the standard two-dimensional momentum equation, by introducing the force \vec{f}_B instead of \vec{f} , with

$$\bar{\rho}b \vec{f}_B = -(\bar{p}\vec{I} - \bar{\tau}_a) \cdot \vec{V}b + \bar{\rho}b\vec{f} \quad (1.2.41)$$

leading to

$$\frac{\partial \vec{V}}{\partial t} + (\vec{V} \cdot \vec{\nabla}) \vec{V} = \frac{-1}{\rho} \vec{\nabla} (\bar{p} \bar{I} - \bar{\tau}_a) + \vec{f}_e + \vec{f}_B - \frac{1}{b \bar{\rho}} \vec{\nabla} (\rho \vec{v}'' \otimes \vec{v}'' b) \quad (1.2.42)$$

With the exception of the last term, this equation and equation (1.1.58) obtained by following a streamsurface, have very similar forms, although the interpretations of each term differ by the fact that here local derivatives of averaged quantities appear while in the former approach one has to do with streamsurface derivatives of the local flow quantities. In both cases however, the quasi-three-dimensional approximation leads to the introduction of variable streamtube thickness (B or b) and to additional forces \vec{f} whose non-viscous components act in the direction normal to the considered surfaces.

In the present approach an additional term appears on the right hand side of the momentum equation. This term, which has the same structure as the Reynolds stress tensor in the turbulent averaged Navier-Stokes equations, contains the influence of the three-dimensionality of the flow on its averaged representation.

It is to be kept in mind that the \vec{v}'' components of the velocity field represent the deviations from flow uniformity in the ξ^3 direction and can therefore be considered as large scale velocity fluctuations around the averaged flow.

Hence, the products $\rho \vec{v}'' \otimes \vec{v}''$ are an expression of the large scale momentum transport around the averaged flow and its gradients act as a diffusion effect on the resulting averaged momentum. If the flow is mildly non-uniform in the averaging direction these terms may become neglectable with respect to the other terms. If not, they can only be evaluated through a knowledge of the flow in a family of surfaces containing the ξ^3 -direction. In the following we will designate these terms as secondary stresses $\bar{\tau}^S$

$$\bar{\tau}^S = -\rho \overline{\vec{v}'' \otimes \vec{v}''} \quad (1.2.43)$$

1.2.3. The Averaged Energy Conservation Equation

The energy equation can be derived in the same way as described above using the local form, corresponding to equations (1.1.62) to (1.1.64)

$$\frac{\partial}{\partial t}(\rho E) + \vec{\nabla} (\rho \vec{v} H - \vec{G}) = Q \quad (1.2.44)$$

where \vec{G} is the flux of the shear stresses work and heat conduction

$$\vec{G} = k\vec{\nabla}T + \vec{\tau} \cdot \vec{v} \quad (1.2.45)$$

The averaging procedure leads to the following form of the averaged energy equation

$$\frac{\partial}{\partial t}(\overline{\rho E} b) + \vec{\nabla}[(\overline{\rho v H} - \vec{G})b] = \bar{Q} \cdot b - [p \frac{\partial b}{\partial t}] + [\vec{G} \cdot \vec{n}] - [\rho H (\vec{v} \cdot \vec{n} - \frac{\partial b}{\partial t})] \quad (1.2.46)$$

The last term vanishes when the boundaries are streamsurfaces, following equations (1.2.12) and (1.2.14).

Two additional contributions to the averaged energy balance appear in the right hand side as source terms. The first one

$$- [p \frac{\partial b}{\partial t}] = p_0 \cdot \frac{\partial b_0}{\partial t} - p_1 \cdot \frac{\partial b_1}{\partial t} \quad (1.2.47)$$

is the work of the pressure forces against the moving boundaries, while the second term

$$[\vec{G} \cdot \vec{n}] = [(k\vec{\nabla}T + \vec{\tau} \cdot \vec{v}) \cdot \vec{n}] \quad (1.2.48)$$

is the transfer of heat flux and work of the viscous stresses across the boundaries of the integration region. These two terms will be grouped in the source term

$$b Q_b = [\vec{G} \cdot \vec{n}] - [p \frac{\partial b}{\partial t}] \quad (1.2.49)$$

When the averaged products on the left hand side are worked out, one obtains

$$\frac{\partial}{\partial t}(\bar{\rho E} b) + \vec{\nabla}[(\bar{\rho v H} - \vec{G})b] = \bar{Q} \cdot b + Q_b \cdot b - \vec{\nabla}(\overline{b \rho v H}) \quad (1.2.50)$$

or by application of the averaged continuity equation

$$\rho [\frac{\partial \bar{H}}{\partial t} + (\vec{v} \cdot \vec{\nabla}) \bar{H}] = \frac{1}{b} \frac{\partial}{\partial t}(\bar{\rho} b) + \frac{1}{b} \vec{\nabla}(\bar{G} b) + \bar{Q} + Q_b - \frac{1}{b} \vec{\nabla}(\overline{b \rho v H}) \quad (1.2.51)$$

This form of the averaged energy conservation equation parallels completely equation (1.1.68) obtained by the streamsurface method with the difference in interpretation already discussed above for the momentum equation. An additional energy flux term appears,

$\overline{\rho v H}$, which represents the effect of the total enthalpy fluctuations as convected by the large scale velocity fluctuations.

Making use of the equations (1.2.12) and (1.2.14), the additional source term Q_b can be written as follows

$$Q_b = \frac{1}{b} [(\bar{\tau} \cdot \vec{v}) \cdot \vec{n} - p \vec{n} \cdot \vec{v}] + \frac{1}{b} [k \vec{\nabla} T \cdot \vec{n}]$$

or

$$Q_b = \frac{1}{b} [(\bar{\tau} \cdot \vec{n}) \cdot \vec{v} - p \vec{n} \cdot \vec{v}] + \frac{1}{b} [k \vec{\nabla} T \cdot \vec{n}] \quad (1.2.52)$$

In general circumstances, the first term of equation (1.2.52) shows that the additional heat source Q_b arises from the difference in the work of the shear stresses and pressure forces along the two limit surfaces b_0 and b_1 , in addition to the balance of heat conduction through these two surfaces.

An interesting particular situation occurs when both end-surfaces b_0 and b_1 have the same velocity, say \vec{v}_s . In this case, the first term of Q_b represents the work of the additional force \vec{f} , equation (1.2.37), acting on the moving boundary surfaces,

$$Q_b = \frac{1}{b} [\bar{\tau} \cdot \vec{n} - p \cdot \vec{n}] \cdot \vec{v}_s + \frac{1}{b} [k \vec{\nabla} T \cdot \vec{n}]$$

or

$$Q_b = \bar{\rho} \vec{f} \cdot \vec{v}_s + \frac{1}{b} [k \vec{\nabla} T \cdot \vec{n}] \quad (1.2.53)$$

A typical situation of this kind occurs in the passage between two blades of a rotating turbomachinery blade row.

The averaged energy equation can be put under different forms, when the stagnation enthalpy fluctuations H'' are separated into the static enthalpy fluctuations h'' and the contributions from the kinetic energy.

The total enthalpy fluctuations can be written as

$$H'' = H - \bar{H} = h'' + \vec{v}'' \cdot \vec{V} + \frac{\vec{v}''^2}{2} - \bar{k} \quad (1.2.54)$$

where the average kinetic energy of the velocity fluctuations is introduced,

$$\bar{\rho} \bar{k} = \rho \overline{\frac{\vec{v}'' \cdot \vec{v}''}{2}} = \overline{\rho k''} \quad (1.2.55)$$

Referring to equation (1.2.50), the last term of the right hand side becomes after introduction of equations (1.2.54) and (1.2.43)

$$\overline{\rho \vec{v}'' H''} = \overline{\rho v'' h''} - \overline{\tau^S \cdot \vec{V}} + \overline{\rho v'' \cdot \frac{\vec{v}''^2}{2}} \quad (1.2.56)$$

where τ^S designates the secondary stresses (1.2.43)

The energy equation (1.2.50) becomes

$$\frac{\partial}{\partial t}(\bar{\rho} b \bar{E}) + \vec{\nabla} \cdot (\bar{\rho} \vec{V} H b) = \vec{\nabla} \cdot [\vec{G} b - \overline{\rho \vec{v}'' (h'' + \frac{\vec{v}''^2}{2}) b}] + \vec{\nabla} \cdot (b \vec{V} \tau^S) + b (\bar{Q} + Q_b) \quad (1.2.57)$$

$$= \vec{\nabla} \cdot (\vec{V} \cdot \overline{\tau} + \vec{V} \cdot \tau^S - \overline{\rho \vec{v}'' h''} + \frac{\mu c}{P_r} \vec{\nabla} T - \overline{\rho \vec{v}'' k''}) b + b (\bar{Q} + Q_b)$$

Note the appearance of the energy due to the work of the secondary stresses τ^S against the averaged flow field \vec{V} , $\vec{\nabla} \cdot (\vec{V} \cdot \tau^S)$, in the right hand side as well as the transport of total energy of the fluctuations $(h'' + \vec{v}''^2/2)$ by the large scale fluctuating flow field \vec{v}'' .

If the deviations from the average velocity are small, this last contribution, being of third order in \vec{v}'' might be neglectable compared to the work of the secondary stresses τ^S against the mean flow \vec{V} . In addition, if the work of the fluctuating viscous (and turbulent) shear stresses is neglected $\overline{\vec{v}'' \tau^1} = 0$, then the averaged energy equation (1.2.57) simplifies to

$$\frac{\partial}{\partial t}(\bar{\rho} b \bar{E}) + \vec{\nabla} \cdot (\bar{\rho} \vec{V} H b) = \vec{\nabla} \cdot [(\vec{V} \cdot \overline{\tau}^T - \overline{\rho \vec{v}'' h''} + \frac{\mu c}{P_r} \vec{\nabla} T) b] + b (\bar{Q} + Q_b) \quad (1.2.58)$$

where the total shear stress appears as the sum of the viscous (plus turbulent) and secondary stresses

$$\overline{\tau}^T = \overline{\tau}_a + \tau^S \quad (1.2.59)$$

One can also introduce the total energy of the averaged flow

$$\hat{H} = \tilde{h} + \frac{\vec{V}^2}{2} = \tilde{H} - \frac{\overline{\rho \vec{v}'' \cdot \vec{v}''}}{2\bar{\rho}} = \tilde{H} - \bar{k} \quad (1.2.60)$$

into equation (1.2.57), in order to obtain an equation for \hat{H} .

1.2.4. Crocco's form for the averaged momentum equation

If the entropy relation is averaged over the width b of the channel, one obtains from equations (1.2.7), (1.2.16) and (1.2.33)

$$\overline{\rho T \vec{V}_s} = \overline{\rho \vec{V}_h} - \overline{\vec{V}_p} \quad (1.2.61)$$

or

$$\overline{\rho T \cdot \vec{V}_s} = \overline{\rho \cdot \vec{V}_h} - \overline{\vec{V}_p} - \overline{(\rho T)''(\vec{V}_s)''} + \overline{\rho'(\vec{V}_h)'} \quad (1.2.62)$$

leading to

$$\bar{T} \vec{V}(b\bar{s}) = \vec{V}(b\bar{h}) - \frac{1}{\bar{\rho}} \vec{V}(b\bar{p}) + \left[(h - \frac{p}{\bar{\rho}} - \bar{T}s)\bar{n} \right] - \frac{b}{\bar{\rho}} \overline{(\rho T)'(\vec{V}_s)'} + \overline{\rho'(\vec{V}_h)'} \quad (1.2.63)$$

or, grouping the three last terms into a force term $b\vec{f}_s$,

$$\bar{T} \vec{V}(b\bar{s}) = \vec{V}(b\bar{h}) - \frac{1}{\bar{\rho}} \vec{V}(b\bar{p}) + b\vec{f}_s \quad (1.2.64)$$

Eliminating the pressure term with the help of equation (1.2.64), one obtains Crocco's form of the momentum equation for the averaged flow,

$$\frac{\partial \vec{V}}{\partial t} - \vec{V} \times \vec{\zeta} = \bar{T} \vec{V}_s - \hat{V}_H + \frac{1}{\bar{\rho}} \vec{V} \cdot \bar{\tau}^T + \vec{f}_e + \vec{f}_s \quad (1.2.65)$$

with

$$\bar{\rho} b \vec{f}_s' = (\vec{f} - \vec{f}_s) \bar{\rho} b + \bar{\rho} (\bar{T}s - \bar{h}) \vec{V}_b \quad (1.2.66)$$

$$= [\bar{\tau} \cdot \bar{n}] + [(\bar{T}s - \bar{h}) \bar{n}] \bar{\rho} + b \overline{(\rho T)'(\vec{V}_s)'} - \overline{\rho'(\vec{V}_h)'} + \bar{\rho} (\bar{T}s - \bar{h}) \vec{V}_b$$

and

$$\vec{\zeta} = \vec{V} \times \vec{V} \quad (1.2.67)$$

Observe that the pressure term is eliminated from the new force term \vec{f}_s' , and the appearance of \hat{H} , the total energy of the average flow, instead of \bar{H} .

STREAMSURFACE APPROACH	AVERAGING APPROACH
<u>CONTINUITY EQUATION</u>	
$\frac{\partial}{\partial t} (\rho B) + \vec{\nabla}(\rho \vec{v} B) = 0$	$\frac{\partial}{\partial t} (\bar{\rho} b) + \vec{\nabla}(\bar{\rho} \vec{v} b) = 0$
<u>MOMENTUM CONSERVATION EQUATION</u>	
$\frac{\partial}{\partial t} (\rho B \vec{v}) + \vec{\nabla} [(\rho \vec{v} \cdot \vec{v} + p \vec{I} - \vec{\tau}) B] = \rho B \vec{f}_e + \rho B \vec{f}$ $\rho \vec{f} = - \frac{b}{B} \partial_3 [(p \vec{I} - \vec{\tau}) \cdot \vec{n}]$	$\frac{\partial}{\partial t} (\bar{\rho} b \vec{v}) + \vec{\nabla} [(\bar{\rho} \vec{v} \cdot \vec{v} + p - \vec{\tau}_a) b] = \bar{\rho} b \vec{f}_e + \bar{\rho} b \vec{f} - \vec{\nabla}(\bar{\rho} \vec{v} \cdot \vec{v} b)$ $\bar{\rho} \vec{f} = - \frac{1}{b} [(p \vec{I} - \vec{\tau}) \cdot \vec{n}]$
<u>ALTERNATIVE FORMULATION - NON-CONSERVATION FORM</u>	
$\frac{\partial \vec{v}}{\partial t} + (\vec{v} \cdot \vec{\nabla}) \vec{v} = - \frac{1}{\rho} \vec{\nabla}(p \vec{I} - \vec{\tau}) + \vec{f}_e + \vec{f}_B$ $\vec{f}_B = \vec{f} - \frac{1}{\rho B} (p \vec{I} - \vec{\tau}) \cdot \vec{\nabla} B = - \vec{n} \partial_3 (p \vec{I} - \vec{\tau})$	$\frac{\partial \vec{v}}{\partial t} + (\vec{v} \cdot \vec{\nabla}) \vec{v} = - \frac{1}{\rho} \vec{\nabla}(p \vec{I} - \vec{\tau}_a) + \vec{f}_e + \vec{f}_B - \frac{1}{b \rho} \vec{\nabla}(\bar{\rho} \vec{v} \cdot \vec{v} b)$ $\vec{f}_B = \vec{f} - \frac{1}{\bar{\rho} b} (p \vec{I} - \vec{\tau}_a) \cdot \vec{\nabla} b$
<u>CROCCO'S FORM</u>	
$\frac{\partial \vec{v}}{\partial t} - \vec{v} \times \vec{\zeta} = \vec{\nabla} \vec{v} \cdot \vec{\nabla} - \vec{\nabla} H + \frac{1}{\rho} \vec{\nabla} \cdot \vec{\tau} + \vec{f}_e + \vec{f}_B$ $\vec{\zeta} = \vec{\nabla} \times \vec{v}$	$\frac{\partial \vec{v}}{\partial t} - \vec{v} \times \vec{\zeta} = \vec{\nabla} \vec{v} \cdot \vec{\nabla} - \vec{\nabla} H + \frac{1}{\rho} \vec{\nabla} \cdot \vec{\tau} + \vec{f}_e + \vec{f}_s$ $\vec{\zeta} = \vec{\nabla} \times \vec{v}$
<u>ENERGY CONSERVATION LAW</u>	
$\frac{\partial}{\partial t} (\rho E B) + \vec{\nabla} [(\rho \vec{v} H - k \vec{\nabla} T - \vec{\tau} \cdot \vec{v}) B] = Q_e B + Q_b B$ $Q_b = \frac{b}{B} \partial_3 [(k \vec{\nabla} T + \vec{\tau} \cdot \vec{v}) \vec{I}_n]$	$\frac{\partial}{\partial t} (\bar{\rho} \bar{E} b) + \vec{\nabla} (\bar{\rho} \vec{v} H - \vec{G}) b = \bar{Q}_e b - \vec{\nabla}(\bar{\rho} \vec{v} \cdot \vec{v} H b) + Q_b \cdot b$ $Q_b = \frac{1}{b} [\vec{G} \cdot \vec{n}] - \frac{1}{b} [p \partial_t b]$ $\vec{G} = k \vec{\nabla} T + \vec{\tau} \cdot \vec{v}$
<u>NON-CONSERVATIVE FORM</u>	
$\rho (\frac{\partial}{\partial t} + \vec{v} \cdot \vec{\nabla}) H = \frac{\partial}{\partial t} p + \vec{\nabla} (k \vec{\nabla} T + \vec{\tau} \cdot \vec{v}) + Q + Q_B$ $Q_B = \vec{n} \cdot \partial_3 (k \vec{\nabla} T + \vec{\tau} \cdot \vec{v})$	$\bar{\rho} [\frac{\partial H}{\partial t} + (\vec{v} \cdot \vec{\nabla}) H] = \frac{1}{b} \frac{\partial}{\partial t} (\bar{p} b) + \frac{1}{b} \vec{\nabla} (\vec{G} b) + \bar{Q} + Q_b - \frac{1}{b} \vec{\nabla}(\bar{\rho} \vec{v} \cdot \vec{v} H b)$
<u>NOTATIONS</u>	
<p>The operators $\vec{\nabla} = (\partial_1, \partial_2)$ are defined by</p> $\vec{\nabla} = \vec{\nabla} - \vec{n} \partial_3$ <p>where \vec{n} is the normal to the surface</p>	<p>The averaged quantities are defined by</p> $\bar{\rho} \vec{A} = \frac{1}{b} \int_{b_0}^{b_1} \rho A d\xi^3$ <p>where ξ^3 is the averaged coordinate direction</p> $b = (b_1 - b_0)$ <p>\vec{v} is the averaged velocity</p> $[A] = A_1 - A_0$

Table 1. : Quasi-Three Dimensional Formulation. Streamsurface and averaging approach

SUMMARY

The system of equations obtained by following the flow along a streamsurface, or the system of equations found by averaging the conservation laws over a chosen direction lead to two equivalent representations of the two-dimensional restriction of a three-dimensional flow. The former approach defines a rigorous iterative procedure between two families of streamsurfaces allowing to reconstruct the complete three-dimensional flow. On the other hand the averaged equations define a "mean" flow in the two remaining coordinates and time, which is not associated with any particular streamsurface. The solution of this two-dimensional mean flow requires however informations from the three-dimensionality of the complete flow, as expressed by the additional force and energy source terms but also by the averaged products of velocity and energy fluctuations around the averaged flow quantities.

The quasi-three-dimensional approximation will consist in introducing some assumptions about the unknown contributions from the three-dimensionality by imposing for instance, a given shape for the (unknown) streamsurface along which the flow is followed or by neglecting certain terms in the equations related to the additional fluxes introduced through the averaging procedure. In both cases, the simplest approximation consists in keeping only the influence of the varying streamtube thickness B or b , and neglecting all other influences.

Both approaches are applied in the field of internal flows, such as turbomachinery and channel flows, while the averaging technique is widely applied in the field of hydraulics, in particular in the analysis of tidal flows of rivers, estuaries and seas. Table 1.1 presents a summary of the flow equations as derived from the two approaches.

REFERENCES

- Abbott, M.B. (1979). Computational Hydraulics. Fearon-Pitman Publishers, Belmont, Ca, USA.
- Abdallah, S.; Hamed, A. (1982). "The Elliptic Solution of the Secondary Flow Problem". 27th ASME Int. Gas Turbine Conferences, ASME Paper 82-GT-242.
- Briley, W.R.; Mc Donald, H. (1979). "Analysis and Computation of Viscous Subsonic Primary and Secondary Flows". Proc. AIAA 4th Computational Fluid Dynamics Conference, AIAA Paper 79-1453, pp. 74-88.
- Hamed, A.; Abdallah, S. (1979). "Streamlike Function : A New Concept in Flow Problems Formulation". Journal of Aircraft, Vol. 16, pp. 801-802.
- Hirsch, Ch.; Warzee, S. (1980). "Quasi 3D Finite Element Computation of Flows in Centrifugal Compressors" in Performance Prediction of Centrifugal Pumps and Compressors, pp. 69-75, ASME Publications.
- Phillips, O.M. (1977). The Dynamics of the Upper Ocean, Cambridge University Press.
- Sheoran, Y.; Tabakoff, W. (1982). "A Study of Viscous Flow in Stator and Rotor Passages". ASME Paper 82-GT-248.
- Wu, C.H. (1952). "A General Theory of Three-Dimensional Flow in Subsonic and Supersonic Turbomachine of Axial- Radial- and Mixed Flow type". NACA TN 2604.
- Wu, C.H. (1976). "Three-Dimensional Turbomachine Flow Equations Expressed with Respect to Non-Orthogonal Curvilinear Coordinates and Methods of Solution". Proc. 3rd Int. Symp. on Air Breathing Engines (ISABE), Munich.
- Yih, C.S. (1979). Fluid Mechanics, West River Press, Ann Arbor, Michigan, 2nd ed.

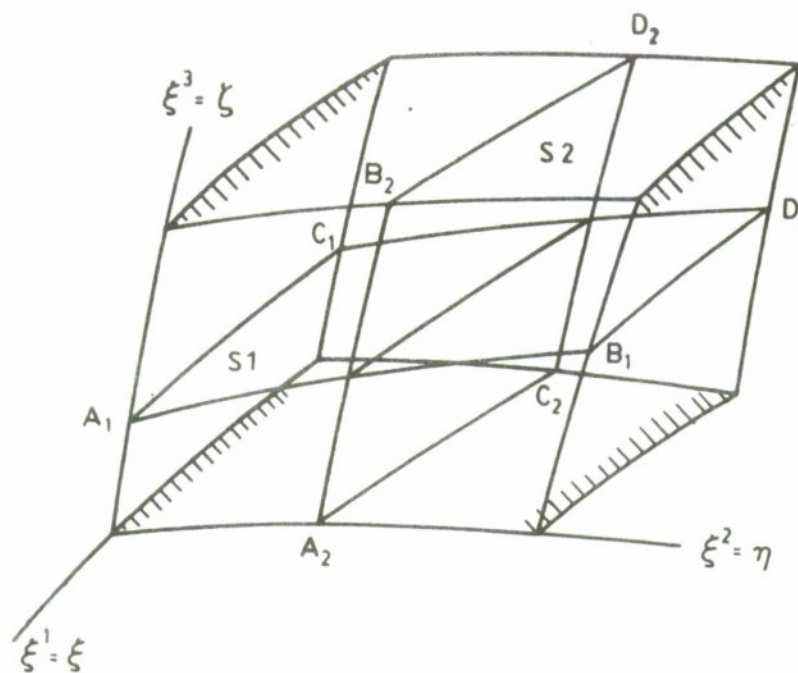


Figure 1.1.1. : General configuration of a channel flow

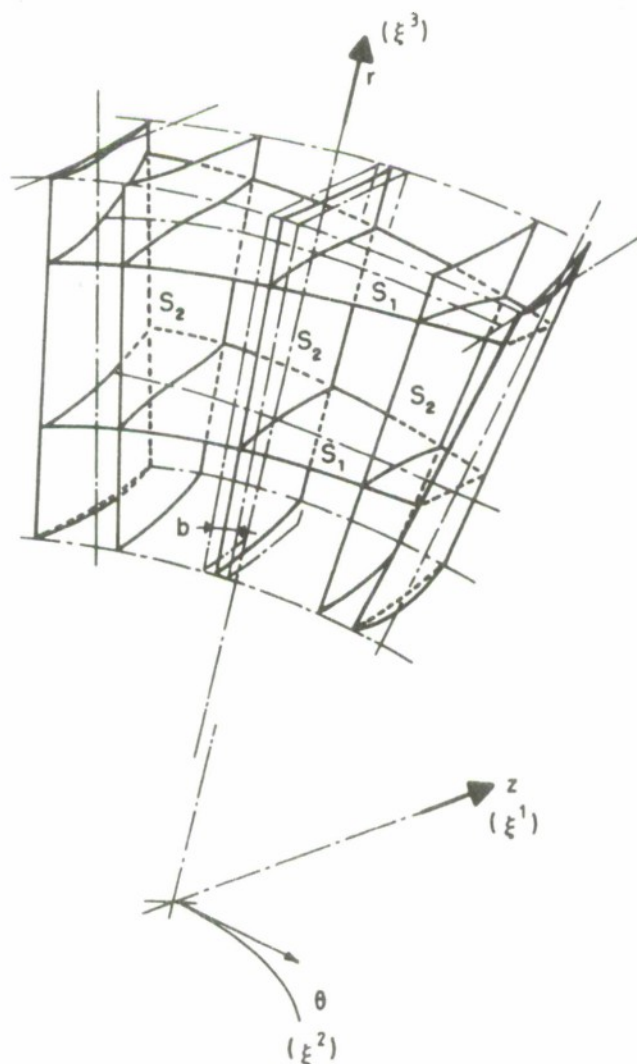


Figure 1.1.2. : Turbomachinery blade passage

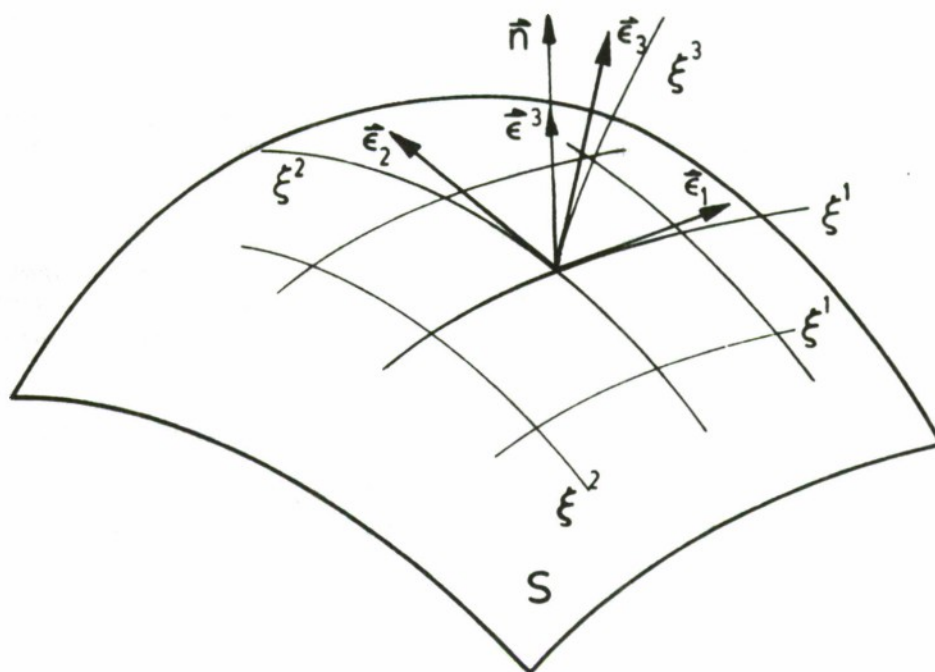


Figure 1.1.3. : S surface generated by ξ^1 and ξ^2 lines and defined by $\xi^3 = \text{constant}$.

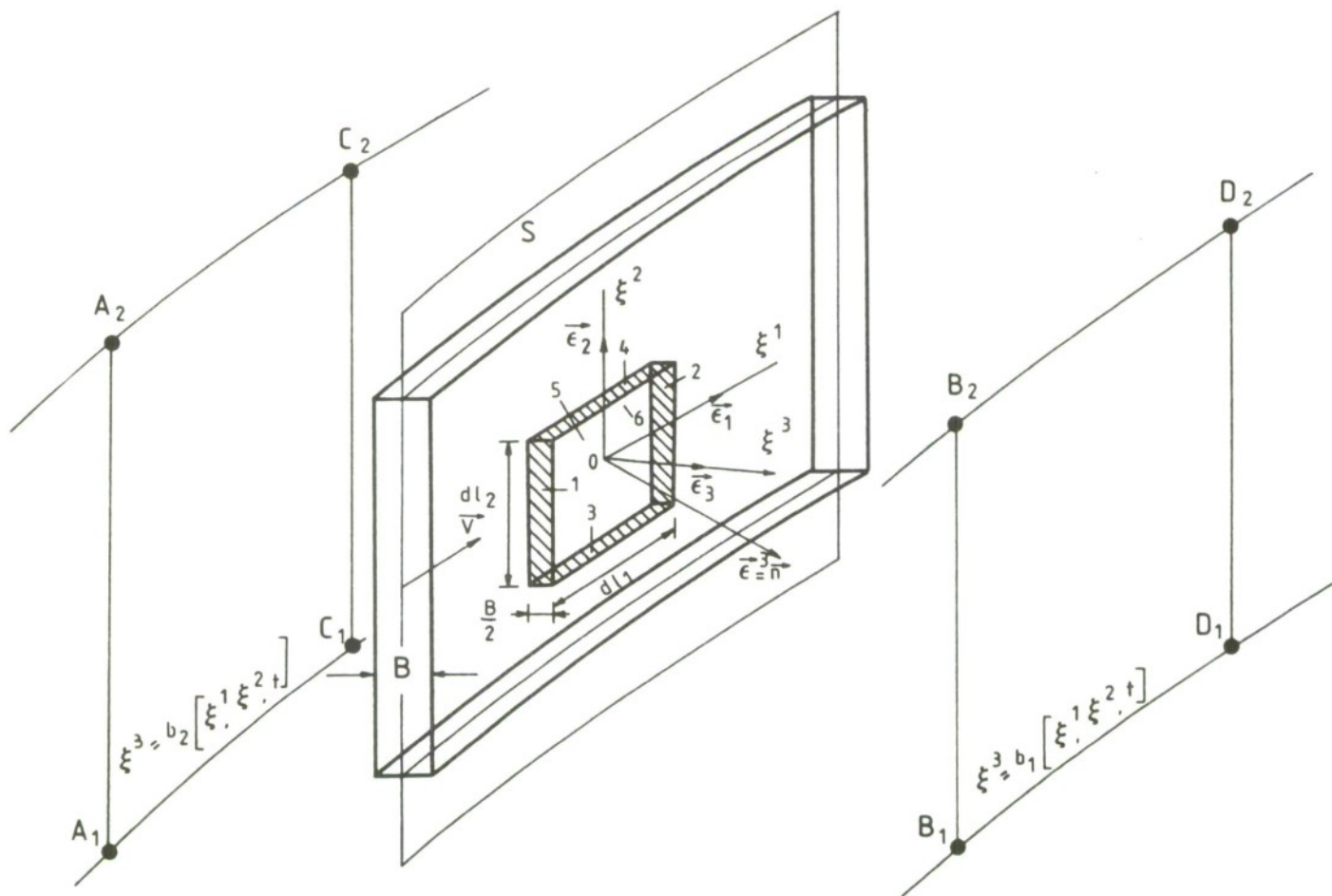


Figure 1.1.4. : Elementary volume of a streamsheet of thickness B .

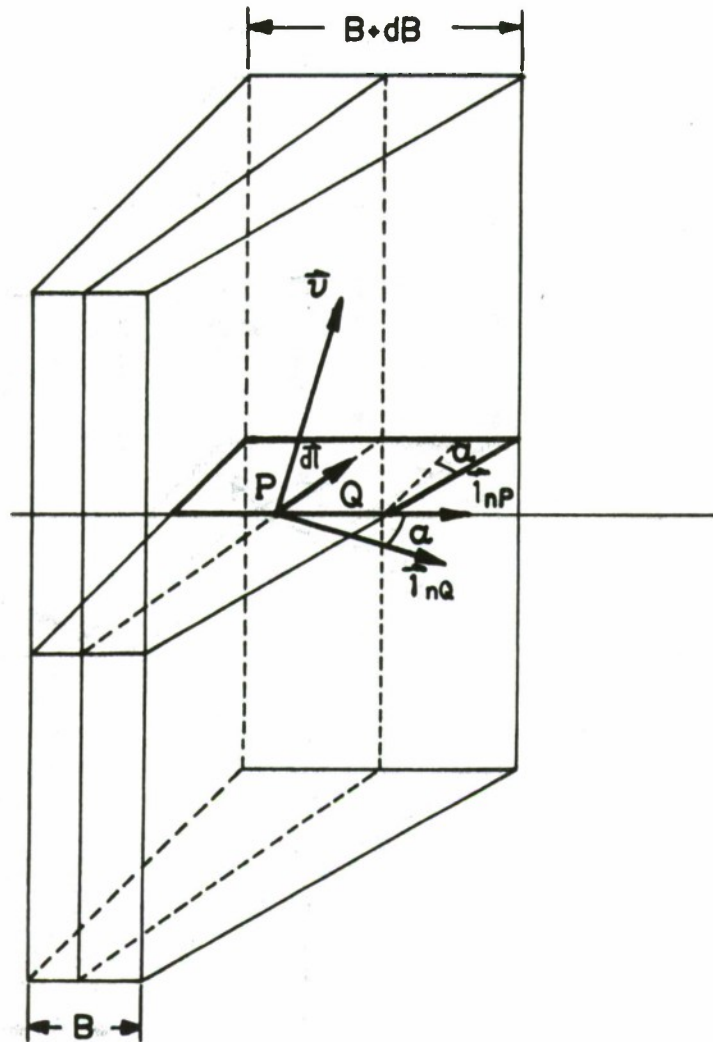


Figure 1.1.5. : Divergence of streamsheet and relation to thickness variation

PART 2 : THE COMPUTATION OF TURBOMACHINERY FLOWS

The second part of this report is devoted to a presentation of some of the computational models and techniques used in the prediction and analysis of multistage turbomachinery flows.

Turbomachinery internal flows constitute one of the most complex flow patterns in the field of technology. The detailed flow behaviour within a blade row is mostly strongly three-dimensional, viscous dominated, and often influenced by the presence of shock waves. Figure 2.I.1 is a sketch of the typical flow phenomena in a compressor blade passage, where the various contributions to the overall flow picture are illustrated. Due to the turning of the flow through the blade passages, an initial boundary layer along one of the end walls of a blade row will generate streamwise vorticity within the passage, through the secondary flow mechanism, and give rise to additional three dimensional effects which can become predominant (as in turbine blades with high turning angles), creating an interaction between the viscous regions and the three-dimensionality of the flow. Another aspect of these phenomena can be found in turbines, where the thick leading edges of modern turbine blade sections generate horse-shoe vortices in the inlet regions which influence strongly the internal passage flow. This is illustrated in figure 2.I.2, showing a visualization of these flow structures. In addition, the clearance space between blade rows and casing (or hub) walls generates leakage flows and local vorticity. Furthermore, in modern, high performance machines the flow reaches supersonic velocities with the consequence of the appearance of shock waves, shock boundary layer interactions and choking phenomena. Figure 2.I.3 represents a typical flow pattern in a two-dimensional tip section of a transonic compressor fan as determined experimentally and figure 2.I.4 shows a possible model for these complex processes.

Even in steady rotating machines, the wakes of an upstream blade row create an unsteady incident flow on the subsequent blades due to the relative motion between rotors and stators. This adds to the overall complexity of the flow, making it a formidable challenge for the developer of computational prediction tools.

The above figures represent typical flow patterns in single blade passages. In multistage configurations, figure 2.I.5, the accumulation of these effects can lead to severe deterioration of initially uniform velocity profiles over the height of the blades, even when circumferential averaged profiles are considered. Figure 2.I.6 illustrates some aspects of the flow migration as visualized by the stagnation pressure distribution in a multistage compressor. The isopressure lines show the distribution and concentration of losses in the exit plane of this blade row.

Notwithstanding these complexities, the design process requires the ability to predict, at least in some approximate way, the flow behaviour in a multistage machine in order to optimize the performance and to be able to localize the sources of dissipation and energy losses. In view of the complexity of the flow, the computation of a flow structure such as depicted in figure 2.I.1 requires high levels of approximation of

flow models, such as is the full Navier-Stokes equations with adequate turbulence models for the Reynolds averaged formulation. Methods able to predict aspects of the viscous three-dimensional nature of the blade row passage flow are appearing, and will be used at increased rates in the future. However, these computations, very instructive at the single passage level, will not be able to be used currently in initial design processes of a multistage machine, at least in the foreseeable future of computer resources. Therefore typical multistage, simplified models have been developed in order to single out an approximate view and prediction of the main aspects of the turbomachinery flow.

For instance, one of the aspects of the simplified models deals with the properties of the flow averaged over the blade spacing in the circumferential direction, that is in the direction of the blade rotation. This passage-averaged flow can be considered for a rotating blade row, as the flow seen by a fixed observer, attached to the stator blade rows, looking at the rotor flow. Referring to figure 2.1.1, if the flow is averaged at a given spanwise position over the blade spacing, the details of the internal three-dimensional flow configuration are lost, but instead, a two-dimensional flow distribution in function of mainstream and spanwise coordinates is obtained. Of course, the lost information will have to be supplied by some form of empirical input as will be discussed in the following. This passage-averaged flow actually removes the secondary and three-dimensional flow details as well as any flow distribution in the blade-to-blade direction. It represents therefore an axisymmetric approximation of the real flow and is called the meridional through-flow, or radial equilibrium flow. From this point of view, the alternative representation of the through-flow by the flow projection along one representative streamsurface of S2-type shown in figure 1.1.2, is an equivalent approximation and either the stream-surface approach discussed in section 1.1 or the averaged formulation of section 1.2 can be used. Hence, the flow description in rotating machines will rely on the quasi-three-dimensional spatial approximation described in Part 1. Indeed, if the through-flow is determined, it can be coupled to flow computations in the blade-to-blade surfaces, of the S1-type of figure 1.1.2, in order to reconstruct an approximate picture of the three-dimensional flow. A still further step consists in determining the through-flow along various S2-type of surfaces attempting in this way to reconstruct the secondary flow pattern in the blade passage. This last step can be considered for simple blade passages but is seldom performed in multistage configurations. A more frequent approach towards this goal consists in computing separately the secondary flow, see for instance Atkins and Smith (1983), based on inviscid secondary flow approximations as developed by Hawthorne (1955), Smith (1955), and many others. The interested reader will find an excellent and rigorous presentation of secondary flow theories in Horlock and Lakshminarayana (1971). In all these approaches the flow is decomposed in combinations of two-dimensional flow components which can be reconstructed in a quasi-three-dimensional way, but which are individually easier to solve.

Consistent with these views and with the loss of information attached to the axisymmetric or passage-averaged approximation, the details of the viscous effects and mechanisms are smeared out and the appropriate approximation which fits into this framework is the distributed loss model. In this model, the viscous stresses are replaced by an external,

distributed friction force which is responsible for the overall energy losses. The lost information with regard to the viscous shear stresses will have to be replaced by empirical informations defining the energy losses as expressed by the entropy production at the level of the through-flow computations. In a full quasi-three-dimensional computation this information might also be provided by two-dimensional blade-to-blade viscous flow calculations including estimations of the three-dimensional effects on the loss distributions.

The flow models for multistage turbomachines are therefore defined by the combination of the quasi-three-dimensional representation with the distributed loss model. Since the distributed loss model is essentially a non-viscous model, coupling with boundary layer computations can be added, in particular in the through-flow, where the interaction with the end wall boundary layers is an important aspect of the overall prediction schemes, Mellor and Wood (1971), Hirsch (1974), De Ruyck, Hirsch and Kool (1979), De Ruyck and Hirsch (1981), (1983).

Section 2.1 will summarize the system of equations used in the turbomachinery flow models namely the distributed loss model. The following sections will discuss and define the quasi-three-dimensional formulation and the two options, the streamsurface approach or the averaging technique will be developed in sections 2.2 and 2.3 respectively, and the differences and similitudes pointed out. Section 2.4 will describe the through-flow computational techniques. These include the widely used streamline curvature method as well as the methods based on the streamfunction formulation discretized by finite differences or by finite elements.

The interested reader may also find some general reviews of computational methods, aimed at turbomachinery flow applications, in Japikse (1976) and more recently in McNally and Sockol (1981).

2.1. THE DISTRIBUTED LOSS MODEL

The distributed loss model retains, from all the effects of heat conduction and viscous shear stresses, the contributions to the entropy production. That is, the dissipation or energy loss resulting from the frictional action of the shear stresses is considered as the dominating contribution. As a consequence, this action is expressed by a distributed friction force \vec{F}_f defined at

every point in the flow field. From a theoretical point of view, the friction force \vec{F}_f is equal to the gradient of the shear stresses,

$$\rho \vec{F}_f = \vec{\nabla} \cdot \vec{\tau} \quad (2.1.1)$$

and the contributions of heat conduction and of the work of the shear stresses to the overall energy balance are either separately neglected, or considered to cancel each other ,

$$\vec{\nabla} (k_T \vec{\nabla} T) + \vec{\nabla} (\vec{\tau} \cdot \vec{w}) \approx 0 \quad (2.1.2)$$

The contribution to the entropy production reduces to the work of the friction force as given by

$$T \frac{ds}{dt} = -\vec{w} \cdot \vec{F}_f \quad (2.1.3)$$

where \vec{F}_f is considered to be in the direction opposite to the relative velocity vector \vec{w} , and is defined by this relation instead of equation (2.1.1).

With

$$\vec{F}_f = -F_f \cdot \vec{i}_w \quad (2.1.4)$$

where \vec{i}_w is the unit vector in the direction of the velocity \vec{w} , equation (2.1.3) becomes

$$T \frac{ds}{dt} = w F_f \quad (2.1.5)$$

Hence, the entropy equation (2.1.5) is added to the system of flow equations as an independent equation and subsequently, one of the three components of the momentum equation is redundant and can be left out of the system.

With the neglect of heat conduction effects, of external forces \vec{f}_e and of external heat sources q_H , the system of flow equations within the distributed loss model will be defined in a relative reference system rotating with a constant angular velocity $\vec{\omega}$ around an axial direction. At a radius \vec{r} , the relative system has a rotation speed equal to $\vec{u} = \vec{\omega} \times \vec{r}$. The system of equations, defining the turbomachinery flows within this approximation level, is therefore

$$\frac{\partial \rho}{\partial t} + \vec{\nabla}(\rho \vec{w}) = 0 \quad (2.1.6)$$

$$\frac{\partial \vec{w}}{\partial t} - \vec{\omega} \times \vec{r} = T \vec{\nabla} s - \vec{\nabla} I + \vec{F}_f \quad (2.1.7)$$

$$\frac{\partial I}{\partial t} + (\vec{\omega} \cdot \vec{\nabla}) I = \frac{1}{\rho} \frac{\partial p}{\partial t} \quad (2.1.8)$$

$$\frac{\partial s}{\partial t} + (\vec{\omega} \cdot \vec{\nabla}) s = \frac{w}{T} \cdot F_f \quad (2.1.9)$$

The rothalpy I is defined as

$$I = h + \frac{\vec{w}^2}{2} - \frac{\vec{u}^2}{2} = H - \vec{u} \cdot \vec{v} \quad (2.1.10)$$

in function of the static enthalpy h or the stagnation enthalpy

$$H = h + \frac{\vec{v}^2}{2} \quad (2.1.11)$$

and $\vec{\zeta}$ is the vorticity of the absolute flow \vec{v} ,

$$\vec{\zeta} = \vec{\nabla} \times \vec{v} \quad (2.1.12)$$

Equation (2.1.7) is in Crocco's form and is most useful in the computation of turbomachinery flow because of the direct use of the energy equation (2.1.8) and of the entropy equation (2.1.9). However the standard form of the momentum equation can also be applied and an alternative form of the above system is provided by the equations in conservation form.

$$\frac{\partial \rho}{\partial t} + \vec{\nabla}(\rho \vec{w}) = 0 \quad (2.1.13)$$

$$\frac{\partial}{\partial t} (\rho \vec{w}) + \vec{\nabla}(\rho \vec{w} \otimes \vec{w}) = -\vec{\nabla} p - 2\rho(\vec{\omega} \times \vec{w}) - \rho \vec{\omega} \times (\vec{\omega} \times \vec{r}) + \rho \vec{F}_f \quad (2.1.14)$$

$$\frac{\partial}{\partial t} (\rho I) + \vec{\nabla}(\rho \vec{w} I) = \frac{\partial p}{\partial t} \quad (2.1.15)$$

$$\frac{\partial}{\partial t} (\rho s) + \vec{\nabla}(\rho \vec{w} s) = \frac{w}{T} \rho F_f \quad (2.1.16)$$

The fluid constitutive equation has to be added to the above system and in the following, the perfect gas model will be considered as representing with sufficient accuracy the fluid state. This is a good approximation for gases and can be used also for steam, at least for dry steam. For saturated steam the steam tables have to be used, but one can still in this case refer to the perfect gas model approximation, at least locally.

Hence, with the perfect gas law $p/\rho = rT$ the entropy variations are connected to the variations of stagnation pressure p_0 and stagnation temperature T_0 .

$$ds = c_p \frac{dT_0}{T_0} - r \frac{dp_0}{p_0} \quad (2.1.17)$$

Note that all equations are written here in the relative system, that is for a rotor flow. The stator flows are obtained by setting $\vec{u}=0$, and from the velocity composition law,

$$\vec{v} = \vec{w} + \vec{u} \quad (2.1.18)$$

\vec{w} is to be replaced by the absolute velocity \vec{v} .

Equation (2.1.7) shows that the multistage turbomachinery flow models can be considered as basically inviscid, as they do not contain explicitly shear stress gradients and \vec{F}_f is considered as an external friction force defined by equations (2.1.4) and (2.1.17) when information is provided with regard to the stagnation pressure losses. In addition, the momentum equation (2.1.7) also shows that the general flow pattern will be rotational due to the gradients of entropy, the gradients of total energy, or rothalpy I , and due to the presence of the distributed friction force \vec{F}_f .

Incompressible flows

For hydraulic turbomachines such as pumps and hydraulic turbines, the incompressible fluid approximation is best adapted. In this case, the system of turbomachinery flow equations simplifies, with $\rho = \text{constant}$, to

$$\vec{\nabla} \cdot \vec{w} = 0 \quad (2.1.19)$$

$$\frac{\partial \vec{w}}{\partial t} - \vec{w} \times \vec{\zeta} = \frac{-1}{\rho} \vec{\nabla} p^* + \vec{F}_f \quad (2.1.20)$$

$$\frac{\partial}{\partial t} \frac{\vec{w}^2}{2} + \frac{1}{\rho} (\vec{w} \cdot \vec{\nabla}) p^* = -w F_f \quad (2.1.21)$$

where p^* is the rotary stagnation pressure defined by

$$p^* = p + \rho \frac{\vec{w}^2}{2} - \rho \frac{u^2}{2} \quad (2.1.22)$$

Note that (2.1.21) is obtained from (2.1.20) by scalar multiplication with the relative velocity \vec{w} and is therefore not an independent equation. This equation replaces the entropy equation (2.1.9). Actually, equation (2.1.21) is used to compute the friction force F_f through the knowledge of the rotary stagnation pressure loss coefficients which have to be provided to the calculation procedure.

Compared to the compressible system of equations, $(-p^*)$ plays the role of the entropy since p^* decreases in the downstream direction as can be seen from equation (2.1.21) in steady state flows.

Steady Flow Assumption

It is also customary, in the field of turbomachinery, to assume that the relative flow is steady for constant rotation speed of the machine. This will be the case if the inlet flow is uniform in the tangential direction, which implies that the effects of the wake of upstream blade rows are neglected. Indeed one has the following relation between the local time-dependency in the relative and absolute systems

$$\left. \frac{\partial q}{\partial t} \right|_A = \left. \frac{\partial q}{\partial t} \right|_R - \omega \frac{\partial q}{\partial \theta} \quad (2.1.23)$$

when θ represents the angular coordinate in the wheel speed direction and A and R denote absolute and relative systems respectively. Therefore, if the absolute outlet flow from a preceding stator is steady, the flow relative to the rotor will be steady if the stator outlet flow is uniform in the tangential direction. This will generally not be the case, due to the presence of wakes and other three-dimensional effects, and hence the physical flow always contains unsteady components. A recent detailed experimental investigation performed by Dring et al. (1982) clearly shows the importance of the unsteady flow and pressure variations, although the time average flow was observed to be in good agreement with the steady state predictions. Another source of unsteadiness is due to the inviscid upstream propagation of pressure waves from a moving rotor to an upstream located stator. This effect, of subsonic nature, can be locally important on the loading of the stator trailing edge or on the heat transfer coefficients and exists even for uniform tangential flows. Therefore, the detailed interaction between two consecutive blade rows is always

unsteady. However, if one neglects this interaction or if time averaged flows are considered, the steady state assumption becomes a valuable approximation.

In this case, the distributed loss model simplifies to

$$\vec{\nabla}(\rho \vec{w}) = 0 \quad (2.1.24)$$

$$-\vec{\omega} \times \vec{\zeta} = T \vec{\nabla} s - \vec{\nabla} I + \vec{F}_f \quad (2.1.25)$$

$$(\vec{\omega} \cdot \vec{\nabla}) I = 0 \quad (2.1.26)$$

$$(\vec{\omega} \cdot \vec{\nabla}) s = \frac{\omega}{T} F_f \quad (2.1.27)$$

for a compressible fluid.

In particular the energy equation takes the simple form of constancy of the rothalpy I along a streamline.

This is nothing else than the Euler equation for the energy exchange in a rotating blade row. If subscripts 1 and 2 denote respectively the inlet and outlet planes of a rotor then from $I = \text{constant}$ one has indeed,

$$\Delta H = H_2 - H_1 = (uv_u)_2 - (uv_u)_1 = \Delta(uv_u) \quad (2.1.28)$$

where v_u is the projection of the absolute velocity \vec{v} on the direction of the rotor velocity $\vec{u} = \vec{\omega} \times \vec{r}$.

As is well known, the stagnation enthalpy variation ΔH is the power per unit of mass flow exchanged between the fluid and the rotor blades. This most widely applied equation, which allows the determination of the power and of efficiencies, from the knowledge of the flow velocity components, is therefore only strictly valid for steady relative flows. The complete energy equation in the relative system, contains also the effects of heat conduction and of viscous energy exchange between streamtubes described by the two terms of equation (2.1.2).

Hence, it is essential to keep in mind that the Euler equation for turbomachinery rotors is an approximation, valid for steady, inviscid behavior. The viscous interactions and unsteadiness which are always present to some degree in turbomachinery flows, introduce variations in rothalpy along flow paths. This is of importance when assessing the results of computations based on the simplified flow model described here. It is known from experimental observations and from comparisons with fully viscous computations, Moore and Moore (1980), that the overall incidence of these effects can reach a few percent on global energy exchange estimations, but might still be more important locally in regions of high viscous effects, for instance in end wall-blade corners and tip regions. For an incompressible flow, one obtains similarly the steady flow model defined by the equations

$$\vec{\nabla} \cdot \vec{w} = 0 \quad (2.1.29)$$

$$-\vec{w} \times \vec{\zeta} = -\frac{1}{\rho} \vec{\nabla} p^* + \vec{F}_f \quad (2.1.30)$$

$$(\vec{w} \cdot \vec{\nabla}) p^* / \rho = -w F_f \quad (2.1.31)$$

2.2. QUASI-THREE-DIMENSIONAL APPROXIMATION FOR TURBOMACHINERY FLOWS : THE STREAMSURFACE MODEL

According to the considerations developed in chapter 3, two ways are open in order to introduce a quasi-three dimensional approximation of the turbomachinery flows.

Either one can follow the flow along families of streamsurfaces, defined by the positions occupied by the fluid particles lying initially on a given line in the inlet section of flow passage, or one can consider the averaged flow over a selected direction and calculate this averaged flow in function of the remaining (two dimensional) variables.

Both methods will be developed here, since they form two equivalent formulations for through-flow and quasi-three-dimensional computations. The first approach, introduced by Wu (1952), has been applied by a large number of authors, among which Katsanis (1964), (1966), Novak (1967), March (1968), Frost (1970), Adler and Krimerman (1974), Biniaris (1975), Novak and Hearsey (1977), Bosman and El-Shaarawi (1977). A more complete list of references, including program development descriptions which have been published outside the journal literature can be found in the review article by G. Serovy in the AGARD report, edited by Hirsch and Denton (1981). The second approach is applied essentially by Smith (1966), Hirsch and Warzee (1976), (1979), Jennions and Stow (1984).

Two families of surfaces are generally considered of the form illustrated in figure 1.1.2. The S1 family is of the blade-to-blade type and can be considered as generated by the particles situated initially on a line at a constant radius r . The S2 family is generated by particles located initially on a radial line and is designated as a hub-to-shroud surfaces. Due to the axisymmetry of the geometry the cylindrical coordinate system is most appropriate as reference system with the z -axis aligned with the axis of the machine and the angular coordinate θ defining the direction of the blade rotation. In the following, the blade rotation direction will be selected as the positive θ -direction and this will also serve as the positive direction for the blade and flow angles.

The general form of the streamsurface equations have been derived earlier and are summarized in Table 1. For a streamsheet thickness B , the conservation equations obtained by following the flow along the considered streamsurface can be written in a two-dimensional space defined by this surface.

In accordance with the distributed loss model, heat conduction and shear stresses are neglected, but a friction force \vec{F}_f is added to the external forces. In addition, we consider the flow relative to a rotating frame of reference. As a consequence, centrifugal and Coriolis forces have to be considered in the streamsurface momentum equations and the stagnation enthalpy H is replaced by the rothalpy I in the energy equation.

This leads to the following system of equations valid on a two-dimensional streamsurface. Overbars on the gradient operator indicate that the derivatives are defined by following the surface of

normal \vec{n} .

For a streamsurface S defined by $\xi^3 = \xi^3(\xi^1, \xi^2)$ in a ξ^α -coordinate system, the derivatives along the surface, indicated by an overbar, are given by, with ∂_α representing $\partial/\partial\xi^\alpha$

$$\vec{\nabla}_g = \vec{\nabla} - \vec{n} \partial_{,g} \quad (2.2.1)$$

and we refer to Part 1 for a detailed analysis. The normal \vec{n} is defined by its components n_α with

$$n_\alpha = \left(-\frac{\partial \xi^3}{\partial \xi^1}, -\frac{\partial \xi^3}{\partial \xi^2}, 1 \right) \quad \alpha=1,2,3 \quad (2.2.2)$$

Written in the relative system one obtains the streamsurface formulation of equations (2.1.13) to (2.1.16), see Part 1 for a full derivation and Table 1 for a summary.

Continuity equation

$$\frac{\partial}{\partial t} (\rho B) + \vec{\nabla} \cdot (\rho \vec{w} B) = 0 \quad (2.2.3)$$

Momentum equation

$$\frac{\partial}{\partial t} (\rho B \vec{w}) + \vec{\nabla} \cdot [(\rho \vec{w} \vec{w} + p) B] = [(\vec{F}_f + \vec{f} - 2\vec{\omega} \times \vec{w} - \vec{\omega} \times (\vec{\omega} \times \vec{r}))] \rho B \quad (2.2.4)$$

or

$$\frac{\partial}{\partial t} \vec{w} - \vec{w} \times \vec{\zeta} = T \vec{\nabla} s - \vec{\nabla} I + \vec{F}_f + \vec{f}_B \quad (2.2.5)$$

Energy equation

$$\frac{\partial}{\partial t} (\rho B I) + \vec{\nabla} \cdot (\rho B \vec{w} I) = \frac{\partial (p B)}{\partial t} \quad (2.2.6)$$

Entropy equation

$$\frac{\partial}{\partial t} (\rho B s) + \vec{\nabla} \cdot (\rho B \vec{w} s) = \frac{W}{T} \rho B F_f \quad (2.2.7)$$

The additional body force \vec{f} is defined by equation (1.1.55)

$$\rho \vec{f}_B = -\vec{n} \cdot \partial_3 p \quad (2.2.8a)$$

if the metric coefficients do not depend on ξ^3 , see equations (1.1.57), and

$$\rho \vec{f} = \rho \vec{f}_B + p \frac{\vec{\nabla} B}{B} \quad (2.2.8b)$$

The streamsheet thickness B is related to the three-dimensional flow behavior by equation (1.1.35) or equation (1.1.40) for $b=B/h_3$, where h_3 is the metric coefficient corresponding to ξ^3 in the curvilinear, orthogonal system ξ^α .

$$\frac{\vec{\nabla} B}{B} = -\partial_3 \vec{n} \quad (2.2.9)$$

$$\frac{1}{b} (\vec{w} \cdot \vec{\nabla}) b = + n_\alpha \cdot \partial_3 w^\alpha = -w^\alpha \cdot \partial_3 n_\alpha \quad (2.2.10)$$

where the summation convention on the repeated index α is assumed.

Note that the absolute vorticity $\vec{\zeta}$ is defined by

$$\vec{\zeta} = \vec{\nabla} \times \vec{v} \quad (2.2.11)$$

The hub-to-shroud equations on the S2 surface are obtained by applying the above equations for surfaces $\xi^3 = \theta = \theta(r,z)$, while the S1 blade-to-blade flow equations will be obtained by setting for instance $\xi^3 = r = r(\theta,z)$.

2.2.1. Equations for Hub-to-Shroud S2 Surfaces - Through-Flow Equations

In the selected cylindrical coordinate system $\theta = \theta(r,z)$, the absolute velocity vector \vec{v} and the relative velocity \vec{w} are defined by their projections along the radial, axial and circumferential (or tangential) directions,

$$\begin{aligned} \vec{v} &= v_r \vec{1}_r + v_z \vec{1}_z + v_\theta \vec{1}_\theta \\ \vec{u} &= \vec{w} \times \vec{r} = \omega r \vec{1}_\theta \end{aligned} \quad (2.2.12)$$

Hence, the relative velocity components are given by

$$\begin{aligned} v_r &= v_r \\ w_z &= v_z \\ w_\theta &= v_\theta + \omega r \end{aligned} \quad (2.2.13)$$

The components of the normal \vec{n} to the streamsurface $\theta = \theta(r, z)$ are defined in the natural coordinate system $\vec{\epsilon}^\alpha$, that is $(\vec{i}_r, \vec{i}_z, \frac{1}{r} \vec{i}_\theta)$, see example E.1.4, by

$$\begin{aligned} n_\theta &= 1 \\ n_z &= -\frac{\partial \theta}{\partial z} \\ n_r &= -\frac{\partial \theta}{\partial r} \end{aligned} \quad (2.2.14)$$

and the streamsurface derivatives are

$$\begin{aligned} \overline{\frac{\partial}{\partial r}} &= \frac{\partial}{\partial r} - n_r \cdot \frac{\partial}{\partial \theta} = \frac{\partial}{\partial r} + \left(\frac{\partial \theta}{\partial r}\right) \cdot \frac{\partial}{\partial \theta} \\ \overline{\frac{\partial}{\partial z}} &= \frac{\partial}{\partial z} - n_z \cdot \frac{\partial}{\partial \theta} = \frac{\partial}{\partial z} + \left(\frac{\partial \theta}{\partial z}\right) \cdot \frac{\partial}{\partial \theta} \end{aligned} \quad (2.2.15)$$

Geometrical Definition of S2-Surfaces (Hub-to-Shroud surfaces)

It is common practice to define the surface S2 by angles β' and ϵ' . The intersection of S2 with the (r, θ) or $z = \text{constant}$ plane, makes an angle ϵ' with the local radial direction and the intersection of the surface with a cylindrical, $r = \text{constant}$ surface, is at an angle β' with the axial direction, figure 2.2.1.

These angles are related to the components of the normal vector \vec{n} , since they define uniquely the local orientation of the streamsurface. They are defined by, referring to figure 2.2.1,

$$r \frac{\partial \theta}{\partial r} = \tan \epsilon' = -r n_r \quad (2.2.16)$$

$$r \frac{\partial \theta}{\partial z} = \tan \beta' = -r n_z \quad (2.2.17)$$

and the \vec{n} vector is obtained, following equation (2.2.14), as

$$\vec{n} = -\frac{1}{r} \tan \epsilon' \cdot \vec{i}_r - \frac{1}{r} \tan \beta' \cdot \vec{i}_z + \frac{1}{r} \vec{i}_\theta = \frac{1}{r} \vec{n} \quad (2.2.18)$$

We will assume in the following that the S2 surface is time independent. The condition for this surface to be a streamsurface is

$$\vec{n} \cdot \vec{w} = 0 \quad (2.2.19)$$

With equations (2.2.16) and (2.2.17), the relation between the velocity components valid on S2, is obtained

$$w_{\theta} = w_z \tan \beta' + w_r \tan \epsilon' \quad (2.2.20)$$

If an axial flow angle $\hat{\beta}$ is introduced on a cylindrical surface of constant radius r , figure 2.2.2, by

$$\tan \hat{\beta} = w_{\theta} / w_z \quad (2.2.21)$$

and a meridional angle σ in the meridional plane (r - z) by

$$\tan \sigma = w_r / w_z \quad (2.2.22)$$

one obtains the relation

$$\tan \hat{\beta} = \tan \beta' + \tan \sigma \cdot \tan \epsilon' \quad (2.2.23)$$

Generally, a flow angle β is defined with respect to the meridional velocity component w_m , making an angle σ with the axial direction,

$$w_m = \sqrt{w_r^2 + w_z^2} \quad (2.2.24)$$

$$\tan \beta = \frac{w_{\theta}}{w_m} \quad (2.2.25)$$

Between β and $\hat{\beta}$ one has the relation

$$\tan \beta = \tan \hat{\beta} \cdot \cos \sigma \quad (2.2.26)$$

and from equation (2.2.11)

$$\tan \beta = \cos \sigma \cdot \tan \beta' + \sin \sigma \cdot \tan \epsilon' \quad (2.2.27)$$

Since \vec{w} is in the surface S2, this relation can also be interpreted as defining the angle β of the intersection of the S2 surface with a conical surface forming an angle σ with the axial direction.

Blockage coefficients, friction and body forces

The dimensionless streamtube thickness b , also called the tangential blockage factor, is related to the circumferential velocity variations of the flow by equation (2.2.10), with $b = B/r$. In order to distinguish between the two families of surfaces, S_2 and S_1 , we will indicate the thickness of the S_2 streamsheet by a subscript 2. Hence we have here $b_2 = B_2/r$ and equation (2.2.10) becomes

$$\begin{aligned} \frac{1}{b_2} \frac{db_2}{dt} &= \frac{1}{r} (-\tan \beta' \cdot \frac{\partial w_z}{\partial \theta} - \tan \epsilon' \cdot \frac{\partial w_r}{\partial \theta} + \frac{\partial w_\theta}{\partial \theta}) \\ &= \frac{1}{b_2} (w_r \frac{\partial b_2}{\partial r} + w_z \frac{\partial b_2}{\partial z}) \end{aligned} \quad (2.2.28)$$

With the knowledge of the normal vector to the streamsurface and the vector relation (2.2.9), one has here

$$\frac{\vec{\nabla} B_2}{B_2} = - \frac{\partial \vec{n}}{\partial \theta} = - \frac{1}{r} \frac{\partial \vec{n}}{\partial \theta} \quad (2.2.29)$$

For an axisymmetric flow, the tangential blockage factor b_2 will be constant. But inside blade rows, the blade-to-blade flow creates a tangential variation of the flow field and hence variations of b_2 . As shown by Novak and Hearsey (1977), the streamwise variations of the tangential blockage factor can be quite strong in particular in the vicinity of the leading edge region of the blades. In absence of any other information, the blockage factor b_2 may be approximated by the tangential spacing variation between two adjacent blades. A better approximation can be obtained from the knowledge of the flow in the θ -direction, that is from the flow along the S_1 -blade-to-blade surfaces. In this case b_2 can be represented by the distance between two adjacent streamlines.

The body force \vec{f}_B , appearing in the streamsurface momentum equation, and defined by equation (2.2.8) is given here by

$$\vec{f}_B = \frac{-\vec{n}}{\rho} \frac{\partial p}{\partial \theta} = - \frac{\vec{n}}{\rho} \frac{1}{r} \frac{\partial p}{\partial \theta} \quad (2.2.30)$$

This force, which results from the confinement of the flow description to a two-dimensional surface, is directed along the normal, and hence is orthogonal to the local velocity vector following equation (2.2.19),

$$\vec{f}_B \cdot \vec{w} = 0 \quad (2.2.31)$$

This relation actually allows the determination of two force components f_{Br} and f_{Bz} in function of the third one $f_{B\theta}$. One has from equation (2.2.18)

$$f_{Br}/f_{B\theta} = -\tan \epsilon' = n_r/n_\theta \quad (2.2.32a)$$

$$f_{Bz}/f_{B\theta} = -\tan \beta' = n_z/n_\theta \quad (2.2.32b)$$

$$f_{B\theta} = \frac{-1}{\rho r} \frac{\partial p}{\partial \theta} \quad (2.2.33)$$

The direction of the friction force \vec{F}_f is defined by equation (2.1.4) as being opposed to the relative velocity vector \vec{w} . Hence, two components of \vec{F}_f are determined by the flow angles in function of the third one, or alternatively in function of the magnitude of \vec{F}_f ,

$$F_{f\theta} = -F_f \cdot \frac{w_\theta}{w} \quad (2.2.34a)$$

$$F_{fr} = -F_f \frac{w_r}{w} \quad (2.2.34b)$$

$$F_{fz} = -F_f \frac{w_z}{w} \quad (2.2.34c)$$

Through-Flow Equations in Cylindrical and Axisymmetric Coordinates

Finally, the through-flow equations take the following form within the streamsurface approach in cylindrical coordinates when Crocco's form, equation (2.2.5) is selected for the momentum equation, see Problem 2.2.1.

$$\frac{\partial}{\partial t} (\rho b_2 r) + \frac{\partial}{\partial r} (\rho b_2 r w_r) + \frac{\partial}{\partial z} (\rho b_2 r w_z) = 0 \quad (2.2.35)$$

$$\frac{\partial}{\partial t} w_r - w_z \left(\frac{\partial}{\partial r} w_z - \frac{\partial}{\partial z} w_r \right) - \frac{w_\theta}{r} \frac{\partial}{\partial r} (r v_\theta) = T \frac{\partial s}{\partial r} - \frac{\partial I}{\partial r} + F_{fr} + f_{Br} \quad (2.2.36)$$

$$\frac{\partial}{\partial t} w_z + w_r \left(\frac{\partial}{\partial r} w_z - \frac{\partial}{\partial z} w_r \right) - \frac{w_\theta}{r} \frac{\partial}{\partial z} (r v_\theta) = T \frac{\partial s}{\partial z} - \frac{\partial I}{\partial z} + F_{fz} + f_{Bz} \quad (2.2.37)$$

$$\frac{\partial}{\partial t} w_\theta + \frac{1}{r} \frac{\partial}{\partial m} (rv_\theta) = F_{f\theta} + f_{B\theta} \quad (2.2.38)$$

$$\frac{\partial}{\partial t} s + w_m \frac{\partial s}{\partial m} = \frac{w}{T} F_f \quad (2.2.39)$$

$$\frac{\partial}{\partial t} I + w_m \frac{\partial I}{\partial m} = \frac{1}{\rho} \frac{\partial}{\partial t} p \quad (2.2.40)$$

The operator $\vec{w} \cdot \vec{\nabla}$ is defined here by

$$\vec{w} \cdot \vec{\nabla} = w_m \frac{\partial}{\partial m} = w_r \frac{\partial}{\partial r} + w_z \frac{\partial}{\partial z} \quad (2.2.41)$$

where m indicates the distance along the meridional streamline, see figure 2.2.3.

Another interesting coordinate system is provided by the axisymmetric (θ, m, n) system. With the assumption that the coordinate m is a meridional streamline, that is obtained by the projection of the velocity on a meridional plane, figure 2.2.3., then $w_n = v_n = 0$ everywhere. This leads to the following system of streamsurface equations

$$\frac{\partial}{\partial t} w_m - \frac{w_\theta}{r} \frac{\partial}{\partial m} (rv_\theta) = T \frac{\partial s}{\partial m} - \frac{\partial I}{\partial m} + F_{fm} + f_{Bm} \quad (2.2.42)$$

$$- \left[\frac{w_\theta}{r} \frac{\partial}{\partial n} (rv_\theta) + w_m \frac{\partial w_m}{\partial n} + \frac{w_m^2}{R_m} \right] = T \frac{\partial s}{\partial n} - \frac{\partial I}{\partial n} + f_{Bn} \quad (2.2.43)$$

$$\frac{\partial}{\partial t} w_\theta + \frac{w_m}{r} \frac{\partial}{\partial m} (rv_\theta) = F_{f\theta} + f_{B\theta} \quad (2.2.44)$$

The projection of \vec{F}_f along the direction n is zero since \vec{F}_f is directed opposite to \vec{w} , equation (2.1.4). The radius of curvature $1/R_m$ is connected to the angle σ by

$$\frac{\partial \sigma}{\partial m} = -1/R_m \quad (2.2.45)$$

The continuity equation becomes,

$$\frac{\partial}{\partial t} (\rho b_2 r h_2) + \frac{\partial}{\partial m} (\rho r w_m b_2 h_2) = 0 \quad (2.2.46)$$

or, for a steady flow

$$\rho w_m b_2 h_2 = \text{constant along the meridional streamline } m \quad (2.2.47)$$

Equation (2.2.47) expresses the conservation of mass in a streamtube around the meridional streamline m , see figure 2.3.1. Indeed, h_2 (h_2 being the metric coefficient associated to the n -coordinate) is proportional to the thickness of the streamtube centered on m . Calling this meridional streamtube thickness B_1 , measured perpendicularly to the m -line, one has from equation (2.2.47)

$$\rho w_m b_2 r B_1 = \text{constant} \quad (2.2.48)$$

Note that $B_2 = b_2 r$ is the thickness of the S2 streamsheet, while B_1 can be considered as the thickness of the S1 streamsheet.

As mentioned earlier, it is fully consistent with the already assumed approximations to consider that, for steady inlet flow conditions to the machine and steady rotations, the relative flow remains steady. In this case, the set of streamsurface-S2-equations simplify to the following form, in cylindrical coordinates

$$\frac{\partial}{\partial r} (\rho r b_2 w_r) + \frac{\partial}{\partial z} (\rho r b_2 w_z) = 0 \quad (2.2.49)$$

$$-w_z \left(\frac{\partial}{\partial r} w_z - \frac{\partial}{\partial z} w_r \right) = T \frac{\partial s}{\partial r} - \frac{\partial I}{\partial r} + \frac{w_\theta}{r} \frac{\partial}{\partial z} (r v_\theta) + F_{fr} + f_{Br} \quad (2.2.50)$$

$$w_r \left(\frac{\partial}{\partial r} w_z - \frac{\partial}{\partial z} w_r \right) = T \frac{\partial s}{\partial z} - \frac{\partial I}{\partial z} + \frac{w_\theta}{r} \frac{\partial}{\partial z} (r v_\theta) + F_{fz} + f_{Bz} \quad (2.2.51)$$

$$\frac{1}{r} w_m \frac{\partial}{\partial m} (r v_\theta) = F_{f\theta} + f_{B\theta} \quad (2.2.52)$$

$$w_m \frac{\partial s}{\partial m} = \frac{w}{T} F_f \quad (2.2.53)$$

$$w_m \frac{\partial}{\partial m} I = 0 \quad (2.2.54)$$

Note that one of the above equations is not independent from the others.

The last equation (2.2.54) states that the total energy or rothalpy I is constant along a meridional projection of the streamline along the S2-surface. This implies, the following relations :

$$I = H - u v_\theta = \text{constant along } m, \text{ for a rotating blade row, or} \quad (2.2.55)$$

$H = \text{constant along the meridional streamline in a non-rotating system}$

Equation (2.2.52) defines the meridional variations of the angular momentum (rv_θ) as determined by the component of the friction force and the body force. In practical computations, equation (2.2.53) determines the magnitude of the friction force F_f , while $f_{B\theta}$ will be deduced from equation (2.2.52) when the necessary information is provided for the variations of rv_θ as will be discussed in the next section. The entropy variations are obtained from the total pressure loss coefficients as discussed next.

The remaining equations (2.2.50) and (2.2.51) form a system for the velocity components w_r, w_z . Since the entropy equation has been used explicitly, the two momentum equations are not independent and one of them can be applied, while the other is discarded.

The radial component of the momentum equation (2.2.50) is known in the turbomachinery literature as the radial equilibrium equation.

2.2.2. Principles of Through-Flow Computations

Three sets of external information have to be provided to the system of equations (2.2.49) to (2.2.54), expressing the missing information with regard to viscous effects (\vec{F}_f) as well as to the properties of the flow in the omitted direction, that is the θ or tangential direction (b_2, rv_θ).

i) The tangential blockage or streamsheet thickness b_2

This information has to be defined by the flow along the other family of surfaces, namely the S1 or blade-to-blade surfaces according to equation (2.2.28). In absence of this information, the following approximation is usually applied

$$b_2 = \frac{\text{geometrical width of channel}}{\text{inlet width of channel}}$$

whereby b_2 is made flow independent. For the S2-surface this implies

$$b_2 = 1 - \frac{d}{s} \quad (2.2.56)$$

where d is the blade thickness in the tangential direction and s the blade spacing or pitch, see figure 2.3.1. In duct regions, outside blade rows, b_2 can be taken equal to 1.

ii) The angular momentum rv_θ

Since equations (2.2.50), or (2.2.51), solve for the velocity components in the meridional plane w_r and w_z , the tangential

row. From the knowledge of the loss coefficient $\bar{\omega}$, one obtains the entropy variation

$$\frac{s - s_A}{r} = -\ln\left(1 - \bar{\omega} \frac{p_d}{p_o^{(is)'}}\right) \quad (2.2.66)$$

from which the friction force F_f can be defined.

The determination of the stagnation pressure losses are strictly outside the present level of approximation and have to be provided by external sources such as empirical informations. Note however, that within the blade-to-blade flow computations, viscous calculations could be performed, for instance with boundary layer methods in order to estimate the losses occurring along the blade sections. These two-dimensional profile losses form only a part of the total loss and they would have to be supplemented by additional contributions from full three-dimensional effects such as, for instance, the secondary and tip leakage losses.

Therefore, as with the flow angles, reference is made to empirical correlations relating loss coefficients to a limited number of geometrical and flow parameters considered to have a dominating influence. These loss correlations complete the missing information of the S2-surface flow as defined by the equations (2.2.49) to (2.2.54) above. A large body of literature is available in this field and a recent overview of the problem and limitations of loss and turning correlations can be found in Hirsch and Denton (1981).

iv) The calculation of the density

The density is computed from the knowledge of the flow velocities and the local stagnation conditions, for instance from equation (2.1.29), with

$$H'_O = C_p T'_O = I + \frac{\vec{u}^2}{2} = h + \frac{\vec{w}^2}{2} \quad (2.2.67)$$

$$\frac{\rho}{\rho'_O} = \left(1 - \frac{\vec{w}^2}{2 H'_O}\right)^{1/(\gamma-1)} = \left(1 - \frac{w_m^2 + w_\theta^2}{2 H'_O}\right)^{1/(\gamma-1)} \quad (2.2.68)$$

With the relation

$$\frac{\rho}{\rho_A} = \left(\frac{h}{h_A}\right)^{1/(\gamma-1)} e^{-(s-s_A)/r} \quad (2.2.69)$$

one can relate the local density to stagnation values at another point A on the same streamline.

$$\frac{\rho}{\rho'_{OA}} = \left(\frac{h}{H'_{OA}}\right)^{1/(\gamma-1)} e^{-(s-s_A)/r} \quad (2.2.70)$$

$$= \left(1 - \frac{\vec{w}^2 + \vec{u}_A^2 - \vec{u}^2}{2 H'_{OA}}\right)^{1/(\gamma-1)} e^{-(s-s_A)/r}$$

2.2.3. Alternative forms of through-flow equations

As mentioned earlier, one of the momentum equations is redundant and the choice between equations (2.2.50) and (2.2.51) depends on the general flow configuration. Equation (2.2.50), the radial component of the momentum equation, has a coefficient w_z in the left hand side and will not be suitable for a machine with a predominant radial flow, that is for radial or centrifugal machines. Similarly, the axial component of the momentum equation, equation (2.2.51), cannot be applied for axial machines where w_r might vanish in all or part of the flow domain. For mixed flow machines one would have to use one or the other equation according to the flow region. An elegant way to avoid this has been introduced by Bosman and Marsh (1974) and consists in using the projection of the momentum equation on a direction \vec{N} situated in the S_2 surface and perpendicular to the velocity vector \vec{w} , see figure 2.2.1.

The \vec{N} -direction is actually perpendicular to the body force \vec{f}_B , which is normal to S_2 , as well as to the friction force \vec{F}_f , which is parallel to \vec{w} . Hence, one has

$$\vec{N} \cdot \vec{F}_f = 0 \quad \text{and} \quad \vec{N} \cdot \vec{f}_B = 0 \quad (2.2.71)$$

Defining \vec{N} by the vector product

$$\vec{N} = (\vec{f}_B \times \vec{w}) \quad (2.2.72)$$

the projection of the streamsurface momentum equations can be obtained from equation (2.2.5) for steady state flows, as

$$-\vec{N} \cdot (\vec{w} \times \vec{\zeta}) = \vec{N} \cdot (\vec{T} \vec{\nabla} s - \vec{\nabla} I) \quad (2.2.73)$$

or

$$(\vec{f}_B \cdot \vec{\zeta}) \cdot \vec{w}^2 = T(\vec{N} \cdot \vec{V})s - (\vec{N} \cdot \vec{V})I = T(N_r \frac{\partial s}{\partial r} + N_z \frac{\partial s}{\partial z}) - (N_r \frac{\partial I}{\partial r} + N_z \frac{\partial I}{\partial z}) \quad (2.2.74)$$

With equations (2.2.32) and (2.2.33) defining the direction of the body force \vec{f}_B , equation (2.2.74) becomes

$$\begin{aligned} \vec{w}^2 [f_{B\theta} (\frac{\partial}{\partial z} w_r - \frac{\partial}{\partial r} w_z) + \frac{1}{r} f_{Bz} \frac{\partial}{\partial r} (rv_\theta) - \frac{1}{r} f_{Br} \frac{\partial}{\partial z} (rv_\theta)] \\ = (f_{B\theta} w_z - f_{Bz} w_\theta) (T \frac{\partial s}{\partial r} - \frac{\partial I}{\partial r}) + (f_{Br} w_\theta - f_{B\theta} w_r) (T \frac{\partial s}{\partial z} - \frac{\partial I}{\partial z}) \end{aligned}$$

or

$$\begin{aligned} \vec{w}^2 (\frac{\partial}{\partial z} w_r - \frac{\partial}{\partial r} w_z) = (w_z - \frac{n_z}{n_\theta} w_\theta) (T \frac{\partial s}{\partial r} - \frac{\partial I}{\partial r}) \\ - (w_r - \frac{n_r}{n_\theta} w_\theta) (T \frac{\partial s}{\partial z} - \frac{\partial I}{\partial z}) + \frac{\vec{w}^2}{r} [\frac{n_r}{n_\theta} \frac{\partial}{\partial z} (rv_\theta) - \frac{n_z}{n_\theta} \frac{\partial}{\partial r} (rv_\theta)] \end{aligned} \quad (2.2.75)$$

The coefficient in the left hand side of the above equation is now \vec{w}^2 , independent of the flow direction. This equation has another advantage in that the force terms have disappeared from the right hand side, although they are not neglected. Hence, equation (2.2.75) does not require the explicit calculation of the force components, but does however require the explicit knowledge of the normal to the streamsurface, that is the angles ϵ' and β' . Introducing these angles explicitly, equation (2.2.75) becomes

$$\begin{aligned} \vec{w}^2 (\frac{\partial}{\partial z} w_r - \frac{\partial}{\partial r} w_z) = (w_z + w_\theta \tan \beta') (T \frac{\partial s}{\partial r} - \frac{\partial I}{\partial r}) \\ - (w_r + w_\theta \tan \epsilon') (T \frac{\partial s}{\partial z} - \frac{\partial I}{\partial z}) + \frac{\vec{w}^2}{r} [\tan \beta' \frac{\partial}{\partial r} (rv_\theta) - \tan \epsilon' \frac{\partial}{\partial z} (rv_\theta)] \end{aligned} \quad (2.2.76)$$

In a duct region, where no blades are present there is no body force because of the axisymmetric assumption and the direction \vec{N} cannot be defined. In this case, because of the axisymmetry, one can select the direction perpendicular to the meridional streamline m in the $(r-z)$ space as the projection direction, see figure 2.2.2. With

$$\vec{N} = \vec{i}_\theta \times \vec{w} = w_z \vec{i}_r - w_r \vec{i}_z \quad (2.2.77)$$

one obtains instead of equation (2.2.74),

$$\begin{aligned}
w_m^2 \left(\frac{\bar{\partial}}{\partial r} w_z - \frac{\bar{\partial}}{\partial z} w_r \right) &= w_r \left(T \frac{\bar{\partial} s}{\partial z} - \frac{\bar{\partial} I}{\partial z} \right) - w_z \left(T \frac{\bar{\partial} s}{\partial r} - \frac{\bar{\partial} I}{\partial r} \right) \\
&+ \frac{w_\theta}{r} \left[w_r \frac{\bar{\partial}}{\partial z} (rv_\theta) - w_z \frac{\bar{\partial}}{\partial r} (rv_\theta) \right]
\end{aligned}
\tag{2.2.78}$$

Note that, in a duct region one can consider the flow from the absolute reference system and set $I=H$, $\vec{w}=\vec{v}$ since $\vec{u}=0$. Also the overbars on the derivatives can be suppressed because the flow is considered as axisymmetric.

2.2.4. Properties of the through-flow equations

It is important to analyze the mathematical properties of the system formed by the continuity equation and the momentum equation, for instance the radial component for an axial machine, with regard to the characteristics and their elliptic or hyperbolic properties. This is best obtained after setting the equations into the quasi-linear form. The radial momentum equation is best written, for this analysis, in the form of equation (2.2.4), after introduction of the continuity equation (2.2.3), for steady flows

$$\begin{aligned}
w_r \frac{\bar{\partial}}{\partial r} w_r + w_z \frac{\bar{\partial}}{\partial z} w_r + \frac{1}{\rho} \frac{\bar{\partial}}{\partial r} p &= F_{fr} + f_{Br} + \omega^2 r + 2\omega \cdot w_\theta + w_\theta^2 / r \\
&= F_{fr} + f_{Br} + v_\theta^2 / r
\end{aligned}
\tag{2.2.79}$$

where the right hand side is unimportant for the properties of the system. The continuity equation is transformed to the quasi-linear form, developing equation (2.2.49)

$$\rho \frac{\bar{\partial}}{\partial r} w_r + \rho \frac{\bar{\partial}}{\partial z} w_z + w_r \frac{\bar{\partial}}{\partial r} \rho + w_z \frac{\bar{\partial}}{\partial z} \rho = -\rho \frac{\vec{w} \cdot \vec{\nabla} B_z}{B_z}
\tag{2.2.80}$$

The derivatives of density and pressure can be expressed in function of the velocity derivatives. One has, from the definition, equation (2.2.68), for any variation δ

$$\delta \rho = -\frac{\rho}{a^2} (w_r \delta w_r + w_z \delta w_z + w_\theta \delta w_\theta)
\tag{2.2.81}$$

and

$$\delta p = \left(\frac{\partial p}{\partial \rho} \right) \delta \rho = a^2 \delta \rho
\tag{2.2.82}$$

where a^2 is the square of the speed of sound.

The dependent variables are w_r and w_z and as discussed above, w_θ is supposed to be known from the blade-to-blade information.

If w_θ is defined by the flow angle $\hat{\beta}$, equation (2.2.21), then w_θ will be function of w_z and contribute to the definition of the properties of the equation. In the other case, if w_θ is given as a function of coordinates, as in the design option, w_θ will be considered independent of the velocity component w_z . We will combine these two cases by writing formally

$$\delta w_\theta = v \cdot \tan \hat{\beta} \cdot \delta w_z \quad (2.2.83)$$

where $v=1$ when the flow angle $\hat{\beta}$ is given and $v=0$ when w_θ is imposed. Hence, equation (2.2.81) can be written as

$$\delta \rho = - \frac{\rho}{a^2} [w_r \delta w_r + w_z (1 + v \tan^2 \hat{\beta}) \delta w_z] \quad (2.2.84)$$

The continuity and radial momentum equations can be written under the system form as follows, writing $K = 1 + v \tan^2 \hat{\beta}$

$$(1-M_r^2) \frac{\partial}{\partial r} w_r - M_r M_z K \frac{\partial}{\partial r} w_z - M_z M_r \frac{\partial}{\partial z} w_r + (1-KM_z^2) \frac{\partial}{\partial z} w_z = - \frac{\vec{w} \cdot \vec{\nabla} B_2}{B_2} \quad (2.2.85)$$

$$-w_z K \frac{\partial}{\partial r} w_z + w_z \frac{\partial}{\partial z} w_r = F_{fr} + f_{Br} + \frac{v_\theta^2}{r} \quad (2.2.86)$$

M_r and M_z are the Mach numbers corresponding to w_r and w_z , that is

$$M_r = w_r/a \quad \text{and} \quad M_z = w_z/a \quad (2.2.87)$$

In matrix form, the above system can be written as

$$A \cdot \frac{\partial}{\partial r} \begin{vmatrix} w_r \\ w_z \end{vmatrix} + B \cdot \frac{\partial}{\partial z} \begin{vmatrix} w_r \\ w_z \end{vmatrix} = \begin{vmatrix} q_1 \\ q_2 \end{vmatrix} \quad (2.2.88)$$

or explicitly

$$\begin{vmatrix} (1 - M_r^2) - KM_r M_z & \frac{\partial}{\partial r} \begin{vmatrix} w_r \\ w_z \end{vmatrix} \\ 0 & -w_z K \end{vmatrix} + \begin{vmatrix} -M_r M_z & 1 - KM_z^2 \\ w_z & 0 \end{vmatrix} \frac{\partial}{\partial z} \begin{vmatrix} w_r \\ w_z \end{vmatrix} = \begin{vmatrix} q_1 \\ q_2 \end{vmatrix} \quad (2.2.89)$$

where the right hand sides represent the terms independent of the velocity derivatives. The system (2.2.89) is elliptic or hyperbolic if the characteristics are imaginary or real. The characteristic directions λ are determined by the solutions of the determinant $|A + \lambda B| = 0$. That is

$$\begin{vmatrix} 1 - M_r^2 - \lambda M_r M_z & -M_r M_z K + \lambda(1 - KM_z^2) \\ \lambda w_z & -w_z \end{vmatrix} = 0 \quad (2.2.90)$$

leading to the two solutions

$$\lambda_{\pm} = [M_r M_z K \pm \sqrt{K(M_r^2 + KM_z^2 - 1)}] / (1 - KM_z^2) \quad (2.2.91)$$

One obtains the following important properties, valid for all quasi-three dimensional descriptions along the S2 type of surfaces :

- The system of equations (2.2.49) to (2.2.54) is elliptic if the expression under the square root is negative, that is for

$$M_m^2 + \nu M_\theta^2 < 1 \quad (2.2.92)$$

Hence, the through-flow model is elliptic for subsonic meridional Mach numbers when w_θ is imposed ($\nu=0$), while the system is elliptic for subsonic relative Mach numbers $M^2 = M_m^2 + M_\theta^2 < 1$, when the flow angle $\hat{\beta}$ is given ($\nu=1$). Any solution method will have to take these properties into account.

The first case, namely the design option, whereby w_θ is considered as a known function, is of particular interest and deserves some comments. The condition (2.2.92) indicates that the through-flow problem can be treated in an elliptic way for subsonic meridional Mach numbers, although the relative Mach number can be supersonic. Hence, for given w_θ distributions, one can handle relative supersonic flows inside the blade rows in the same way as the subsonic relative flows and compute the meridional velocity components within the blade rows by implementing in the appropriate way, the information about w_θ to be transferred from the blade-to-blade surfaces. However, if this information is transmitted under the form of the flow angles β or $\hat{\beta}$, no calculation method of "elliptic" type (for instance the methods described in section 2.4.) will be able to handle correctly supersonic relative flows, at calculation points situated inside the blade rows, unless the computational procedure is adapted for supersonic flows, by allowing a correct treatment of hyperbolic regions. For instance, by applying techniques similar to those developed for the computation of transonic

potential flows, or time dependent formulations of the type applied to the resolution of the system of Euler equations.

Note that outside blade rows, that is in the duct regions, the above conditions automatically apply since v_θ is always given, as a consequence of equation (2.2.58) expressing the constancy of angular momentum. Hence in duct regions the problem will always be elliptic for subsonic meridional Mach numbers.

This situation is closely connected to the analysis of the time-like direction in three dimensional supersonic flows. An arbitrary direction is to be considered as time-like if the projection of the velocity along this direction is supersonic. When this projection is subsonic, the problem is elliptic with respect to the corresponding direction, since an upstream propagation of information in this direction is possible. The same properties appear here, since upstream propagation of information in the meridional direction is possible, from outlet to inlet of a blade row for instance, when the meridional Mach number is subsonic even for relative supersonic flows. This apparently contradictory situation can be understood, even in the presence of choked blade-to-blade passages, because of the way the information is transmitted from the blade-to-blade flow to the S2-surface. Indeed, the supersonic flow occurs in the blade-to-blade-S1-surface, which is not resolved by equations (2.2.49) to (2.2.54) and, as discussed above, the information on the properties of this flow have to be transferred through the entropy (or stagnation pressure) and w_θ variations. If the flow passage is choked, implying that no upstream influence can be transmitted in the relative flow direction, and with the mass flow defined by the inlet conditions independently of the outlet flow conditions, there is still an upstream propagation of pressure waves in the meridional direction, assuming subsonic meridional flow. This is illustrated on figures 2.2.4 and 2.2.5 in the case of choked compressor and turbine passages, respectively. In these cases, the entropy variation $s=s(r,z)$ or $s=s(r,m)$ will have to take into account the entropy discontinuity over the normal shock in figure 2.2.4 and the transmitted tangential flow components will have to be consistent with the choked mass flow. Similarly, the value of w_θ transmitted at blade outlet of the choked turbine of figure 2.2.5, will have to be defined by the local value of the mass flow in such a way as to respect mass conservation between the throat area and the outlet. This has of course implications on the way the computation of the through-flow is performed since, for a fully choked passage, the mass flow cannot be imposed but will result from the calculations for an imposed pressure ratio.

A similar situation occurs for the supersonic compressor inlet flow where the phenomena of unique incidence, at the leading edge of the blades, for supersonic incident velocities, has to be taken into account and the corresponding tangential velocity at inlet has to be transferred to the through-flow computation. Similarly, if the flow is choked the outlet tangential velocity should be consistent with the critical mass flow.

Therefore, when information on w_θ is transmitted, this decouples the meridional velocity field (w_r, w_z) from the tangential velocity field

and, provided the w_θ distribution is consistent with the physical phenomena in the blade-to-blade surfaces, one is left with an elliptic or hyperbolic problem in the (r,z) space according to the meridional Mach number. However, when the flow angle is transmitted this couples the tangential flow field to the meridional one through equation (2.2.21) or (2.2.25) and the full three-dimensional conditions for ellipticity are maintained, namely subsonic relative velocities.

2.2.5. Flow Equations along Blade-to-Blade S1 Surfaces

The equations for the blade-to-blade surfaces of the S1 type in figure 1.1.2, are obtained by following the same procedure as in the previous section starting from equations (2.2.1) to (2.2.11).

If the S1 surfaces are defined by $r=r(\theta,z)$ families, the continuity equation becomes, indicating by b_1 the thickness of the S1 streamsheet, see also equation (E.1.1.16),

$$\frac{\partial}{\partial t} (B_1 \rho) + \frac{1}{r} \frac{\partial}{\partial \theta} (\rho B_1 w_\theta) + \frac{1}{r} \frac{\partial}{\partial z} (\rho B_1 w_z r) = 0 \quad (2.2.93)$$

The streamtube thickness B_1 is defined by

$$\frac{1}{B_1} \frac{dB_1}{dt} = \frac{1}{B_1} \left(\frac{\partial B_1}{\partial t} + \frac{w_\theta}{r} \frac{\partial B_1}{\partial \theta} + w_z \frac{\partial B_1}{\partial z} \right) = \left(\frac{\partial}{\partial r} w_r + n_z \frac{\partial}{\partial r} w_z + n_\theta \frac{\partial}{\partial r} (w_\theta / r) \right) \quad (2.2.94a)$$

or

$$\frac{\vec{\nabla} B_1}{B_1} = - \frac{\partial \vec{n}}{\partial r} \quad (2.2.94b)$$

with

$$\begin{cases} n_z = - \left(\frac{\partial r}{\partial z} \right) \\ n_\theta = - \left(\frac{\partial r}{\partial \theta} \right) \\ n_r = 1 \end{cases} \quad (2.2.95)$$

as the components of the normal vector to the surface $r=r(\theta,z)$. This form of the continuity equation is not suitable for radial blade rows, where the blade-to-blade sections are essentially in the $(\theta-r)$ planes (when the angle σ comes close to 90 degrees) and the S1 surfaces would have to be defined by $z=z(\theta,r)$.

Therefore a more general form valid for any blade geometry is obtained by defining surfaces in the (m, θ) coordinate system where m is the meridional projection of the streamlines, see figure 2.2.3.

Hence, in the axisymmetric orthogonal coordinate system (θ, m, n) shown on figure 2.2.3, the S_1 surfaces will be defined by surfaces $n=n(\theta, m)$.

The continuity equation takes on the general form given by equation (2.2.3), leading to

$$\frac{\partial}{\partial t} (\rho B_1) + \frac{1}{r} \frac{\partial}{\partial m} (\rho r B_1 w_m) + \frac{1}{r} \frac{\partial}{\partial \theta} (\rho B_1 w_\theta) = 0 \quad (2.2.96)$$

where $B_1 = b_1 h_3$, h_3 being the metric coefficient associated to the coordinate n , and with the definition of the b_1 -coefficient, following equation (2.2.10),

$$\frac{1}{b_1} \left(\frac{\partial b_1}{\partial t} + \frac{w_\theta}{r} \frac{\partial b_1}{\partial \theta} + w_m \frac{\partial b_1}{\partial m} \right) = \left(\frac{\partial}{\partial n} w_n + n_\theta \frac{\partial}{\partial n} (w_\theta / r) + n_m \frac{\partial}{\partial n} w_m \right) \quad (2.2.97)$$

with

$$\begin{aligned} n_\theta &= - \frac{\partial n}{\partial \theta} (\theta, m) \\ n_m &= - \frac{\partial n}{\partial m} (\theta, m) \end{aligned} \quad (2.2.98)$$

The streamsurface derivatives are defined by equation (2.2.1)

$$\begin{aligned} \frac{\partial}{\partial \theta} &= \frac{\partial}{\partial \theta} - n_\theta \frac{\partial}{\partial n} \\ \frac{\partial}{\partial m} &= \frac{\partial}{\partial m} - n_m \frac{\partial}{\partial n} \end{aligned} \quad (2.2.99)$$

Some confusion might be possible here between the normal \vec{n} and the n coordinate of the axisymmetric coordinate system n, m, θ . However, it should be clear from the text that equation (2.2.98) for instance, relates the θ component of the vector \vec{n} to the θ derivative of the surface defined by relation $n=n(\theta, m)$ in the (n, m, θ) coordinate system.

For a permanent relative flow, the steady state continuity equation becomes

$$\frac{\partial}{\partial m} (\rho B_1 r w_m) + \frac{1}{r} \frac{\partial}{\partial \theta} (\rho B_1 r w_\theta) = 0 \quad (2.2.100)$$

Note that B_1 is measured here in a direction perpendicular to m .

In practical calculations the function $B_1=B_1(\theta, m)$ has to be determined from the hub-shroud S2-flow according to equations (2.2.96). An interesting and widely used approximation is obtained from equation (2.2.48) which states the mass conservation along a streamsheet centered on m .

Hence one can define the function $B_1=B_1(m)$ as follows

$$\frac{B_1(m)}{B_1(m_0)} = \frac{(\rho w_m b_2)_0}{\rho w_m b_2} \quad (2.2.101)$$

where (ρw_m) is obtained from the hub-shroud S2 streamsurface solutions to equations (2.2.49) to (2.2.54) and where the subscript 0 indicates a reference state, generally the inlet of the considered blade row. The inverse of equation (2.2.101), namely the quantity $B_1(m_0)/B_1(m)$ is often called the Axial Velocity-Density ratio or AVDR, in the literature.

The momentum equation (2.2.5) becomes in the (θ, m, n) coordinate system, with $w_n=0$ and $F_{fn}=0$ for a streamsurface $n=n(m, \theta)$

$$\frac{\partial}{\partial t} w_\theta + \frac{w_m}{r} \left(\frac{\partial}{\partial m} r v_\theta - \frac{\partial}{\partial \theta} w_m \right) = \frac{T}{r} \frac{\partial}{\partial \theta} s - \frac{1}{r} \frac{\partial}{\partial \theta} I + F_{f\theta} + f_{B\theta} \quad (2.2.102)$$

$$\frac{\partial}{\partial t} w_m + \frac{w_\theta}{r} \left(\frac{\partial}{\partial \theta} w_m - \frac{\partial}{\partial m} r v_\theta \right) = T \frac{\partial}{\partial m} s - \frac{\partial}{\partial m} I + F_{fm} + f_{Bm} \quad (2.2.103)$$

$$\frac{-w_m^2}{R_m} = f_{Bn} \quad (2.2.104)$$

while the energy and entropy equations can be written as

$$\frac{\partial I}{\partial t} + w_m \frac{\partial I}{\partial m} + \frac{w_\theta}{r} \frac{\partial I}{\partial \theta} = \frac{1}{\rho B_1} \frac{\partial}{\partial t} (p B_1) \quad (2.2.105)$$

$$\frac{\partial s}{\partial t} + w_m \frac{\partial s}{\partial m} + \frac{w_\theta}{r} \frac{\partial s}{\partial \theta} = \frac{w}{T} F_f \quad (2.2.106)$$

where R_m is the radius of curvature of the meridional streamline. The body force \vec{f}_B is defined here by

$$\rho \vec{f}_B = -\vec{n} \cdot \frac{\partial p}{\partial n} \quad (2.2.107)$$

In particular, if the S1-streamsurface is assumed to be close to an axisymmetric streamsurface, then S1 is a surface $n=\text{constant}$ and the body force \vec{f}_B is purely directed along the n -axis, which is the normal to the $m-\theta$ axisymmetric surface. This follows from the same considerations as those which lead to equation (2.2.30). Under these conditions, one would have

$$f_{B\theta} = f_{Bm} = 0 \quad (2.2.108)$$

Equation (2.2.104) defines the n -component of the body force as balanced by the centrifugal force in this direction and can be considered to be responsible for the curvature of the meridional streamline. The radius of curvature R_m will be positive if the pressure increases with n , that is from hub to shroud.

In analogy with the discussion of the S2-streamsurface computation, the blade-to-blade S1 computations require the knowledge of the streamsheet thickness B_1 , and of the forces \vec{F}_f and \vec{f}_B .

The thickness B_1 , defined by equation (2.2.97) can be approximated by equation (2.2.101), while the force \vec{f}_B requires the knowledge of the pressure gradients in the n direction at every point. Both quantities are to be obtained from the S2-streamsurface solutions. As discussed previously, the friction force on the other hand has to be provided by empirical data or can be calculated at least partly in the blade-to-blade surfaces (for instance by a boundary layer approximation) and averaged out over the blade-to-blade spacing for transmission to the S2-hub-to-shroud surfaces.

The Axisymmetric Blade-to-Blade Surface Approximation

A considerable simplification of the whole quasi-three dimensional interaction occurs when the blade-to-blade S1 streamsurfaces can be considered as surfaces of revolution. This assumption does not imply, however, that the flow is to be considered as axisymmetric. The blade-to-blade equations can be simplified in the following way, as a consequence of the axisymmetry and of additional assumptions with regard to the tangential uniformity of total energy I and entropy s .

- i) the surface $n=n(\theta, m)$ is the surface of revolution, $n=\text{constant}$, generated by the rotation of the meridional streamline m , see figure 2.2.3. The blade force reduces to a force in the n direction according to equation (2.2.108) and the normal \vec{n} to the surface is in the direction of the n -axis.

Hence

$$n_m = n_\theta = 0 \quad (2.2.109)$$

- ii) In a steady flow the total energy I is constant along a streamline,

equation (2.2.105) and hence, the total energy will remain constant in the whole S1 flow field if it is assumed to be uniform in the θ -tangential direction in the inlet section of the blade-to-blade calculation domain. Thus, if

$$\frac{\partial I}{\partial \theta} = 0 \quad \text{in the inlet surface} \quad (2.2.110)$$

one has

$$I = \text{constant in the whole S1 surface} \quad (2.2.111)$$

- iii) In accordance with the distributed loss model, the friction force and hence the entropy, are considered as an average representation of the losses generated by the shear stresses. Therefore it is consistent to assume that the entropy and F_f do not vary in the tangential direction θ .

This corresponds to the assumption that the entropy is a unique function of the meridional distance m , that is

$$s = s(m) \quad \text{or} \quad \frac{\partial s}{\partial \theta} = 0 \quad (2.2.112)$$

With these simplifications, the blade-to-blade equations for an axisymmetric streamsurface and tangentially uniform energy and entropy distributions reduce to the following equations, where the overbars have been removed from the derivatives as a consequence of (2.2.109)

$$\frac{\partial}{\partial t} (\rho B_1) + \frac{\partial}{\partial m} (\rho B_1 r w_m) + \frac{\partial}{\partial \theta} (\rho B_1 w_\theta) = 0 \quad (2.2.113)$$

$$\frac{\partial}{\partial t} w_\theta + \frac{w_m}{r} \left(\frac{\partial}{\partial m} (r v_\theta) - \frac{\partial}{\partial \theta} w_m \right) = F_{f\theta} = - \frac{w_\theta}{w} F_f \quad (2.2.114)$$

$$\frac{-w_m^2}{R_m} = f_{Bn} \quad (2.2.115)$$

$$\frac{\partial I}{\partial t} + w_m \frac{\partial I}{\partial m} = \frac{1}{\rho B_1} \frac{\partial}{\partial t} (\rho B_1) \quad (2.2.116)$$

$$\frac{\partial s}{\partial t} + w_m \frac{\partial s}{\partial m} = \frac{w}{T} F_f \quad (2.2.117)$$

A further simplification is introduced for steady flows, leading to the system

$$\frac{\partial}{\partial m} (\rho B_1 r w_m) + \frac{\partial}{\partial \theta} (\rho B_1 w_\theta) = 0 \quad (2.2.118)$$

$$\frac{w_m}{r} \left(\frac{\partial}{\partial m} (r v_\theta) - \frac{\partial}{\partial \theta} w_m \right) = F_{f\theta} \quad (2.2.119)$$

$$\frac{-w_m^2}{R_m} = f_{Bn} \quad (2.2.120)$$

$$\frac{\partial I}{\partial m} = 0 \quad (2.2.121)$$

$$w_m \frac{\partial s}{\partial m} = \frac{w}{T} F_f \quad (2.2.122)$$

In particular for steady flows, equation (2.2.119) shows that the n-component of the absolute vorticity ζ_n is given by

$$\zeta_n = -r F_{f\theta} / w_m = r \frac{w_\theta}{w_m} \frac{F_f}{w} = \frac{r \tan \beta}{w} \cdot F_f \quad (2.2.123)$$

and hence, if the effects of the friction force are neglected in the blade-to-blade surface, the absolute flow will be irrotational. In this case the absolute velocity will depend on a potential function ϕ , which satisfies equation (2.2.118), in the steady state case.

$$\vec{v} = \vec{\nabla} \phi \quad (2.2.124)$$

$$\frac{\partial}{\partial m} (\rho B_1 r \frac{\partial \phi}{\partial m}) + \frac{\partial}{\partial \theta} (\rho \frac{B_1}{r} \frac{\partial \phi}{\partial \theta}) - \frac{\partial}{\partial \theta} (\rho B_1 \omega r) = 0 \quad (2.2.125)$$

However, it is to be noticed that this assumption is not consistent with the S2-hub-shroud through-flow since, neglecting the friction forces consists in assuming constant stagnation pressure and hence constant entropy in the blade-to-blade surface, while this is not the case at the corresponding points of the S2-surface. The introduction of the losses leads to a stagnation pressure variation along the meridional m-line in the through-flow calculation, while the above assumptions neglects the same variation in the blade-to-blade surface.

In addition, the application of the isentropic potential equation (2.2.125) to the internal blade-to-blade flows is faced with the non-uniqueness problems associated with transonic potential flows. Therefore, equation (2.2.125) can be considered as a good approximation for subsonic and mildly supersonic flows, but is not recommended for choked transonic blade-to-blade flows. In this latter case, it is advised to apply the equations (2.2.113) and (2.2.114) supplied by equation (2.2.116) and (2.2.117).

Another option consists in introducing a streamfunction $\psi(m, \theta)$, defined by

$$\rho B_1 r w_m = \frac{\partial \psi}{\partial \theta} \quad (2.2.126)$$

$$\rho B_1 w_\theta = - \frac{\partial \psi}{\partial m} = \rho B_1 v_\theta - \rho B_1 \omega r \quad (2.2.127)$$

the vorticity ζ_n of the absolute flow can be written as

$$\frac{\partial}{\partial \theta} \left(\frac{1}{\rho B_1 r} \frac{\partial \psi}{\partial \theta} \right) + \frac{\partial}{\partial m} \left(\frac{r}{\rho B_1} \frac{\partial \psi}{\partial m} \right) = \zeta_n + \frac{\partial}{\partial m} (\rho B_1 \omega r^2) = r \frac{w_\theta}{w_m} \frac{1}{w_m} F_f + \frac{\partial}{\partial m} (\rho B_1 \omega r^2) \quad (2.2.128)$$

The application of the streamfunction to the 2D blade-to-blade flow, allows to take into account, the effect of the friction force on the inviscid blade-to-blade flow. However the non-unique relation between density and streamfunction makes the application of this formulation difficult for transonic flows.

2.2.6. The Streamsurface Quasi-Three-Dimensional Interaction

The complete Quasi-three dimensional interaction can now be described as follows, for an analysis problem whereby the geometry of the machines is given. Detailed considerations with regard to the design options can be found in Wu (1952).

- i) Define a series of S2-streamsurfaces as a reasonable approximation to the passage flow configurations. A valid starting option is to consider only one S2-surface assuming an initial axisymmetric approximation.
- ii) For each streamsurface S2, initial approximations have to be selected for the tangential blockage or sheet thickness coefficient B_2 . The through-flow is computed following sections 2.2.1 to 2.2.3.
- iii) From the computed S2-flows, the following information is extracted in order to define the various S1 blade-to-blade flows :
 - the geometrical coordinates $n=n(\theta, m)$ of the selected blade-to-blade surfaces,
 - the streamsheet thickness $B_1=B_1(\theta, m)$ according to equation (2.2.101)
 - the body force
 - the boundary conditions upstream and downstream of each blade to blade section.
- iv) The various S1 blade-to-blade flows are computed following section 2.2.5.

v) From the computed blade-to-blade flows, improved S2-streamsurface coordinates are defined as well as blockage coefficients $B_2=B_2(r,z)$ and body force.

vi) The whole process is repeated until a satisfactory convergence is obtained.

This complete iterative procedure has been applied by Krimerman and Adler (1978) and is schematically illustrated in figure 2.2.6

The iterative process can be quite complex and lengthy, especially in configurations where the blade-to-blade surfaces become highly twisted, but it allows to recover the full three-dimensional flow.

Simplified Quasi-Three-Dimensional Interaction - Mean Streamsheet

An important simplification of the complete process consists in assuming that the S1-blade-to-blade surfaces are surfaces of revolution generated by the rotation of the meridional projection of the streamlines. This will be valid when the blade-to-blade surface twist, induced by secondary flows remains small. In addition, it is considered that the through-flow can be represented by a single, mean streamsurface S2, which is considered to be representative of all of the S2 surfaces. Hence the quasi-three dimensional flow model will consist of one S2-through-flow surface and several, axisymmetric, blade-to-blade surfaces.

The main problem in this simplified approach is to define the mean streamsheet. Intuitively it is to be considered as a kind of average or representative surface of all the S2 surfaces. However, the present approach does not give any indication as how to select this surface.

Various choices have been attempted in order to generate the mean S2 surface: the mean camber line, Senoo and Nakase (1972); the streamlines of the blade-to-blade flows separating equally the mass flow between pressure side and friction side, Novak and Hearsey (1977); the mass averaged blade-to-blade streamlines, these "streamlines" being different from any actual streamline, Bosman and El-Shaarawi (1977).

No indications are available as to which choice is to be recommended. As discussed by Novak and Hearsey (1977), the local flow values can be quite sensitive to the choice of the distributions of the β' and ϵ' angles defining the mean streamsurface. In particular, figure 2.2.7 shows a comparison of the meridional variation of the streamsurface angle β' in function of meridional distance for the mean camber line and the equally dividing streamline ($\psi=0.5$ on figure 2.2.8), for a turbine nozzle such as illustrated in figure 2.2.8,.

Clearly, the strong gradients of β' along the camber line are difficult to accept as representative of the mean hub-shroud flow. In addition, the angle ϵ' (lean angle) can have a considerable influence on the resulting flow distributions. This is illustrated in figure 2.2.9 from Novak and Hearsey (1977), showing a comparison of two calculations of the through-flow along an S2-surface. A first calculation (Run 10)

corresponds to $\epsilon' = 0$, while the second case (Run 20) had a mean streamsheet lean angle ϵ' of 10 degrees at the inner radius and varying such that the surface was straight. The computed configuration is a turbine nozzle with radius ratio of 0.88, outlet angle of 72 degrees and an outlet Mach number close to 0.6. In the second run, the blades were given the same lean as the streamsurface, with the pressure surface facing towards the inner radius. As can be seen from figure 2.2.9, the radial static pressure gradient is completely altered at the inner section AA, although minor differences occur at the trailing edge.

The third parameter necessary to define the mean streamsurface through-flow is the thickness parameter B_2 . As already observed by Wu (1952) and illustrated by Novak and Hearsey (1977), the application of equation (2.2.28) leads to variations of B_2 with very strong gradients as shown on figure 2.2.9 for the same computation as figures 2.2.7 and 2.2.8. In addition, for subsonic flows, the influence of the blades extend upstream and hence modifies the value of B_2 from the value of unity valid in bladeless regions. More generally, Horlock and Marsh (1971) have shown that no choice of the mean streamsurface can be made such that the calculated flow along this mean surface would represent exactly the actual average flow over the passage width, see also section 2.3.2.

However, the overall change, from leading edge to trailing edge can be correctly modeled if the streamsheet angles are adapted to the flow angles at these locations. But there is no guaranty that the local values of the flow variables, calculated within the blade passage, are representative of the actual averaged flow.

Therefore, although the simplification provided by the mean streamsurface model is an important one, its precise choice can lead to uncertainties as to the representativity of the calculated local flow behavior inside the blade rows with regard to the real passage averaged flow.

An alternative approach, which avoids the arbitrariness of the choice of the mean S2 surface, can be defined by the averaging procedure to be discussed next. As will be seen, this approach which solves the exact through-flow equations for the passage averaged flow in a meridional plane does not have the same uncertainties on the angular parameters, β' , ϵ' . The third variable B_2 on the other hand, will be seen to be only function of geometry, see equation (2.3.5). However, the through-flow equations contain additional terms depending on the blade-to-blade flow distributions, which have to be estimated. Since the estimation of these terms can be derived, if necessary from the blade-to-blade solutions, one has a general, rigorous approach for the simplified quasi-three-dimensional flow model consisting of the passage averaged flow and axisymmetric blade-to-blade surfaces. The averaging procedure on the other hand cannot be applied to the estimation of the full three-dimensional flow, as can be done with the streamsurface approach.

2.3. THE PASSAGE-AVERAGED QUASI-THREE DIMENSIONAL APPROXIMATION

The averaging procedure for obtaining a quasi-three dimensional approximation to the turbomachinery flow consists in defining a two-dimensional flow in the meridional cross-section of the machine, representative of an average flow over the passage width of the blade row.

Referring to figure 2.3.1, the averaged flow at a given point P of the meridional cross-section is obtained by performing an integration of the flow properties from the pressure surface to the suction surface of the next blade along the axisymmetric cross section generated by the rotation of the meridional streamline m. In order to apply the general theory of section 1.2, a cylindrical coordinate system (r,θ,z) is chosen and the integration direction $\xi^3 = \theta$. The limits of integration are defined by the blade surfaces and the width b of the integration region is given by $b = \theta_p - \theta_s$ where θ_p and θ_s are the angular position of the pressure and suction surfaces of two consecutive blades. If N is the number of blades, d the tangential thickness of an individual blade, and s the pitch or blade spacing at radius r, one has

$$b = \frac{2\pi}{N} - \frac{d}{r} = \frac{2\pi}{N} \left(1 - \frac{d}{s}\right) = \frac{2\pi}{N} b_2 \quad (2.3.1)$$

defining a streamtube thickness parameter b_2 , function of the geometry,

$$b_2 = 1 - d/s \quad (2.3.2)$$

The averaged equations have the following form, obtained from section 1.2 (Table 3.1) by removing the shear stress and heat conduction terms.

Continuity

$$\frac{\partial}{\partial t} (\bar{\rho} b_2) + \vec{\nabla} \cdot (\bar{b}_2 \bar{\rho} \vec{w}) = 0 \quad (2.3.3)$$

Momentum

$$\frac{\partial}{\partial t} (\bar{\rho} \vec{w} b_2) + \vec{\nabla} \cdot (\bar{\rho} \vec{w} \otimes \vec{w} + \bar{p}) b_2 = -2\bar{\rho} (\vec{\omega} \times \vec{w}) b_2 + \bar{\rho} \omega^2 r b_2 + \bar{\rho} \vec{F}_f b_2 + \bar{\rho} \vec{f} b_2 \quad (2.3.4)$$

Energy

$$\frac{\partial}{\partial t} (\overline{\rho E^* b_2}) + \vec{\nabla} \cdot (\overline{\rho \vec{w} I} b_2) = 0 \quad (2.3.5)$$

A body force \vec{f} appears in the momentum equation as a result of the averaging process as seen in section 1.2. This additional force \vec{f} is defined by equation (1.2.37) and represents here the resultant of the pressure forces on the blade sections

$$\overline{\rho \vec{f}} = \frac{-1}{b} [p \vec{n}] = (p_p \vec{n}^{(p)} - p_s \vec{n}^{(s)}) \frac{1}{\frac{2\pi b_2}{N}} \quad (2.3.6)$$

where $\vec{n}^{(p)}$ and $\vec{n}^{(s)}$ are the normals to the pressure and suction surfaces, respectively.

The energy equation is written in the relative system with

$$E^* = e + \frac{\vec{w}^2}{2} - \frac{\vec{u}^2}{2} \quad (2.3.7)$$

The above equations are fully rigorous.

Various averaged quantities can be defined and the most frequently occurring choices are the geometrical, density weighted or mass flux weighted averages. A consistent set of equations can be obtained for the density weighted average which has the property of satisfying exactly mass conservation, Hirsch and Warzee (1979).

The density weighted average of a quantity A is defined by

$$\overline{\rho A} = \frac{1}{b} \int_{\theta_p}^{\theta_s} \rho A d\theta = \overline{\rho (A - A'')} \quad (2.3.8a)$$

with

$$\overline{\rho} = \frac{1}{b} \int_{\theta_p}^{\theta_s} \rho d\theta \quad (2.3.8b)$$

$$A = \overline{A} + A'' \quad (2.3.9a)$$

and

$$\overline{\rho A''} = 0 \quad (2.3.9b)$$

where A'' are the deviations of the quantity A from the axisymmetric value \bar{A} .

Applying this definition with the general procedure of section 1.2, leads to the following averaged equations for the through-flow in a meridional cross section of the machine.

2.3.1. Passage Averaged Continuity Equation

The averaged continuity equation (2.3.3), in the relative system, becomes

$$\frac{\partial}{\partial t} (\bar{\rho} b_2 r) + \frac{\partial}{\partial r} (\bar{\rho} b_2 r W_r) + \frac{\partial}{\partial z} (\bar{\rho} b_2 r W_z) = 0 \quad (2.3.10)$$

where W_r and W_z are the density weighted averaged relative velocity components.

$$\bar{\rho} \vec{W} = \frac{1}{b} \int_{\theta_p}^{\theta_s} \rho \vec{w} d\theta \quad (2.3.11)$$

This is an exact equation to be compared with equation (2.2.35) where b_2 is given by equation (2.2.28). Formally, both equations are identical, but in the streamsurface approach b_2 is flow dependent and is only approximately equal to the value given by equation (2.3.2), see equation (2.2.56). On the other hand, equation (2.2.35) is the mass conservation law for the local velocities along an S2 streamsurface which has to be defined, while equation (2.3.10) is the mass conservation law for the averaged meridional flow considered in a true meridional cross section of the machine.

For an axisymmetric flow, however, both approaches lead to exactly the same equations.

2.3.2. Passage Averaged Momentum Equation

Applying the results summarized in equation (1.2.39) with the body force \vec{f} defined by equation (2.3.6), the momentum equations in the relative system become

$$\begin{aligned} \frac{1}{b_2} \frac{\partial}{\partial t} (\bar{\rho} \vec{W} b_2) + \frac{1}{b_2} \vec{\nabla} [\bar{\rho} \vec{W} \otimes \vec{W} b_2] &= \frac{1}{b_2} \vec{\nabla} (\bar{\rho} b_2) - 2\bar{\rho} (\vec{\omega} \times \vec{W}) + \bar{\rho} \omega^2 \vec{r} \\ &+ \bar{\rho} \vec{F}_f + \bar{\rho} \vec{f} - \frac{1}{b_2} \vec{\nabla} (\bar{\rho} \vec{w}'' \otimes \vec{w}'' b_2) \end{aligned} \quad (2.3.12)$$

where $\vec{\nabla}$ is the gradient operating on the r and z coordinate space. That is, the explicit components of the gradient operator are obtained from the three-dimensional projections, where all derivatives with respect to θ are put to zero.

The normals \vec{n} to the blade surfaces, figure 2.3.2, appearing in the body force term \vec{f} , are defined by the angles β' and ϵ' as in equations (2.2.16) and (2.2.17) and are given respectively, for the blade pressure and suction surfaces, by

$$-n_r^{(p)} = \frac{\partial \theta}{\partial r} = \frac{1}{r} \tan \epsilon'_p \quad (2.3.13a)$$

$$-n_z^{(p)} = \frac{\partial \theta}{\partial z} = \frac{1}{r} \tan \beta'_p \quad (2.3.13b)$$

$$n_\theta^{(p)} = 1 \quad (2.3.13c)$$

and similar equations for the suction surface, defining the angles β'_s , ϵ'_s

$$-n_r^{(s)} = \frac{\partial \theta}{\partial r} = \frac{1}{r} \tan \epsilon'_s \quad (2.3.14a)$$

$$-n_z^{(s)} = \frac{\partial \theta}{\partial z} = \frac{1}{r} \tan \beta'_s \quad (2.3.14b)$$

$$n_\theta^{(s)} = 1 \quad (2.3.14c)$$

Hence, the components of the body force \vec{f} are

$$\bar{\rho} f_r = \frac{-1}{b_2 s} (p_p \tan \epsilon'_p - p_s \tan \epsilon'_s) \quad (2.3.15a)$$

for the radial component and for the axial component

$$\bar{\rho} f_z = \frac{-1}{b_2 s} (p_p \tan \beta'_p - p_s \tan \beta'_s) \quad (2.3.15b)$$

while the tangential component f_θ is

$$\bar{\rho} f_\theta = \frac{1}{b_2 s} (p_p - p_s) \quad (2.3.15c)$$

This last relation shows that the body force originates from the presence of the blades in the flow field as solid surfaces able to sustain pressure forces. Actually f_θ is nothing else than the tangential projection of the local lift force on the blade. Hence, outside the blade row $\vec{f} = 0$ and the flow is considered as axisymmetric.

It is customary to separate in the body force the effect of the blade camber from the blade thickness. If θ_1 is the angular coordinate of the mean camber line, one has

$$\theta_p = \theta_1 + \frac{\pi b_2}{N} \quad (2.3.16)$$

and

$$\theta_s = \theta_1 - \frac{\pi b_2}{N} + \frac{2\pi}{N} \quad (2.3.17)$$

Introducing these relations in the definition of the blade force, equation (2.3.6), leads to

$$\vec{\rho f} = \frac{r}{b_2 s} (p_p - p_s) \vec{n}^{(1)} + \frac{(p_p + p_s)}{2} \frac{\vec{V} b_2}{b_2} = \vec{\rho f}^{(1)} + \vec{\rho f}^{(b)} \quad (2.3.18)$$

The first term $\vec{\rho f}^{(1)}$ corresponds to the lift force generated by the mean camber line and is orthogonal to the mean camber surface. The second term $\vec{\rho f}^{(b)}$ is a correction depending on the radial and axial variations of the blade thickness blockage factor b_2 . Explicitly, one has

$$\vec{\rho f}_r = \frac{-1}{b_2 s} (p_p - p_s) \tan \epsilon'_1 + \frac{p_p + p_s}{2 b_2} \frac{\partial b_2}{\partial r} \quad (2.3.19a)$$

$$\vec{\rho f}_z = \frac{-1}{b_2 s} (p_p - p_s) \tan \beta'_1 + \frac{p_p + p_s}{2 b_2} \frac{\partial b_2}{\partial z} \quad (2.3.19b)$$

The last term of equation (2.3.12), has the same structure as the Reynolds stress terms in turbulent averaged Navier-Stokes equations and describes the influences of the full three-dimensional flow on its averaged components. We will define a secondary stress tensor by

$$\vec{\tau}^{(s)} = -\overline{\rho \vec{w}'' \otimes \vec{w}''} \quad (2.3.20)$$

since the velocity fluctuations \vec{w}'' are generated by the deviations from axisymmetry, in particular the secondary flow contributions, or the blade-to-blade flow variations. We will designate the gradients of the secondary stresses as the interaction terms, since their influence arises essentially from the interaction between the averaged flow and the secondary flows. These terms can be considered as the sole contributions from the three-dimensional flow distribution to the averaged momentum equation.

An alternative form to equation (2.3.12) is obtained by taking into account the continuity equation (2.3.9), leading to

$$\begin{aligned} \bar{\rho} \frac{\partial}{\partial t} \vec{W} + \bar{\rho} (\vec{W} \cdot \vec{\nabla}) \vec{W} \\ = -\vec{\nabla} \bar{p} - 2\bar{\rho} (\vec{\omega} \times \vec{W}) + \bar{\rho} \omega^2 \vec{r} + \bar{\rho} \vec{F}_f + \bar{\rho} \vec{F}_B - \frac{1}{b_2} \vec{\nabla} (\overline{\rho \vec{w}'' \otimes \vec{w}'' b_2}) \end{aligned} \quad (2.3.21)$$

where the body force \vec{F}_B is defined by

$$\begin{aligned} \bar{\rho} \vec{F}_B = \frac{\bar{p}}{b_2} \vec{\nabla} b_2 + \bar{\rho} \vec{f} = \vec{f}^{(1)} - \left(\bar{p} - \frac{p_p + p_s}{2} \right) \frac{\vec{\nabla} b_2}{b_2} \\ = \vec{f}^{(1)} - \frac{p'_p + p'_s}{2} \cdot \frac{\vec{\nabla} b_2}{b_2} \end{aligned} \quad (2.3.22)$$

where the pressure fluctuations have been introduced in the second term.

The projections of the momentum equation (2.3.21) can be obtained from the general transformation laws to cylindrical coordinates, as follows :

Radial momentum equation

$$\begin{aligned} \frac{\partial W_r}{\partial t} + W_r \frac{\partial}{\partial r} W_r + W_z \frac{\partial}{\partial z} W_r - \frac{W_\theta^2}{r} \\ = - \frac{1}{\rho} \frac{\partial}{\partial r} \bar{p} + \omega^2 r + 2\omega W_\theta + \bar{F}_{fr} + f_{Br} + \frac{1}{\rho_2 b} [\vec{\nabla}(\vec{\tau}^{(S)} b_2)]_r \end{aligned} \quad (2.3.23)$$

where the secondary stresses are represented by the following three contributions

$$-[\vec{\nabla}(\vec{\tau}^{(S)} b_2)]_r = \frac{1}{r} \frac{\partial}{\partial r} (b_2 r \overline{\rho w''_r w''_r}) + \frac{1}{r} \frac{\partial}{\partial z} (b_2 r \overline{\rho w''_r w''_z}) - \frac{b_2}{r} \overline{\rho w''_\theta w''_\theta} \quad (2.3.24)$$

Observe that the non-derivative velocity terms of equation (2.3.23) can be grouped as

$$\frac{V_\theta^2}{r} = \frac{(W_\theta + \omega r)^2}{r} = \frac{W_\theta^2}{r} + \omega^2 r + 2\omega W_\theta \quad (2.3.25)$$

Similarly the axial component of the momentum equation becomes

$$\frac{\partial}{\partial t} W_z + W_r \frac{\partial}{\partial r} W_z + W_z \frac{\partial}{\partial z} W_z = -\frac{1}{\rho} \frac{\partial \bar{p}}{\partial z} + \bar{F}_{fz} + f_{Bz} + \frac{1}{\rho b_z} [\vec{V}(\vec{\tau}^{(S)} b_z)]_z \quad (2.3.26)$$

where the last term represents

$$-[\vec{V}(\vec{\tau}^{(S)} b_z)]_z = \frac{1}{r} \frac{\partial}{\partial r} (b_z r \overline{\rho w''_r w''_z}) + \frac{1}{r} \frac{\partial}{\partial z} (b_z r \overline{\rho w''_z w''_z}) \quad (2.3.27)$$

Tangential component

$$\begin{aligned} \frac{\partial}{\partial t} W_\theta + W_r \frac{\partial}{\partial r} W_\theta + W_z \frac{\partial}{\partial z} W_\theta + \frac{1}{r} W_r W_\theta \\ = -2\omega W_r + \bar{F}_{f\theta} + f_{B\theta} + \frac{1}{\rho b_z} [\vec{V}(\vec{\tau}^{(S)} b_z)]_\theta \end{aligned} \quad (2.3.28)$$

where

$$-[\vec{V}(\vec{\tau}^{(S)} b_z)]_\theta = \frac{1}{r} \frac{\partial}{\partial r} (b_z r \overline{\rho w''_r w''_\theta}) + \frac{1}{r} \frac{\partial}{\partial z} (b_z r \overline{\rho w''_z w''_\theta}) + \frac{1}{r} \overline{\rho w''_\theta w''_r} b_z \quad (2.3.29)$$

Here also the non-derivative velocity terms can be written as

$$\frac{1}{r} W_r (W_\theta + 2\omega r) = \frac{1}{r} W_r (V_\theta + \omega r) \quad (2.3.30)$$

A detailed investigation of the influence and order of magnitude of the interaction terms, originating from the blade-to-blade flow variations inside a compressor blade row, has been presented by Smith (1966). The main conclusion is that the interaction terms are proportional to the blade loading or lift coefficient but that their effect is rather small, although their influence might be non-negligible in certain configurations with high loadings and secondary flows, for instance in turbine passages.

A similar analysis, performed by Hirsch (1975), for the contributions arising from the two-dimensional wakes of the blades shows that the interaction terms are proportional, outside the blade passage in the vicinity of the trailing edge, to the loss coefficients of the

corresponding blade section. The influence of these terms has been found to be generally negligible although, in regions of high losses such as the sections close to the end-walls, their effect might need to be accounted for.

In addition to the two-dimensional effects, three-dimensional effects due to secondary flows and local vorticity production can strongly influence the averaged flow, through significant contributions to the interaction terms.

This is also confirmed by an experimental investigation in a transonic compressor rotor, Sehra (1979). It was shown that the magnitude of these terms has a non-negligible effect on the averaged flow in the end wall regions and that the omission of their contribution led to an inaccurate prediction of the radial flow distribution, see also Sehra and Kerrebrock (1981). A recent evaluation of the relative importance of these interaction terms has been presented by Jennions and Stow (1985), for turbine vanes with strong three-dimensional flow patterns.

Hence in general, the contributions of the secondary stresses will have some influence on the averaged flow, mainly in the endwall regions and in the main blade part, unless the blade rows contain lightly loaded blades or generate small secondary flows.

2.3.3. Passage averaged energy equation

The averaged energy equation is obtained from the general form given by equations (1.2.50) to (1.2.52) written for a relative system. Writing I instead of H and \vec{w} instead of \vec{v} , one obtains, within the assumptions of the distributed loss model, equation (2.1.9),

$$\frac{\partial}{\partial t} (\bar{\rho} E^* b_2) + \vec{\nabla} \cdot (\bar{\rho} \vec{w} I b_2) = - \vec{\nabla} \cdot (\bar{\rho} \vec{w}'' I'' b_2) + b_2 Q_b \quad (2.3.31)$$

where the additional source term Q_b is defined by equation (1.2.52), but takes on the particular form of equation (1.2.53) in the present case of a turbomachinery blade passage.

$$Q_b = \frac{-1}{b_2} \left[p \frac{\partial b_2}{\partial t} \right] = \bar{\rho} \vec{f} \cdot \vec{u}_B \quad (2.3.32)$$

In this relation, \vec{f} is the body force defined by equation (2.3.6) or (2.3.15), and \vec{u}_B is the blade displacement speed in the considered reference system. That is, for a rotor in the relative system

$$\vec{u}_B = 0 \quad (2.3.33)$$

and

$$\vec{u}_B = \vec{u} = \vec{\omega} \times \vec{r}$$

in the absolute system.

It is seen from the above equations that the density weighted averaged total energy represented by the averaged rothalpy \tilde{I}

$$\begin{aligned} \tilde{I} &= \tilde{H} - u\tilde{V}_\theta = \tilde{h} + \frac{\tilde{w}^2}{2} - \frac{\tilde{u}^2}{2} \\ &= \tilde{h} + \frac{\tilde{w}^2}{2} - \frac{\tilde{u}^2}{2} + \frac{\overline{\rho\vec{w}'' \cdot \vec{w}''}}{2\bar{\rho}} = \hat{I} + \frac{\overline{\rho\vec{w}'' \cdot \vec{w}''}}{2\bar{\rho}} \end{aligned} \quad (2.3.34)$$

cannot be considered as constant anymore along a streamline for the steady relative flow. Indeed, in the relative steady state situation, equation (2.3.31) becomes, after introduction of the continuity equation

$$(\bar{\rho}\vec{w} \cdot \vec{\nabla})\tilde{I} = - \frac{1}{b_2} \vec{\nabla}(\overline{\rho\vec{w}'' I'' b_2}) \quad (2.3.35)$$

or

$$\bar{\rho} w_m \frac{\partial}{\partial m} \tilde{I} = - \frac{1}{b_2} \vec{\nabla}(\overline{\rho\vec{w}'' I'' b_2}) \quad (2.3.36)$$

where

$$w_m \frac{\partial}{\partial m} = w_r \frac{\partial}{\partial r} + w_z \frac{\partial}{\partial z} \quad (2.3.37)$$

is the derivative along the averaged meridional streamline m . This important equation (2.3.35) shows that the averaged total energy varies along a streamline, as a consequence of the non-axisymmetric energy fluxes $\overline{\rho\vec{w}'' I''}$.

These energy fluxes are due to the transport of the energy fluctuations I'' by the non-axisymmetric velocity field \vec{w}'' , where

$$I'' = h'' + \vec{w}'' \cdot \vec{w} + \frac{\vec{w}'' \cdot \vec{w}''}{2} - \frac{\overline{\rho\vec{w}'' \cdot \vec{w}''}}{2\bar{\rho}} \quad (2.3.38)$$

represents the deviations from the axisymmetric energy \tilde{I} .

One of the main contributions to these energy fluxes will come from the secondary flows, transporting low energy fluid from the end wall regions to the blade surfaces and the main stream region of the blade passage. These effects can be important and influence the overall energy exchange within a blade row, see for instance Sehra and Kerrebrock (1981), Adkins and Smith (1981).

The energy conservation law can also be written for the total energy of the averaged flow \hat{I} defined by equation (2.3.34). One obtains, instead of equation (2.3.31)

$$\frac{\partial}{\partial t} (\bar{\rho} \hat{I} b_2) + \vec{\nabla}(\bar{\rho} \vec{W} \cdot \hat{I} b_2) = \frac{\partial \bar{p} b_2}{\partial t} - \vec{\nabla}(\bar{\rho} \vec{W}'' \cdot \hat{I}'' b_2) - \vec{\nabla}(\bar{\rho} \vec{W} \cdot \tilde{k} b_2) + b_2 Q_b \quad (2.3.39)$$

where \tilde{k} represents the average kinetic energy of the large scale fluctuations,

$$\tilde{\rho} \tilde{k} = \frac{\overline{\rho \vec{W}'' \cdot \vec{W}''}}{2} = \rho k'' \quad (2.3.40)$$

Equation (2.3.39) shows that the total energy of the density averaged flow does not remain constant along an averaged streamline following \vec{W} , in the steady state limit. This is an essential limitation of the averaged flow model for turbomachinery computation, since the general procedure in practical calculations is based on the constancy of energy, in conjunction with Crocco's form of the momentum equation.

2.3.4. Crocco's Form for the Averaged Momentum Equations

In the averaged formulation, Crocco's form can be derived either directly by averaging the three-dimensional form of equation (2.1.8), Hirsch and Warzee (1979), or by introducing the entropy and the enthalpy in the averaged momentum equation (2.3.21), following section 1.2.4. This second procedure requires the averaging of the entropy relation

$$\rho T \vec{\nabla} s = \rho \vec{\nabla} h - \vec{\nabla} p \quad (2.3.41)$$

The averaged pressure gradient gives rise to the body force as seen from section 1.2. and the definition (2.3.6). Hence one has, after averaging

$$\vec{\nabla} \bar{p} - \bar{\rho} \vec{f}_B = \frac{1}{b_2} \vec{\nabla}(\bar{p} b_2) - \bar{\rho} \vec{f} = \overline{\rho \vec{\nabla} h} - \overline{\rho T \vec{\nabla} s} \quad (2.3.42)$$

This could be worked out following section 1.2.4; but the second term on the right hand side can be simplified if it is considered, in

accordance with the distributed loss model assumptions, that the entropy s and the friction force \vec{F}_f are averaged, mean quantities. Hence with $s=\bar{s}$, the entropy term becomes equal to $\bar{\rho} \vec{T} \vec{\nabla} \bar{s}$. The enthalpy term is averaged in the following way, applying the rules of section 1.2.

$$\overline{\rho \vec{\nabla} h} = \frac{1}{b_2} \vec{\nabla}(\bar{\rho} \tilde{h} b_2) + [\rho h \cdot \vec{n}] \frac{1}{b} - \overline{h \vec{\nabla} \rho} \quad (2.3.43)$$

The last term can be decomposed as follows, introducing $h = \tilde{h} + h''$

$$\overline{h \cdot \vec{\nabla} \rho} = \frac{\tilde{h}}{b_2} \vec{\nabla} \bar{\rho} b_2 + \overline{h'' \cdot \vec{\nabla} \rho} + \frac{\tilde{h}}{b} [\rho \vec{n}] \quad (2.3.44)$$

Combining this relation with equation (2.3.43), gives finally

$$\overline{\rho \vec{\nabla} h} = \bar{\rho} \vec{\nabla} \tilde{h} + [\rho h'' \cdot \vec{n}] \frac{1}{b} - \overline{h'' \vec{\nabla} \rho} \quad (2.3.45)$$

where the second term on the right hand side is the new expression of the body force

$$\bar{\rho} b_2 \vec{f}^{(h)} = -[\rho h'' \cdot \vec{n}] \frac{1}{2\pi/N} \quad (2.3.46)$$

Equation (2.3.42) becomes

$$\vec{\nabla} \bar{p} - \bar{\rho} \vec{f}_B = \frac{1}{b_2} \vec{\nabla} \bar{\rho} b_2 - \bar{\rho} \vec{f} = \bar{\rho} \vec{\nabla} \tilde{h} - \bar{\rho} \vec{f}^{(h)} - \overline{h'' \vec{\nabla} \rho} - \bar{\rho} \vec{T} \vec{\nabla} \bar{s} \quad (2.3.47)$$

An additional interaction term is introduced here, namely $\overline{h'' \vec{\nabla} \rho}$ which can be approximated in practical computations by

$$\overline{h'' \vec{\nabla} \rho} = \bar{h}'' \vec{\nabla} \bar{\rho} + \overline{h'' \vec{\nabla} \rho'} = \bar{h}'' \vec{\nabla} \bar{\rho} \quad (2.3.48)$$

since the second term can be expected to be of a lower order of magnitude.

Introducing equation (2.3.47) in the averaged momentum equations leads to the following form of the averaged Crocco's momentum equation

$$\frac{\partial}{\partial t} \vec{W} - \vec{W} \times \vec{\zeta} = \bar{T} \vec{\nabla} \bar{s} - \vec{\nabla} \hat{I} + \vec{F}_f + \vec{f}^{(h)} - \frac{1}{b_2 \bar{\rho}} \vec{\nabla}(\bar{\rho} \vec{w}'' \times \vec{w}'' b_2) + \frac{\bar{h}'' \vec{\nabla} \bar{\rho}}{\bar{\rho}} \quad (2.3.49)$$

where the averaged absolute voriticity is defined by

$$\vec{\zeta} = \vec{\nabla} \times \vec{V} \quad (2.3.50)$$

The total energy gradient term appearing in this equation contains the total energy of the averaged flow \bar{I} . In practical computations, where the averaged quantities \bar{h} , \vec{W} are calculated, this quantity is the obvious one to consider, since it is only dependent on the averaged flow variables. This is not the case for the averaged total energy \bar{I} which depends also on the large scale flow deviations from axisymmetry \vec{w}'' . However, neither of these quantities are conserved along a streamline of the density averaged flow in steady state conditions. The implications of this situation have been discussed by Sehra (1979) with respect to the interpretations of overall radial equilibrium as described by equation (2.3.49) and more recently by Hirsch and Dring (1986).

Compared to the corresponding momentum equation (2.2.5) of the streamsurface approach, similar terms are obtained here, with the addition of the already discussed interaction terms. The projections of equation (2.3.49) follow closely the formulas given in section 2.2.1, with the projections of the interaction terms calculated in section 2.3.2. The particular projection defined by equation (2.2.73) is obtained in the same way but the projection of the secondary stress gradients on the direction \vec{N} , has to be added.

Alternative formulation of the averaged energy equation

By introducing the total energy fluctuations (2.3.38) into the energy equation (2.3.39), one obtains

$$\begin{aligned} \frac{\partial}{\partial t} (\bar{\rho} \bar{I} b_2) + \vec{\nabla}(\bar{\rho} \vec{W} \bar{I} b_2) &= \frac{\partial}{\partial t} (\bar{\rho} b_2) - \vec{\nabla}(\bar{\rho} \vec{w}'' h'' b_2) - \vec{\nabla}(\bar{\rho} \vec{w}'' k'' b_2) \\ &+ \vec{\nabla}(\bar{\tau}^{(s)} \cdot \vec{W} b_2) + b_2 Q_D \end{aligned} \quad (2.3.51)$$

One can notice the appearance of a contribution from the work of the secondary stresses against the averaged flow, in addition to terms describing a diffusive effect of the fluctuating energies h'' and k'' .

Observe also that the term $\vec{\nabla}(\bar{\rho} \vec{w}'' k'' b_2)$ contains the full velocity vector $\vec{w} = \vec{W} + \vec{w}''$.

In steady state conditions, the above equation becomes

$$\vec{\nabla}(\rho \vec{W} \hat{b}_2) = -\vec{\nabla}(\rho \vec{W}'' n'' b_2) - \vec{\nabla}(\rho \vec{W} k'' b_2) + \vec{\nabla}(\vec{\tau}^s \vec{W} b_2) + b_2 Q_b \quad (2.3.52)$$

The secondary stress term can be decomposed, in analogy with the viscous shear stress contributions in a pseudo dissipation term $(\vec{\tau}^s \cdot \vec{\nabla}) \vec{W}$ and an energy producing term $(\vec{W} \cdot \vec{\nabla}) \vec{\tau}^s$. Sehra and Keerebrock (1981) postulated that the former term plus the kinetic energy term $\vec{\nabla}(\rho \vec{W} k'' b_2)$ were lost to the main flow and hence dissipated, leading to an irreversible entropy production.

However, there is presently too little experimental evidence to confirm or infirm this hypothesis.

2.3.5. Blade-to-Blade Flow Equations in the Averaged Flow Model

Since the through-flow is represented by an average flow, the only consistent assumption with regard to the blade-to-blade flows consists in assuming the corresponding streamsurfaces to be surfaces of revolution.

In (θ, m, n) coordinates, the blade-to-blade flow equations are obtained by considering the tangential component of the momentum equations for a streamsheet of thickness $B_1 = B_1(m)$. Therefore one obtains exactly the same equations as described in section 2.2.5.

2.3.6. Quasi-Three Dimensional Interaction for the Averaged Flow Model

The only quasi-three dimensional interaction possible here is the simplified interaction whereby the role of the mean streamsheet is played by the averaged flow considered in a true meridional plane.

The blade-to-blade streamsheet thickness B_1 as well as the location of the meridional streamlines m are an output of the through-flow computation of the averaged flow. The averaged flow is first computed with an initial approximation whereby all the secondary stresses are set to zero, that is, an axisymmetric flow approximation. This delivers also the boundary conditions on the different blade-to-blade sections. After the computation of the blade-to-blade flows an estimation of the interaction terms can be obtained from the blade-to-blade flows distribution, but also from additional, direct estimations of secondary flows and streamwise vorticity, Hawthorne (1955). A new iteration cycle can then be initiated for the through-flow including the interaction terms.

This procedure has been applied, and developed into a prediction and design system, by Jennions and Stow (1985), who performed also a detailed investigation of the comparative influence of the different

contributions to the radial equilibrium equation, including the interaction terms.

Relation between streamsurface and averaged formulations

The question arises actually in the description of turbomachinery flows as to the equivalence of the averaged flow representation and the mean streamsheet representation used in the simplified quasi-three dimensional flow description discussed in the previous section. This topic has been discussed in particular by Horlock and Marsh (1971).

If a mean streamsheet is defined by angles β' and ϵ' , is there a choice of values of β' and ϵ' which will render the two representations identical ?

Comparing the equations of the two models, a first conclusion arises from the energy equations (2.2.54) and (2.3.35). It is clear that neither the total energy of the averaged flow \bar{I} , nor the averaged total energy \tilde{I} , are able to represent the total energy along the mean S2 streamsurface. For a steady state flow, equation (2.2.54) gives with the definitions (2.2.14), (2.2.15) and the orthogonality relation (2.2.19)

$$w_m \frac{\partial \bar{I}}{\partial m} = -(w_\theta \frac{\partial \bar{I}}{\partial \theta}) \quad (2.3.53)$$

while equation (2.3.36) leads to

$$\bar{\rho} \tilde{W}_m \frac{\partial \tilde{I}}{\partial m} = - \frac{1}{b_2 r} \left[\frac{\partial}{\partial r} (\bar{\rho} \tilde{W}_r \tilde{I}'' b_2 r) + \frac{\partial}{\partial z} (\bar{\rho} \tilde{W}_z \tilde{I}'' b_2 r) \right] \quad (2.3.54)$$

Unless the right hand sides of both equations are zero, which is the case in an axisymmetric flow, no general choice of \tilde{I} would render the energy fluxes of the interaction terms zero. With regard to the body forces in the two models, a comparison has to take into account the contributions represented by equation (2.3.22).

If the pressure variation between pressure and suction surface, at a constant radial and axial position, is linear, equation (2.3.22) shows that the force $\rho \vec{f}_B$ becomes identical to the corresponding term in equation (2.2.8) if the mean S2 streamsurface is selected to be identical with the camber line.

Indeed, with this assumption the body force equation (2.2.30) becomes

$$\rho \vec{f}_B = - \vec{n} \left(\frac{\partial p}{\partial \theta} \right) = - \vec{n} \left(\frac{p_s - p_p}{b_2 s} \right) \quad (2.3.55)$$

and is identical to $\rho f^{(1)}$ if $\beta' = \beta'_1$ and $\epsilon' = \epsilon'_1$.

However, for a more general pressure variation law, the two body forces will not be equal, unless the blade thickness is constant or zero. This corresponds to an infinitely thin blade and a mean streamsheet following the blade surface.

In addition, as discussed previously the interaction terms in the momentum equations are non-negligible except for lightly loaded blades generating negligible secondary flow effects. This would be the case for instance for highly spaced, low cambered cascade blades or with thin, many bladed cascades.

Some direct estimations in simplified cases of the different contributions to various flow representations can be found in Horlock and Marsh (1971).

It is to be concluded from these considerations, that in general, it is not possible to define a mean S2 streamsurface on which the flow variations are identical to the averaged flow variations. Considering that the averaged flow model describes correctly the behavior of the real physical average flow over the blade spacing, the flow on a mean streamsurface will not be able to represent correctly the averaged flow.

Only in the hypothetical case of an axisymmetric flow, will both models be identical. Therefore, the interpretation of the calculated local behavior of the flow variables along a mean S2 streamsurface should be taken with caution when considering them as representative of the averaged actual flow.

2.4. THROUGH-FLOW COMPUTATIONAL METHODS

Several methods have been developed for the numerical resolution of the through-flow equations in an arbitrary, multistage, turbomachine and they can be classified in two broad families. The first family is based on the solution of the momentum and continuity equations for the physical variables, while the second family is based on the introduction of a streamfunction in the meridional coordinates (r,z) leading to a second order partial differential equation for the streamfunction.

Within the first family, the streamline curvature method is based on an equation for the meridional velocity $w_m (=v_m)$, along a given calculation station, obtained from the stationary momentum equation. The dependence of the flow on the other coordinate is expressed through the curvature of the meridional projection of the streamlines; hence the name of the method. The streamline curvature method was developed for through-flow computations in its contemporary form in the early sixties, Katsanis (1964), (1966), Smith (1966), Novak (1967), Jansen and Moffatt (1967) and is still widely used.

The streamfunction approach was introduced by Wu (1952) in a finite difference discretization and renamed matrix through-flow method by Marsh (1968). The same approach has been followed by Davis and Millar (1972), (1976), Davis (1975), Biniaris (1975), Bosman and Marsh (1974), Bosman and El Shaarawi (1977).

The discretization of the same streamfunction equations by finite elements has been introduced independently by Adler and Krimmerman (1974) and Hirsch and Warzee (1974), (1976).

The various methods will be discussed in this section from the point of view of the numerical approach, leaving aside any detailed considerations with regard to the necessary empirical input under the form of loss coefficients and turning angles as discussed in section 2.2.1.

2.4.1. Axisymmetric Through-Flow Equations

The current approximations in through-flow computations assume relative steady flow situations at constant wheel speed ωr and some form of axisymmetry of the flow configuration. Actually, within the streamsurface approach, the equations along the S2 streamsheet are formally identical to the axisymmetric flow equations since the replacement of the streamsurface derivatives by ordinary derivatives leads to the axisymmetric equations. Hence, within the streamsurface approach, the distinction between the flow along an arbitrary S2 streamsheet and an axisymmetric flow is a matter of interpretation, the numerical resolution techniques being identical in both cases.

This is not the case within the passage averaged model, since the extra terms represented by the secondary stresses $\vec{V} \cdot \vec{\tau} = S$ in the momentum

equations and by the additional energy exchange and dissipation terms in the energy equations, vanish only in the axisymmetric assumption. Within a complete quasi-three-dimensional computation, as discussed in section 2.3.6, the first step of the calculation will be based on an axisymmetric through-flow, while the next iterations will introduce some estimations of the interaction terms between the averaged flow and the non-axisymmetric contributions, and take into account their contributions to the momentum equations as well as on the energy and entropy equations. Since the basic approximation is based on the axisymmetric assumption, we will consider in the following all methods as applied to the axisymmetric through-flow models.

As shown in the previous sections, the through-flow equations consist of the steady state form of the mass conservation equation, one of the meridional (axial, radial or any combination such as the N-component) projections of the momentum conservation law, the tangential momentum equations, the energy conservation and the entropy equation connecting the stagnation pressure variation to the empirical loss coefficients.

The through-flow equations can be summarized, within the axisymmetric assumption as follows, in cylindrical coordinates

Continuity equation

$$\frac{\partial}{\partial r} (\rho b r w_r) + \frac{\partial}{\partial z} (\rho b r w_z) = 0 \quad (2.4.1)$$

Radial equilibrium equation

$$w_m \frac{\partial}{\partial m} w_r = - \frac{1}{\rho} \frac{\partial p}{\partial r} + \frac{v_\theta^2}{r} + F_{fr} + f_{Br} \quad (2.4.2)$$

Alternate form

$$w_z \left(\frac{\partial}{\partial z} w_r - \frac{\partial}{\partial r} w_z \right) = T \frac{\partial s}{\partial r} - \frac{\partial I}{\partial r} + F_{fr} + f_{Br} + \frac{w_\theta}{r} \frac{\partial}{\partial r} (r v_\theta) \quad (2.4.3)$$

Axial momentum component

$$w_m \frac{\partial}{\partial m} w_z = - \frac{1}{\rho} \frac{\partial p}{\partial z} + F_{fz} + f_{Bz} \quad (2.4.4)$$

Alternate form

$$w_r \left(\frac{\partial}{\partial r} w_z - \frac{\partial}{\partial z} w_r \right) = T \frac{\partial s}{\partial z} - \frac{\partial I}{\partial z} + \frac{w_\theta}{r} \frac{\partial}{\partial z} (rv_\theta) + F_{fz} + f_{Bz} \quad (2.4.5)$$

Tangential momentum component

$$\frac{1}{r} w_m \frac{\partial}{\partial m} (rv_\theta) = F_{f\theta} + f_{B\theta} \quad (2.4.6)$$

Energy equation

$$\rho w_m \frac{\partial I}{\partial m} = 0 \quad (2.4.7)$$

Entropy equation

The friction force $\vec{F}_f = -F_f \vec{i}_w$ is defined by

$$T w_m \frac{\partial s}{\partial m} = -\vec{w} \cdot \vec{F}_f = w \cdot F_f \quad (2.4.8)$$

and the meridional convection operator is defined by

$$w_m \frac{\partial}{\partial m} = w_r \frac{\partial}{\partial r} + w_z \frac{\partial}{\partial z} \quad (2.4.9)$$

The body force is normal to the streamsurface S2, in the streamsurface approach, or to the mean camber line in the averaged formulation, under the axisymmetric assumption, that is

$$\vec{f}_B = r f_B \vec{n} \quad (2.4.10)$$

according to equations (2.2.30) to (2.2.32) or equations (2.3.22) in the appropriate interpretation with

$$\frac{n_r}{n_\theta} = -\tan \epsilon' \quad \frac{n_z}{n_\theta} = -\tan \beta' \quad (2.4.11)$$

and

$$\vec{f}_B \cdot \vec{w} = 0 \quad (2.4.12)$$

For the averaged flow model it is assumed that the flow is tangent to the mean camber line, according to equations (2.3.18) and (2.3.22).

The above equations are valid outside the boundary layer regions, since the friction force \vec{F}_f is not resolved and is related to overall empirical loss coefficients. However the complete through flow is influenced by the end wall boundary layers, through the blockage effect introduced by their displacement thickness and through their effect on the overall energy exchange process, Smith (1969).

The passage averaged equations allow in addition to define a coherent interaction between the meridional through-flow and the end-wall boundary layers developing along the hub and shroud walls of a turbomachine, figure 2.4.1.

A consistent theory describing the influence and interaction of the end wall regions and the main flow has been presented by Mellor and Wood (1971), and further extended by Hirsch (1974), (1976); Horlock and Perkins (1974), De Ruyck, Hirsch and Kool (1979), De Ruyck and Hirsch (1981), (1983).

Within the passage-averaged flow representation, the mainstream through flow will be described, for instance by the radial component of the momentum equation in an axial flow machine, in addition to the continuity equation and the energy and entropy laws. Within the same representation, the end wall boundary layer equations will make use of the other two components of the momentum equations.

2.4.2. The Streamline Curvature Method

The streamline curvature method is based on the transformation of the "meridional" momentum equation, that is either the radial or axial component or the projection of the momentum equation along any direction in the (r,z) surface, into an ordinary differential equation for the meridional velocity w_m in function of the distance along selected calculation stations joining corresponding points on the hub and shroud surfaces.

An arbitrary calculation station is displayed on figure 2.4.2, joining two points A and B on the hub and shroud surfaces. The station may be curved and is defined by the local angle γ with respect to the local radial direction. The angle γ is defined as positive from the radial axis towards the station AB. Hence γ is positive on figure 2.4.2.

The distance along the calculation station AB is denoted by l and an equation is sought for the variation dw_m/dl along that station AB.

The whole computational procedure consists in sweeping through the meridional section of the machine, from a calculation station at inlet

of the machine towards the outlet station, solving for the radial distribution of flow properties along each station. The meridional velocity distribution along a calculation station is adapted in order to satisfy mass flow conservation along each station and the whole procedure is repeated until convergence is reached. The radial flow distributions at different stations have to be consistent with each other and the normal acceleration which a fluid particle undergoes has to be taken into account as it influences the interaction of flow properties between successive stations. This is obtained through assumptions for the meridional streamline shape and its slope and curvature as it interconnects the different stations. The details of the procedure are given in the following.

The basic equation for dw_m/dl can be obtained in a variety of ways and written in many different, but equivalent forms, Katsanis (1964), (1966), Smith (1966), Novak (1967), Wennerstrom (1974).

Defining a total force vector \vec{F}^T

$$\vec{F}^T = \vec{F}_f + \vec{f}_B \quad (2.4.13)$$

the radial equilibrium equation becomes

$$w_m \frac{\partial}{\partial m} w_r = - \frac{1}{\rho} \frac{\partial p}{\partial r} + \frac{v_\theta^2}{r} + F_r^T \quad (2.4.14)$$

or

$$w_z \left(\frac{\partial}{\partial z} w_r - \frac{\partial}{\partial r} w_z \right) = T \frac{\partial s}{\partial r} - \frac{\partial I}{\partial r} + F_r^T + \frac{w_\theta}{r} \frac{\partial}{\partial r} (rv_\theta) \quad (2.4.15)$$

while the axial component takes the form

$$w_m \frac{\partial}{\partial m} w_z = - \frac{1}{\rho} \frac{\partial p}{\partial z} + F_z^T \quad (2.4.16)$$

or

$$w_r \left(\frac{\partial}{\partial r} w_z - \frac{\partial}{\partial z} w_r \right) = T \frac{\partial s}{\partial z} - \frac{\partial I}{\partial z} + \frac{w_\theta}{r} \frac{\partial}{\partial z} (rv_\theta) + F_z^T \quad (2.4.17)$$

If the complete form of the passage averaged equations are solved, \vec{F}^T will be defined by adding the secondary stress term to equation (2.4.13), see equations (2.3.21) to (2.3.30).

Momentum equations along calculation stations

Referring to figure 2.4.2, the derivatives with respect to (r,z) can be replaced by derivatives with respect to m and l along the meridional

streamline and the calculation station AB.

One has, with γ positive when l is located left of the radial axis, as on figure 2.4.2,

$$\frac{\partial}{\partial l} = \cos \gamma \frac{\partial}{\partial r} - \sin \gamma \frac{\partial}{\partial z} \quad (2.4.18)$$

$$\frac{\partial}{\partial m} = \sin \sigma \frac{\partial}{\partial r} + \cos \sigma \frac{\partial}{\partial z} \quad (2.4.19)$$

or

$$\cos(\sigma - \gamma) \frac{\partial}{\partial r} = \cos \sigma \frac{\partial}{\partial l} + \sin \gamma \frac{\partial}{\partial m} \quad (2.4.20)$$

and

$$\cos(\sigma - \gamma) \frac{\partial}{\partial z} = \cos \gamma \frac{\partial}{\partial m} - \sin \sigma \frac{\partial}{\partial l} \quad (2.4.21)$$

The radial and axial momentum equations are combined by multiplying equation (2.4.14) by $\cos \gamma$ and equation (2.4.16) by $(-\sin \gamma)$ and adding up, applying equation (2.4.18)

$$w_m (\cos \gamma \frac{\partial}{\partial m} w_r - \sin \gamma \frac{\partial}{\partial m} w_z) = -\frac{1}{\rho} \frac{\partial p}{\partial l} + \frac{v_\theta^2}{r} \cos \gamma + F_l^T \quad (2.4.22)$$

where

$$F_l^T = \cos \gamma F_r^T - \sin \gamma F_z^T \quad (2.4.23)$$

is the projection of the total force \vec{F}^T on the l direction.

With

$$w_r = w_m \sin \sigma \quad (2.4.24)$$

one has

$$\frac{\partial}{\partial m} w_r = \sin \sigma \frac{\partial}{\partial m} w_m - \frac{w_m \cdot \cos \sigma}{R_m} \quad (2.4.25)$$

where the radius of curvature of the meridional streamline R_m has been introduced according to equation (A.6.40)

$$\frac{-1}{R_m} = \frac{\partial \sigma}{\partial m} \quad (2.4.26)$$

Note that with this definition R_m is negative for a concave streamline, such as shown on figure 2.4.2.

Similarly

$$\frac{\partial}{\partial m} w_z = \cos \sigma \frac{\partial}{\partial m} w_m + \frac{\sin \sigma}{R_m} \cdot w_m \quad (2.4.27)$$

leading to

$$\frac{1}{\rho} \frac{\partial p}{\partial l} = \frac{w_m^2}{R_m} \cos(\sigma - \gamma) - \sin(\sigma - \gamma) w_m \frac{\partial}{\partial m} w_m + \frac{v_\theta^2}{r} \cos \gamma + F_1^T \quad (2.4.28)$$

This equation has to be coupled to the energy equation in order to obtain an equation for $\partial_l w_m$. This is achieved explicitly by using Crocco's form of the momentum equations, equations (2.4.15) and (2.4.16).

The same procedure leads to the equation for $w_m = w_m(l)$ along the calculation station AB :

$$w_m \frac{\partial}{\partial l} w_m = \sin(\sigma - \gamma) w_m \frac{\partial}{\partial m} w_m - \cos(\sigma - \gamma) \frac{w_m^2}{R_m} - T \frac{\partial s}{\partial l} + \frac{\partial I}{\partial l} - \frac{w_\theta}{r} \frac{\partial}{\partial l} (rv_\theta) - F_1^T \quad (2.4.29)$$

The estimation of the gradients of s , rv_θ and I is performed according to the discussion of section 2.2.1. Note that the particular case $\gamma=0$ corresponds to a radial station, while $\gamma=\pm\pi/2$ is an axially oriented station. For a radial station, one obtains

$$w_m \frac{\partial}{\partial r} w_m = \sin \sigma w_m \frac{\partial}{\partial m} w_m - \cos \sigma \frac{w_m^2}{R_m} - T \frac{\partial s}{\partial r} + \frac{\partial I}{\partial r} - \frac{w_\theta}{r} \frac{\partial}{\partial r} (rv_\theta) - F_r^T \quad (2.4.30)$$

Outside bladed regions, the force components F_1^T vanish as well as the meridional entropy and total energy gradients because of the assumption of axisymmetry. However, if wake effects are taken into account these terms might not be zero and have to be estimated through the introduction of appropriate wake flow models, Hirsch (1975), Hearsey (1975).

When the computing station AB is orthogonal to the meridional streamline, that is, $\gamma=\sigma$, the first term on the right hand side of equation (2.4.29), describing the streamwise acceleration due to the meridional variation of the meridional velocity component w_m , vanishes.

However, for arbitrary calculation stations, this will not be the case

and this term has to be evaluated. In early through-flow calculations in axial flow machines, with calculation stations located only outside the bladed regions this term was often neglected. In more general cases and when calculation stations are located inside blade rows, this will not be justified and the term $\frac{\partial w_m}{\partial m}$ has to be taken into account. So more that its variation might become important at transonic Mach number ranges. Indeed, equation (2.2.84) shows that the variation of mass flux ρw_m is related to the variation of w_m by the following equation valid for isentropic, isoenergetic conditions, $H=\text{constant}$, in an absolute reference system

$$\delta(\rho w_m) = \rho(1 - M_m^2)\delta w_m - \rho M_m M_\theta \cdot \delta v_\theta \quad (2.4.31)$$

Hence an alternative form of the meridional velocity equation is obtained from an explicit evaluation of $\frac{\partial}{\partial m} w_m$.

Evaluation of meridional streamwise acceleration - Design problem

In order to evaluate the term $\frac{\partial w_m}{\partial m}$, the continuity equation is introduced with equations (2.4.20) and (2.4.21), leading to

$$\frac{w_m}{\rho b r} \frac{\partial}{\partial m} (\rho b r) + \frac{1}{\cos(\gamma + \sigma)} \left[w_m \frac{\partial \sigma}{\partial l} + \cos(\sigma - \gamma) \frac{\partial}{\partial m} w_m + \sin(\sigma - \gamma) \frac{w_m}{R} \right] = 0 \quad (2.4.32)$$

Since, in general the turbomachinery flow is not isentropic because of the friction force F_f representing the stagnation pressure losses, equation (2.2.82) has to be replaced by the more general relation,

$$\frac{\delta \rho}{\rho} = \frac{\delta h}{a^2} - \frac{\delta s}{R} \quad (2.4.33)$$

where δh is obtained from the energy equation (2.4.7)

Here R has been used for the gas constant in order to avoid confusion with the radius r .

Equation (2.4.31) is to be replaced by a more general expression obtained from (2.4.33) where the definition of I has been used. Since the right hand side of equation (2.4.31) corresponds to the first term of (2.4.32), the density variation in the m -direction becomes

$$\frac{w_m}{\rho} \cdot \frac{\partial \rho}{\partial m} = -M_m^2 \frac{\partial}{\partial m} w_m - M_\theta^{(r)} M_m \frac{\partial}{\partial m} w_\theta + \frac{w_m}{r} \cdot \frac{u^2}{a^2} \sin \sigma - \frac{w_m}{R} \frac{\partial s}{\partial m} \quad (2.4.34)$$

where the relative Mach number component $M_\theta^{(r)}$ is introduced

$$M_{\theta}^{(r)} = \frac{w_{\theta}}{a} = M_{\theta} - \frac{u}{a} \quad (2.4.35)$$

with the definition $\sin \sigma = \partial r / \partial m$.

Introducing equation (2.4.34) into equation (2.4.32) leads to the following expression for the acceleration term $\partial w_m / \partial m$

$$\begin{aligned} (1-M_m^2) \frac{\partial}{\partial m} w_m = & -w_m \left[\frac{1}{b} \frac{\partial b}{\partial m} + (1 + \frac{u^2}{a^2}) \frac{\sin \sigma}{r} + \frac{1}{\cos(\sigma-\gamma)} \frac{\partial \sigma}{\partial l} + \frac{\tan(\sigma-\gamma)}{R_m} \right] \\ & + M_{\theta}^{(r)} M_m \frac{\partial}{\partial m} w_{\theta} + \frac{w_m}{R} \frac{\partial s}{\partial m} \end{aligned} \quad (2.4.36)$$

The meridional derivative of the tangential relative velocity can be eliminated through the use of the tangential momentum equation (2.4.6), written as

$$\frac{w_m}{r} \frac{\partial}{\partial m} (r v_{\theta}) = F_{\theta}^T \quad (2.4.37)$$

where F_{θ}^T will generally be taken to be zero outside the blade rows. In the design problem, $r v_{\theta}$ is specified within a blade row, while in the analysis case v_{θ} has to be expressed in function of meridional velocity and the specified flow angles. The $\partial w_{\theta} / \partial m$ term in equation (2.4.36) becomes

$$M_{\theta}^{(r)} M_m \frac{\partial}{\partial m} w_{\theta} = \frac{w_{\theta}}{a^2} F_{\theta}^T - w_m [M_{\theta}^2 - (\frac{u}{a})^2] \frac{\sin \sigma}{r} \quad (2.4.38)$$

leading to the following form for the meridional variation of w_m ,

$$\begin{aligned} (1-M_m^2) \frac{\partial}{\partial m} w_m = & -w_m \left[\frac{1}{b} \frac{\partial b}{\partial m} + \frac{1}{\cos(\gamma+\sigma)} \frac{\partial \sigma}{\partial l} + \frac{\tan(\sigma-\gamma)}{R_m} + (1+M_{\theta}^2) \frac{\sin \sigma}{r} \right] \\ & + \frac{w_{\theta}}{a^2} F_{\theta}^T + \frac{w_m}{R} \frac{\partial s}{\partial m} \end{aligned} \quad (2.4.39)$$

Introduced in equation (2.4.29), the basic equation written as an ordinary differential equation for $w_m = w_m(l)$ along the station AB, is obtained

$$w_m \frac{\partial}{\partial l} w_m = A w_m^2 + B \quad (2.4.40)$$

$$A = \frac{1 - M_m^2 \cos^2(\sigma - \gamma)}{(1 - M_m^2) R_m \cos(\sigma - \gamma)} - \frac{\sin(\sigma - \gamma)}{1 - M_m^2} \left[\frac{1}{b} \frac{\partial b}{\partial m} + \frac{1}{\cos(\sigma - \gamma)} \frac{\partial \sigma}{\partial l} + \frac{\sin \sigma}{r} (1 + M_\theta^2) \right] + \frac{\sin(\sigma - \gamma)}{(1 - M_m^2) a^2} \cdot \frac{w_\theta}{w_m} \cdot F_\theta^T + \frac{\sin(\sigma - \gamma)}{R(1 - M_m^2)} \frac{\partial s}{\partial m} \quad (2.4.41)$$

$$B = \frac{\partial I}{\partial l} - T \frac{\partial s}{\partial l} - \frac{w_\theta}{r} \frac{\partial}{\partial l} (rv_\theta) - F_1^T \quad (2.4.42)$$

The equations (2.4.40) to (2.4.42) are to be used outside blade rows with

$$F_\theta^T = 0 \quad \text{outside blade rows} \quad (2.4.43)$$

and also inside blade rows with a design option whereby rv_θ is specified as the input information from the blade-to-blade flow. Note also the appearance of the $(1 - M_m^2)$ factor which is an expression of the range of ellipticity of the through-flow equations as discussed in section 8.2, when rv_θ is specified.

When flow angles are specified, - the analysis case - the terms containing derivatives of tangential velocity components have to be explicitly calculated in function of meridional velocity and flow angle.

Analysis Problem - Flow angles specified

With

$$\frac{v_\theta}{w_m} = \tan \alpha = \frac{w_\theta}{w_m} + \frac{u}{w_m} = \tan \beta + \frac{u}{w_m} \quad (2.4.44)$$

one has

$$\begin{aligned} \frac{\partial}{\partial m} (rv_\theta) &= w_m \frac{\partial}{\partial m} (r \tan \alpha) + r \tan \alpha \frac{\partial}{\partial m} w_m \\ &= w_m \frac{\partial}{\partial m} (r \tan \beta) + r \tan \beta \frac{\partial}{\partial m} w_m + 2u \sin \sigma \end{aligned} \quad (2.4.45)$$

and

$$\begin{aligned} \frac{\partial}{\partial l} (rv_\theta) &= w_m \frac{\partial}{\partial l} (r \tan \alpha) + r \tan \alpha \frac{\partial}{\partial l} w_m \\ &= w_m \frac{\partial}{\partial l} (r \tan \beta) + r \tan \beta \frac{\partial}{\partial l} w_m + 2u \cos \gamma \end{aligned} \quad (2.4.46)$$

Within blade rows, the full dependence of $\partial w_m / \partial m$ on the other flow variables, in particular the flow angle β , becomes instead of equation (2.4.36)

$$(1 - M_m^2 - M_\theta^{(r)^2}) \frac{\partial}{\partial m} w_m = -w_m \left[\frac{1}{b} \frac{\partial b}{\partial m} + \frac{1}{\cos(\sigma - \gamma)} \frac{\partial \sigma}{\partial l} + \frac{\tan(\sigma - \gamma)}{R_m} \right. \\ \left. - M_\theta^{(r)} M_m \frac{\partial}{\partial m} \tan \beta + \left(1 + \frac{u^2}{a^2}\right) \frac{\sin \sigma}{r} \right] + \frac{w_m}{R} \frac{\partial s}{\partial m} \quad (2.4.47)$$

Introducing equation (2.4.47) in equation (2.4.29) and replacing the term $w_\theta / r \frac{\partial}{\partial l}(rv_\theta)$ with equation (2.4.46), leads to the following form for the momentum equation

$$(1 + \tan \beta \tan \alpha) w_m \frac{\partial}{\partial l} w_m = A_1 w_m^2 + B_1 \quad (2.4.48)$$

$$A_1 = - \frac{1 - M^{(r)^2} \cos^2(\sigma - \gamma)}{(1 - M^{(r)^2}) R_m \cos(\sigma - \gamma)} - \frac{\sin(\sigma - \gamma)}{1 - M^{(r)^2}} \left[\frac{1}{b} \frac{\partial b}{\partial m} + \frac{1}{\cos(\sigma - \gamma)} \frac{\partial \sigma}{\partial l} + \frac{\sin \sigma}{r} \right. \\ \left. \left(1 + \frac{u}{a}\right)^2 - \frac{1}{R} \frac{\partial s}{\partial m} \right] \quad (2.4.49)$$

$$B_1 = \frac{\partial I}{\partial l} - T \frac{\partial s}{\partial l} - F_1^T \quad (2.4.50)$$

Note the appearance of the factor $(1 - M^{(r)^2})$ in the denominator. This form is limited to problems with fully subsonic relative Mach numbers (or fully supersonic).

In practical computations inside blade rows, it might be more appropriate to calculate $\partial w_m / \partial m$ directly by a finite difference approximation, using values from the previous iteration and apply equation (2.4.29) with equation (2.4.46) introduced for the last term when dealing with the analysis case.

For incompressible flows, equation (2.4.32) becomes

$$\frac{w_m}{b} \frac{\partial b}{\partial m} + \frac{w_m \sin \sigma}{r} + \frac{1}{\cos(\sigma - \gamma)} \left[w_m \frac{\partial \sigma}{\partial l} + \frac{\sin(\sigma - \gamma)}{R_m} w_m \right] + \frac{\partial}{\partial m} w_m = 0 \quad (2.4.51)$$

while equation (2.4.28) can be transformed to the following form after the introduction of the rotary stagnation pressure

$$p^* = p + \rho \frac{\vec{v}^2}{2} - \rho u v_\theta = p + \rho \frac{\vec{w}^2}{2} - \rho \frac{u^2}{2} \quad (2.4.52)$$

$$\frac{1}{\rho} \frac{\partial p^*}{\partial l} = \frac{w_m^2}{R_m} \cos(\sigma - \gamma) - \sin(\sigma - \gamma) w_m \frac{\partial}{\partial m} w_m + w_m \frac{\partial}{\partial l} w_m + \frac{w_\theta}{r} \frac{\partial}{\partial l} (rv_\theta) + F_1^T \quad (2.4.53)$$

Combining both equations, one obtains the ordinary differential equation for $w_m = w_m(l)$ valid for incompressible flows

$$w_m \frac{\partial}{\partial l} w_m = A w_m^2 + B \quad (2.4.54)$$

with

$$A = - \frac{1}{R_m \cos(\sigma - \gamma)} - \sin(\gamma + \sigma) \left[\frac{1}{b} \frac{\partial b}{\partial m} + \frac{1}{\cos(\sigma - \gamma)} \frac{\partial \sigma}{\partial l} + \frac{\sin \sigma}{r} \right] \quad (2.4.55)$$

$$B = \frac{1}{\rho} \frac{\partial p^*}{\partial l} - \frac{w_\theta}{r} \frac{\partial}{\partial l} (rv_\theta) - F_1^T \quad (2.4.54)$$

The above equations are the basic formulation for streamline curvature methods, coupled to the mass flow conservation law in integral form, stating that the mass flow rate \dot{m} is constant throughout the machine. One has, for the mass flow through station AB

$$\dot{m}_{AB} = \dot{m} = 2\pi \int_{AB} \rho w_m \cos(\sigma - \gamma) b \cdot B^{(e)} r dl \quad (2.4.57)$$

where $B^{(e)}$ is the blockage factor introduced by the presence of the end wall boundary layers. If δ_H^* and δ_T^* are respectively the hub and tip displacement thickness for the meridional velocity profiles along the station AB, then the factor $B^{(e)}$ is defined by

$$\dot{m}_{AB} = 2\pi \int_{l_A + \delta_H^*}^{l_B - \delta_T^*} \rho w_m \cos(\sigma - \gamma) b r dl \quad (2.4.58)$$

For uniform flow conditions, one has equating (2.4.57) and (2.4.58)

$$B^{(e)} \cdot S_{AB} = S_{AB} - 2\pi r_A \delta_H^* - 2\pi r_B \delta_T^* \quad (2.4.59)$$

where S_{AB} is the geometrical section through AB, given by

$$S_{AB} = 2\pi \int_{AB} r dl = 2\pi \left(\frac{r_A + r_B}{2} \right) \sqrt{(r_B - r_A)^2 + (z_B - z_A)^2} \quad (2.4.60)$$

for a straight, non curved, station AB.

Equation (2.4.59) can be used to define the blockage factor $B^{(e)}$ when the displacement thicknesses are known or estimated.

Determination of force terms

The total force component F_1^T can be obtained from the tangential momentum equation (2.4.37) and the definitions (2.4.8) to (7.4.12).

The blade force component f_{B1} is defined by

$$\begin{aligned} f_{B1} &= f_{Br} \cos \gamma - f_{Bz} \sin \gamma \\ &= f_{B\theta} (\tan \beta' \cdot \sin \gamma - \tan \epsilon' \cdot \cos \gamma) \end{aligned} \quad (2.4.61)$$

If a blade angle ϵ'_b is defined in the plane (AB, θ) that is by a section along the calculation station, then

$$\begin{aligned} \tan \epsilon'_b &= r \left(\frac{\partial \theta}{\partial l} \right) \\ &= r \left(\frac{\partial \theta}{\partial r} \right) \frac{\partial r}{\partial l} + r \left(\frac{\partial \theta}{\partial z} \right) \frac{\partial z}{\partial l} \\ &= \tan \epsilon' \cdot \cos \gamma - \tan \beta' \sin \gamma \end{aligned} \quad (2.4.62)$$

Hence, the blade force component f_{B1} can be written as

$$f_{B1} = -f_{B\theta} \tan \epsilon'_b \quad (2.4.63)$$

The friction force is obtained from the entropy variation, as

$$\begin{aligned} F_{f\theta} &= -F_f \frac{w_\theta}{w_m} = -T \frac{w_m w_\theta}{w^2} \frac{\partial s}{\partial m} \\ &= -T \sin \beta \cos \beta \frac{\partial s}{\partial m} \end{aligned} \quad (2.4.64)$$

The tangential component of the total force is given by

$$F_\theta^T = F_{f\theta} + f_{B\theta} = \frac{w_m}{r} \frac{\partial}{\partial m} (rv_\theta) \quad (2.4.65)$$

and from equation (2.4.63)

$$\begin{aligned}
 f_{B1} &= -\tan \epsilon'_b \frac{w_m}{r} \frac{\partial}{\partial m} (rv_\theta) + F_{f\theta} \tan \epsilon'_b \\
 &= -\tan \epsilon'_b \cdot \frac{w_m}{r} \frac{\partial}{\partial m} (rv_\theta) - T \frac{\partial s}{\partial m} \sin \beta \cos \beta \tan \epsilon'_b
 \end{aligned}
 \tag{2.4.66}$$

The 1-component of the friction force is obtained from

$$\begin{aligned}
 F_{f1} &= F_{fr} \cos \gamma - F_{fz} \sin \gamma \\
 &= -F_f \left(\frac{w_r}{w} \cos \gamma - \frac{w_z}{w} \sin \gamma \right) \\
 &= -F_f \cos \beta \sin (\sigma - \gamma) \\
 &= -T \frac{\partial s}{\partial m} \cdot \cos^2 \beta \sin (\sigma - \gamma)
 \end{aligned}
 \tag{2.4.67}$$

Finally, the 1-component of the total force can be calculated from

$$\begin{aligned}
 F_1^T &= F_{f1} + f_{B1} \\
 &= -\tan \epsilon'_b \frac{w_m}{r} \frac{\partial}{\partial m} (rv_\theta) - T \frac{\partial s}{\partial m} [\cos \beta \sin (\sigma - \gamma) + \sin \beta \tan \epsilon'_b] \cos \beta
 \end{aligned}
 \tag{2.4.68}$$

In duct regions, outside blade rows, $f_{B1} = 0$ and eventually only the friction force might be accounted for due to wake effects. Then F_{f1} is given by equation (2.4.67).

2.4.3: Numerical Techniques for Streamline Curvature Methods

The complete numerical procedure for streamline curvature methods can be described by the following steps and considerations.

a. Initial mesh point distribution

Given the meridional cross-section of the machine, calculation stations are distributed between an inlet and an outlet section and the current station is indicated by I (figure 2.4.3).

In addition, the through-flow is divided into a specified number of M streamtubes separated by (M + 1) meridional streamlines, the hub wall being streamline j=1, the shroud wall is streamline j=M+1. Since the streamline slopes σ and curvatures R_m have to be determined at every point (I,j), the positions of the streamlines separating the different streamtubes has to be known. Therefore, from one iteration to the other, the streamline position will be shifted in order to be in accordance with the newly obtained meridional velocity distribution w_m .

This distinguishes the streamline curvature method from classical finite difference or finite element methods, in that the mesh points (I,j) are not fixed in the flow domain but are displaced along the I-stations such as to follow the streamlines. Hence, at any iteration, the j-lines will be considered as formed by streamlines limiting streamtubes of constant mass flow (\dot{m}/M) and displaced at the end of the iteration after the w_m distributions have been obtained at all stations.

An initial location of the streamlines can be obtained by assuming uniform w_m distribution along each calculation station.

b. Estimation of streamline slopes and curvatures

This is a central point in the calculation procedure, since the curvature corresponds to a second derivative of the function $r = r(z)$ along a streamline and its numerical estimation from a limited number of points generates high frequency errors.

One has

$$\frac{1}{R_m} = \frac{d^2r / dz^2}{(1 + \tan^2 \sigma)^{3/2}} \quad (2.4.69)$$

A detailed investigation of various formulas for dr/dz and d^2r/dz^2 along a streamline has been presented by Wilkinson (1970). From this analysis results that the best choice between

i) spline curve fitting on streamline positions and (or) on its derivatives,

ii) standard finite difference formulas of second order accuracy,

iii) various polynomial fittings,

is undoubtedly obtained for the standard finite difference formulas.

Hence the best recommendation is to use the following formulas

$$\left. \frac{dr}{dz} \right|_{I,j} = \frac{1}{2} \left(\frac{r_{I+1,j} - r_{I,j}}{z_{I+1,j} - z_{I,j}} + \frac{r_{I,j} - r_{I-1,j}}{z_{I,j} - z_{I-1,j}} \right) = \tan \sigma_{I,j} \quad (2.4.70)$$

$$\left. \frac{d^2r}{dz^2} \right|_{I,j} = \frac{1}{\frac{z_{I+1,j} - z_{I-1,j}}{2}} \left(\frac{r_{I+1,j} - r_{I,j}}{z_{I+1,j} - z_{I,j}} - \frac{r_{I,j} - r_{I-1,j}}{z_{I,j} - z_{I-1,j}} \right) \quad (2.4.71)$$

Another variant is used by Hearsey (1975), to the same order of accuracy

$$\sigma_{I,j} = \left(\tan^{-1} \frac{r_{I+1,j} - r_{I,j}}{z_{I+1,j} - z_{I,j}} + \tan^{-1} \frac{r_{I,j} - r_{I-1,j}}{z_{I,j} - z_{I-1,j}} \right) \frac{1}{2} \quad (2.4.72)$$

$$= \frac{\sigma_{I,j}^+ + \sigma_{I,j}^-}{2}$$

$$\frac{1}{R_m} = - \frac{\frac{\sigma_{I,j}^+ - \sigma_{I,j}^-}{m_{I+1,j} - m_{I-1,j}}}{2} \quad (2.4.73)$$

The theoretical analysis of Wilkinson has been confirmed by Novak (1976).

Another way of investigating the influence of the estimation of streamline slopes and curvatures on the solution is reported by J. Denton in Hirsch and Denton (1981).

A simple test case was chosen, consisting of a single blade row in an axial channel with a hub wall at constant radius and a casing wall formed by two circular arcs and straight lines such that discontinuities in wall curvature at the leading and trailing edge, from circular to straight lines, and at mid-chord between the two circular arcs, provide severe tests of the approximations.

The number of stations was varied between a coarse grid with no internal stations except at leading and trailing edge and a finer grid with 1, 3 and 5 additional internal stations. Using the same second order difference formulas, it is shown that with no internal stations the curvature at leading edge is underestimated leading to an inaccurate, overpredicted estimation of axial velocity and hence of flow angles. The inadequacy of computations with no internal stations is also confirmed by Novak in the same reference, Hirsch and Denton (1981), page

245. A single internal station covers most of the effects of curvature although the accuracy is moderately improved by additional stations. Similar conclusions on the necessity of including internal stations have also been reached by Frost (1970). At the trailing edge, the curvature is shown to be insensitive to the number of internal stations as a consequence of the imposed values of flow angles.

However, the estimation of the streamline curvature at trailing edge has a strong effect on the prediction of the downstream flow field. This can be shown in various ways, through equation (2.4.29). Assuming that s, I and rv_θ as well as w_m are uniform at trailing edge, the downstream variation of meridional profiles is uniquely influenced by the radius of curvature, since equation (2.4.39) reduces to

$$\tan(\sigma - \gamma) \frac{\partial}{\partial m} w_m = \frac{w_m}{R_m}$$

It can also be shown from actuator disk theories, Horlock (1978) that a shift in streamline of (Δr) will generate a curvature of the order of $\Delta r/(\Delta z)^2$ where Δz is the axial distance between two points and inaccuracies on $1/R_m$ greatly affect the meridional velocity distributions. This is fully confirmed by Denton's model calculation (see figure 2.4.4) where the effect of the number of stations used to calculate the curvature is clearly seen. These effects will be amplified for machines with strong curvatures such as centrifugal flow machines for which the computation could be excessively sensitive to the numerical estimation of the curvature.

c. Determination of flow properties at station I + 1

The flow variables are supposed to be known at station I. Within the axisymmetric approximation the stagnation values at point A at station I + 1 are obtained from the known values at station I in the following way.

The variations of angular momentum and entropy are determined as described in section 2.2.2.

Within a blade row :

$$v_\theta = v_\theta(m) \quad \text{for the design problem}$$

$$\beta = \beta(m) \quad \text{for the analysis problem}$$

$$s = s(m)$$

Outside a blade row :

$$\frac{\partial}{\partial m} (rv_\theta) = 0$$

$$\frac{\partial}{\partial m} s = 0$$

when no wake or mixing effects are considered, otherwise equation (2.4.8) has to be applied. The stagnation temperature in the relative system is obtained from the energy equation .

From

$$I_A = I_C$$

and a perfect gas assumption, one obtains the relative stagnation temperature T_0^* through

$$I = c_p T_0^* - \frac{u^2}{2}$$

Evaluation of the density

The density is evaluated from the velocity field through

$$\rho = \rho^* \left(1 - \frac{\vec{w}^2}{2c_p T_0^*} \right)^{1/\gamma-1} \quad (2.4.74)$$

where the velocities are taken from the previous iteration and ρ_0^* is the stagnation density in the relative system.

From the knowledge of the density, stagnation temperature T_0^* and stagnation pressure p_0^* (obtained from the entropy equation, see equation (2.2.60)) one can estimate the static temperature and speed of sound.

The previous steps allow the determination of all quantities in the right hand side of equation (2.4.40), and the new distribution of meridional velocities along station $I+1$ can be obtained from the integration of the ordinary differential equation (2.4.40).

d. Integration of meridional velocity equation

Various methods can be applied to integrate equation (2.4.40), such as a Runge-Kutta method or, when linearising the coefficients, a first order linear equation is obtained, which can be exactly solved.

Whatever method is applied, an initial value at a certain point is needed to initiate the numerical integration. This reference value of w_m, w_{m0} can be taken at hub, shroud or any point along station $(I+1)$. Generally the value at mid station is chosen that is the value at $j = \frac{M+1}{2}$ and the integration proceeds in both directions from $j = \frac{M+1}{2}$ to $(m+1)$ and from this mid-point to $j=1$. The initial value of w_{m0} is arbitrary and

will be corrected iteratively until the $w_m = w_m(1)$ distribution satisfies the conservation of mass flow at that station up to a prescribed accuracy, see equation (2.4.57).

This is not a trivial step since the sign of the variation of mass flow with w_{m0} depends on the Mach number and is different in subsonic and supersonic regions, following equation (2.4.31). Following Hearsey (1975), Novak (1976), the sign of the correction on w_{m0} is obtained from the variation of mass flow with respect to w_{m0} . Taking into account equation (2.4.31) and (2.4.57), one can write for fixed stagnation conditions and tangential velocity v_θ

$$\frac{\partial \dot{m}}{\partial w_{m0}} = \int \rho(1 - M_m^2) \cdot \frac{\delta w_m}{\delta w_{m0}} \cdot dS \quad (2.4.75)$$

where dS is the area element normal to the station

$$dS = 2\pi r b B^{(e)} dl \cos(\sigma - \gamma) \quad (2.4.76)$$

If the flow angle is fixed instead of v_θ , one has from $w_\theta = w_m \tan \beta$ and equation (2.4.31)

$$\frac{\partial \dot{m}}{\partial w_{m0}} = \int \rho(1 - M^{(r)^2}) \frac{\delta w_m}{\delta w_{m0}} dS \quad (2.4.77)$$

where $M^{(r)}$ is the relative mach number $M^{r^2} = \vec{w}^2/a^2$.

The mass flow rate passes through a maximum at sonic meridional Mach number or sonic relative Mach numbers depending on the formulation of the problem that is, v_θ or β fixed. This is an alternative formulation for the properties of the through-flow equations as discussed in 2.2.1.

The variation ratio $\delta w_m / \delta w_{m0}$ can be evaluated either in an approximate way, through

$$\frac{\delta w_m}{\delta w_{m0}} \approx \frac{w_m}{w_{m0}} \quad (2.4.78)$$

or through a more rigorous way by a direct computation.

With the first assumption, equation (2.4.77) becomes

$$\left(\frac{\partial \dot{m}}{\partial w_{m_0}}\right) = \frac{1}{w_{m_0}} \int \rho(1 - M_m^2) w_m dS \quad v_\theta \text{ fixed} \quad (2.4.79)$$

or

$$\left(\frac{\partial \dot{m}}{\partial w_{m_0}}\right) = \frac{1}{w_{m_0}} \int \rho(1 - M^{(r)^2}) w_m dS \quad \beta \text{ fixed} \quad (2.4.80)$$

The sign of the variations of mass flow with respect to w_{m_0} is positive for subsonic Mach numbers and negative for supersonic velocities. Also, the local mass flow in a streamtube dS is maximum at sonic conditions and when this maximum value is reached the streamtube is said to be choked. The large sensitivity of mass flow with respect to w_m , makes the estimation of w_{m_0} delicate particularly in the vicinity of sonic velocities or choking conditions.

If the Mach number M_m or $M^{(r)}$, according to the problem treated, is subsonic, the computed correction on w_{m_0} can be determined from a relation of the following type, for subsonic flows

$$(w_{m_0})_{\text{new}} = (w_{m_0}) + (\dot{m} - \dot{m}_c) / \left(\frac{\partial \dot{m}}{\partial w_{m_0}}\right) \quad (2.4.81)$$

where \dot{m}_c is the calculated mass flow with the current distribution of w_m and the given w_{m_0} . The same relation is used for supersonic velocities when the supersonic solution is desired.

However, when a subsonic solution for instance, is looked for and the calculated derivative $\partial \dot{m} / \partial w_{m_0}$ is negative, which indicates that the initial chosen value of w_{m_0} is on the supersonic side of the $\dot{m}-w_m$ relation then it is necessary to force $(w_m)_{\text{new}}$ to move towards the subsonic branch and impose a relation such as

$$(w_{m_0})_{\text{new}} = K \cdot w_{m_0} \quad (2.4.82)$$

with $K=0.9$ for instance. In the opposite case, K will be taken greater than 1.

Additional recommendations to control the variations of w_{m_0} are given by Hearsey (1975) and Novak (1976). For instance, for a subsonic solution, $(w_{m_0})_{\text{new}}$ should not be lower than a previous estimation w_{m_0} which led to a supersonic solution and inversely when a supersonic solution is searched.

With the new value of $(w_{m_0})_{\text{new}}$ the numerical integration of the momentum equation (2.4.40) is started again and the (w_{m_0}) values recalculated until conservation of mass flow is achieved to an imposed accuracy.

Instead of the approximation (2.4.78) a better estimation of $(\partial w_m / \partial w_{m_0})$ can be obtained by the Taylor expansion, Hearsey (1975)

$$w_m(1) = w_{m_0} + (1-l_0) \frac{\partial}{\partial l} w_m \quad (2.4.83)$$

from which one obtains

$$\frac{\partial w_m}{\partial w_{m_0}} = \frac{1}{1 - (1-l_0) \frac{\partial}{\partial w_m} \left(\frac{\partial}{\partial l} w_m \right)} \quad (2.4.84)$$

The derivative $\partial / \partial w_m$ ($\partial_l w_m$) can be calculated from the momentum equations (2.4.40) - (2.4.42) or similar forms, (2.4.48) to (2.4.50).

The above procedure can allow the computation of relative supersonic flows in the analysis case, when the type of solution which is sought, subsonic corresponding to $\partial \dot{m} / \partial w_m > 0$, or supersonic $\partial \dot{m} / \partial w_m < 0$ is specified by the user at every station inside a blade row. Otherwise, the present formulation does not allow to select the correct solution due to the non-unique relation between mass flow and Mach number; see also Marsh (1971) for a discussion on this point.

e. Displacement of streamlines

Once the new distributions of meridional velocities, consistent with mass flow, are obtained at all the stations, new estimations of the the streamline positions can be calculated.

Referring to figure 2.4.3, the calculated position of streamline j at station I can be obtained from

$$(\Delta l)_{I,j} = l_{I,j} |_{\text{calculated}} - l_{I,j} |_{\text{old}} = \frac{w_{m,I,j} |_{\text{new}} - w_{m,I,j} |_{\text{old}}}{\left(\frac{\partial}{\partial l} w_m \right)_{I,j}} \quad (2.4.85)$$

A detailed theoretical analysis of the stability of the streamline relocation process has been developed by Wilkinson (1970). From this analysis follows that the repositioning of the streamlines has to be strongly underrelaxed in order to achieve convergent iteration cycles. Based on a simple model of a swirling flow in a cylindrical annulus, an estimation of the optimal relaxation factor can be found. A simplified version of Wilkinson's analysis is presented by Hearsey (1975) and Novak (1976).

According to the problem solved, one has the following relaxation procedure

$$l_{I,j} |_{\text{new}} = l_{I,j} |_{\text{old}} + \mu (l_{I,j} |_{\text{calc.}} - l_{I,j} |_{\text{old}}) \quad (2.4.86)$$

$$\mu = \frac{1}{1 + K(1 - M_m^2) \left(\frac{\Delta r}{\Delta z} \right)^2} \quad (2.4.87)$$

where $\Delta r = l_{\text{shroud}} - l_{\text{hub}}$ is the length of the station and Δz is the meridional distance to the nearest station.

Analysis problem

$$\mu = \frac{1}{1 + K(1 - M(r)^2) \left(\frac{\Delta r}{\Delta z} \right)^2} \quad (2.4.88)$$

The constant K is in both cases of the order of $1/8$ to $1/6$. These values of the optimum relaxation factors tend to zero when the spacing between stations is reduced, that is when the mesh is made finer. Therefore, it is necessary to limit the spacing between stations on the lower side in order to avoid excessive slow convergence rates. The new values of $l_{I,j} |_{\text{new}}$ are then used in order to displace the streamlines and start a new iteration cycle with updated values of streamline slopes and curvature. Another variant is applied by Denton (1978), where the curvature is underrelaxed from one iteration to the other.

Summary

The streamline curvature method solves for the meridional velocity distribution along arbitrary calculation stations coupled to the mass conservation equation.

The streamline positions are modified from one iteration to the next and this step, coupled to the estimation of the slope and curvature of the

streamlines, is the most delicate operation in the whole procedure. Practical experience, see for instance Davis and Millar (1975) for an interesting account of some available user's experience, shows that with the necessary care in the estimation of slopes and curvatures, accurate results can be obtained even for radial and mixed flow machines, including return ducts. A recent report on the application of the streamline curvature method to radial compressors has been presented by Casey and Roth (1984).

With regard to Mach number limitations, the general properties discussed in section 2.2.1 are confirmed by the properties of the mass flow derivatives ($\partial \dot{m} / \partial w_m$) through the sign of this function. As pointed out by Marsh (1971), when this derivative has a fixed sign, a unique solution is obtained for the iteration on the meridional distribution. This is the case for subsonic meridional velocities in the design problem and for fully subsonic or fully supersonic relative Mach numbers in the analysis problems. However transonic relative velocities can be treated if the user specifies which, from the subsonic or supersonic solution of the relation between mass flow and Mach number is to be selected.

2.4.4. Streamfunction Methods

An alternative to the streamline curvature method is provided by the introduction of a streamfunction ψ , in order to satisfy the continuity equation. This leads to a second order, quasi-linear, partial differential equation for the streamfunction, which can be discretized on a fixed mesh, either by finite difference or by finite element methods.

The continuity equation, (2.4.1) can be satisfied for any continuous function ψ , by setting

$$\begin{aligned}w_z &= \frac{1}{\rho b r} \frac{\partial \psi}{\partial r} \\w_r &= \frac{-1}{\rho b r} \frac{\partial \psi}{\partial z}\end{aligned}\tag{2.4.89}$$

Inserting these definitions in equation (2.4.15) for instance, leads to the following streamfunction equation

$$\frac{\partial}{\partial r} \left(\frac{1}{\rho b r} \frac{\partial \psi}{\partial r} \right) + \frac{\partial}{\partial z} \left(\frac{1}{\rho b r} \frac{\partial \psi}{\partial z} \right) = \frac{-1}{w_z} \left[T \frac{\partial s}{\partial r} - \frac{\partial I}{\partial r} + \frac{w_\theta}{r} \frac{\partial}{\partial r} (r v_\theta) + F_r^T \right] \tag{2.4.90}$$

This equation can be applied as long as w_z does not vanish, that is for axial flow configurations. For radial flow configurations, the axial momentum equation (2.4.17) can be used, leading to an equivalent streamfunction equation

$$\frac{\partial}{\partial r} \left(\frac{1}{\rho b r} \frac{\partial \psi}{\partial r} \right) + \frac{\partial}{\partial z} \left(\frac{1}{\rho b r} \frac{\partial \psi}{\partial z} \right) = \frac{1}{w_r} \left[T \frac{\partial s}{\partial z} - \frac{\partial I}{\partial z} + \frac{w_\theta}{r} \frac{\partial}{\partial z} (r v_\theta) + F_z^T \right] \tag{2.4.91}$$

This equation in turn ceases to be valid when the radial velocity component vanishes.

A general form, valid for any flow configuration and which can therefore be applied in mixed flow machines with axial-radial transitions is obtained by introducing the N-component of the momentum equation, see section 2.3.4.

Within the notation conventions of this section, where no distinction is made between the streamsheet and the averaging approaches the streamfunction equation becomes

Blade region

$$\begin{aligned}
\frac{\partial}{\partial r} \left(\frac{1}{\rho b r} \frac{\partial \psi}{\partial r} \right) + \frac{\partial}{\partial z} \left(\frac{1}{\rho b r} \frac{\partial \psi}{\partial z} \right) = & -\frac{1}{w^2} [(w_z + w_\theta \tan \beta') (T \frac{\partial s}{\partial r} - \frac{\partial I}{\partial r}) \\
& - (w_r + w_\theta \tan \epsilon') (T \frac{\partial s}{\partial z} - \frac{\partial I}{\partial z})] \\
& - \frac{1}{r} [\tan \beta' \frac{\partial}{\partial r} (r v_\theta) - \tan \epsilon' \frac{\partial}{\partial z} (r v_\theta)]
\end{aligned} \tag{2.4.92}$$

In the axisymmetric approximation β' , ϵ' are the streamsurface or mean Camber surface angles with respect to the axial and radial directions respectively.

Duct region

$$\begin{aligned}
\frac{\partial}{\partial r} \left(\frac{1}{\rho b r} \frac{\partial \psi}{\partial r} \right) + \frac{\partial}{\partial z} \left(\frac{1}{\rho b r} \frac{\partial \psi}{\partial z} \right) = & \frac{-1}{w_m^2} \{ w_z (T \frac{\partial s}{\partial r} - \frac{\partial H}{\partial r}) - w_r (T \frac{\partial s}{\partial z} - \frac{\partial H}{\partial z}) \\
& + \frac{w_\theta}{r} [w_z \frac{\partial}{\partial r} (r v_\theta) - w_r \frac{\partial}{\partial z} (r v_\theta)] \}
\end{aligned} \tag{2.4.93}$$

For incompressible flows, the same equations remain valid with

$$s = 0, \quad I = (p + \rho \frac{\vec{w}^2}{2} - \rho \frac{\vec{u}^2}{2}) / \rho, \quad H = (p + \rho \frac{\vec{v}^2}{2}) / \rho \tag{2.4.94}$$

In the following we will consider either of these three forms, recalling that equation (2.4.92) is valid for all flow configurations.

Hence, the streamfunction equation will be written as

$$\frac{\partial}{\partial r} \left(\frac{1}{\rho b r} \frac{\partial \psi}{\partial r} \right) + \frac{\partial}{\partial z} \left(\frac{1}{\rho b r} \frac{\partial \psi}{\partial z} \right) = q \tag{2.4.95}$$

An alternative form is obtained by working out the left-hand side into a Laplace operator

$$\Delta \psi = [-\frac{\partial \psi}{\partial r} \frac{\partial}{\partial r} \left(\frac{1}{\rho b r} \right) - \frac{\partial \psi}{\partial z} \frac{\partial}{\partial z} \left(\frac{1}{\rho b r} \right) + q](\rho b r) \tag{2.4.96}$$

or

$$\Delta \psi = q \cdot \rho b r - w_r \frac{\partial}{\partial z} (\rho b r) + w_z \frac{\partial}{\partial r} (\rho b r) \tag{2.4.97}$$

Equation (2.4.95) is elliptic for subsonic relative Mach numbers in the analysis case and for subsonic meridional Mach numbers in the design

option when rv_θ is specified. This results from the general analysis of section 2.2.1 but can also be shown directly on equation (2.4.95) using equation (2.2.81).

In the analysis case, the (rv_θ) derivatives of the right-hand-side contribute to the type of the streamfunction equation through equation (2.2.83). For the design problem, applying equation (2.2.81) gives

$$br(1-M_m^2)(w_r \frac{\partial \rho}{\partial z} - w_z \frac{\partial \rho}{\partial r}) = M_r^2 \frac{\partial^2 \psi}{\partial z^2} - 2M_r M_z \frac{\partial^2 \psi}{\partial r \partial z} + M_z^2 \frac{\partial^2 \psi}{\partial r^2}$$

and one can write the streamfunction equation in the following form, with double subscripts on ψ indicating second derivatives

$$(1 - M_r^2)\psi_{rr} - 2M_r M_z \psi_{rz} + (1 - M_z^2)\psi_{zz} = D$$

where D contains the terms of lower order in the ψ -derivatives,

$$D = q.\rho br(1 - M_m^2) + \rho(1 - M_m^2)(w_z \frac{\partial}{\partial r} br - w_r \frac{\partial}{\partial z} br)$$

This equation is elliptic for

$$M_r^2 M_z^2 - (1 - M_r^2)(1 - M_z^2) < 0$$

or

$$M_m^2 < 1 \quad (2.4.98)$$

and hyperbolic for

$$M_m^2 > 1 \quad (2.4.99)$$

In the analysis case, when the flow angle is imposed, the streamfunction equation becomes, Wu (1952), with

$$\tan \hat{\beta} = \frac{w_\theta}{w_z}$$

$$(1 + \tan^2 \hat{\beta})(1 - M_r^2)\psi_{rr} - 2(1 + \tan^2 \hat{\beta})M_r M_z \psi_{rz} + (1 - M_\theta^{(r)^2} - M_z^2)\psi_{zz} = D$$

which is elliptic for

$$M^{(r)^2} = M_{\theta}^{(r)^2} + M_r^2 + M_z^2 < 1 \quad (2.4.100)$$

that is for relative Mach numbers $M^{(r)}$ lower than one, and hyperbolic for supersonic relative Mach numbers.

The determination of density

One of the central problems with the application of streamfunction methods for compressible flows is connected to the non-unique relation between the streamfunction and the density.

From the isentropic relation between static and relative stagnation variables, one has

$$\frac{\rho}{\rho_0} = \left(1 - \frac{w^2}{2 H_0'}\right)^{1/(\gamma-1)} = \left(1 - \frac{|\vec{\nabla}\psi|^2}{2(\rho_0' br)^2 H_0'} - \frac{w_{\theta}^2}{2 H_0'}\right)^{1/(\gamma-1)} \quad (2.4.101)$$

where

$$|\vec{\nabla}\psi|^2 = \left|\frac{\partial\psi}{\partial r}\right|^2 + \left|\frac{\partial\psi}{\partial z}\right|^2 \quad (2.4.102)$$

and where the stagnation quantities are considered in the relative system.

For fixed values of the streamfunction gradient $|\vec{\nabla}\psi|^2$, relative stagnation enthalpy H_0' and stagnation density ρ_0' , equation (2.4.101) has generally two solutions, one corresponding to a supersonic flow, the other to a subsonic relative flow.

Indeed, equation (2.4.101) can be written under the form, valid for the design option, v_{θ} or w_{θ} fixed,

$$\frac{\rho}{\rho_0'} = \left[1 - \frac{w_{\theta}^2}{2 H_0'} - \frac{A}{\left(\frac{\rho}{\rho_0'}\right)^2}\right]^{1/(\gamma-1)} = F\left(\frac{\rho}{\rho_0'}\right) \quad (2.4.103)$$

with

$$A = \frac{|\vec{\nabla}\psi|^2}{2(\rho_0' br)^2 H_0'} = \frac{w_m^2}{2 H_0' \left(\frac{\rho_0'}{\rho}\right)^2} \quad (2.4.104)$$

For the analysis option, β fixed, one has

$$\frac{\rho}{\rho'_0} = \left[1 - \frac{|\vec{V}\psi|^2 (1 + \tan^2 \beta)}{2 H'_0 (\rho br)^2} \right]^{1/(\gamma-1)} \quad (2.4.105)$$

$$= \left(1 - \frac{A}{(\frac{\rho}{\rho'_0})^2} \right)^{1/(\gamma-1)} = F \left(\frac{\rho}{\rho'_0} \right)$$

$$A = \frac{|\vec{V}\psi|^2 (1 + \tan^2 \beta)}{2 H'_0 (\rho'_0 br)^2} = \frac{\vec{w}^2}{2 H'_0 (\frac{\rho'_0}{\rho})^2} \quad (2.4.106)$$

$$= \frac{(\rho w_m)^2 (1 + \tan^2 \beta)}{2 H'_0 \rho'^2}$$

The relations $\rho/\rho'_0 = F(\rho/\rho'_0)$ are represented on figure 2.4.5 and the solutions can be found as the intersections S1 and S2 between the function and the first quadrant bissector.

The function F has an asymptotic limit for large values of ρ given by

$$F_0 = \left(1 - \frac{w_\theta^2}{2 H'_0} \right)^{1/(\gamma-1)} \quad \text{if} \quad rv_\theta \text{ fixed} \quad (2.4.107)$$

$$F_0 = 1 \quad \text{if} \quad \beta \text{ fixed}$$

The number of solutions for the density depends on the value of the constant A. Generally one will have two values of the density, given by the points S1 and S2 of figure 2.4.5, for a given value of the constant A.

Point S1 is the subsonic solution while point S2 corresponds to a supersonic velocity. Points C are defined by the condition that the tangents to F equal one. If point C lies below the line $F = \rho/\rho'_0$ for instance curve 2, there will be no solutions for the density corresponding to the current values of the constants A. Indeed, the condition to be imposed in order to have two solutions

$$F(C) > \left(\frac{\rho}{\rho'_0} \right)_C \quad (2.4.108)$$

where $(\rho/\rho'_0)_C$ is defined by the condition

$$F'(C) = 1 \quad (2.4.109)$$

the notation F' indicating a derivative with respect to (ρ/ρ'_0) .

The limiting case being reached for curve 3 where $F(C3) = (\rho/\rho_0')_{C3}$.

From the definitions above, one has

$$F' = \frac{1}{\gamma - 1} F \frac{2 A}{\left(\frac{h}{H_0'}\right) \left(\frac{\rho}{\rho_0'}\right)^3} = \frac{F}{\frac{\rho}{\rho_0'}} \left(\frac{2}{\gamma - 1} \frac{A}{\left(\frac{\rho}{\rho_0'}\right)^2} \frac{H_0'}{h} \right) \quad (2.4.110)$$

Considering a perfect gas assumption and the particular limiting position of curve 3, for which $F = \rho/\rho_0$ in point C3, one obtains the conditions

$$F'(C3) = M_m^2 \quad \text{design option - } rv_\theta \text{ fixed} \quad (2.4.111)$$

$$F'(C3) = M^{(r)^2} \quad \text{analysis option - } \beta \text{ fixed}$$

This shows that point C3 of curve 3 corresponds to the critical Mach number namely

$$M_{mC3} = 1 \quad \text{design option} \quad (2.4.112)$$

$$M_{C3}^{(r)} = 1 \quad \text{analysis option}$$

and that the critical density ratio is reached

$$(\rho/\rho_0')^*_{C3} = \left(\frac{\gamma+1}{2}\right)^{-1/(\gamma-1)} \left(1 + \frac{\gamma-1}{\gamma+1} M_\theta^{(r)^2}\right)^{-1/(\gamma-1)} \quad \text{design option} \quad (2.4.113)$$

$$(\rho/\rho_0')^*_{C3} = \left(\frac{\gamma+1}{2}\right)^{-1/(\gamma-1)} \quad \text{analysis option}$$

The lowest value of (ρ/ρ_0') is obtained by the intersection of the F curve with the horizontal axis, that is by $F=0$. Hence

$$(\rho/\rho_0')_{\min} = \frac{\sqrt{A} / \sqrt{1 - w_\theta^2 / 2H_0'}}{\sqrt{A}} \quad \begin{array}{l} rv_\theta \text{ fixed - design option} \\ \beta \text{ fixed - analysis option} \end{array} \quad (2.4.114)$$

The critical value of A, A^* corresponds to curve C3, with the condition, deduced from equation (2.4.110), that

$$\left(\frac{2}{\gamma-1} \cdot \frac{A}{(\rho/\rho_0')^2} \cdot \frac{H_0'}{h} \right)^* = 1$$

or

$$A^* = \frac{\gamma-1}{2} \cdot (\rho/\rho_0)^* (\gamma+1) \quad (2.4.115)$$

with $(\rho/\rho_0)^*$ given by equation (2.4.113).

The condition for the density relation, equation (2.4.103), to have solutions, can be expressed by the condition that the values of A corresponding to curve C1 should be larger than A^* .

This is actually a condition on the mass flow per unit area ρw , since the critical mass flow is attained for $w_m^* = c^*$ the speed of sound

$$\begin{aligned} (\rho w_m)^* &= \rho_0 \left(\frac{\rho}{\rho_0} \right)^* \cdot w_m^* \\ &= \rho_0 \cdot \left(\frac{\rho}{\rho_0} \right)^* \cdot \sqrt{(\gamma-1)H_0^*} \left(\frac{\rho^*}{\rho_0} \right)^{\frac{\gamma-1}{2}} \\ (\rho w_m)^* &= \rho_0 \sqrt{(\gamma-1)H_0^*} \left(\frac{\rho^*}{\rho_0} \right)^{\frac{\gamma-1}{2}} = \sqrt{A^*} \rho_0 \sqrt{2H_0^*} \end{aligned} \quad (2.4.116)$$

Hence, the condition $A < A^*$ becomes in all cases, with either w_0 or $\tan \beta$ fixed,

$$\frac{(\rho w_m)^2}{2H_0^* \rho_0^2} < \frac{(\rho w_m)^*^2}{2H_0^* \rho_0^2}$$

or

$$\rho w_m < (\rho w_m)^* \quad (2.4.117)$$

In practical computations, when the computed streamfunction is far from the converged value, a careful check has to be performed in order to insure that the current approximation of $|\vec{\nabla}\psi|^2$ is not too high such as to violate the condition (2.4.117).

When (2.4.117) is satisfied, two solutions occur, corresponding to the subsonic branch point S1, or to the supersonic branch of the mass flow relation versus density or Mach number. In order to solve the density equation and obtain a unique solution, one can apply a Newton method or a fixed point method. The former will allow to obtain either of the two solutions, if the user knows which one to select, while the latter will always lead to the subsonic solution.

Indeed, writing equations (2.4.103) or (2.4.105) under the form

$$G(\rho/\rho_0) = (\rho/\rho_0)^{\gamma-1} - B + \frac{A}{(\rho/\rho_0)^2} = 0 \quad (2.4.118)$$

where

$$B = 1 - w_0^2/2H_0 \quad \text{design option} \quad (2.4.119)$$

$$B = 1 \quad \text{analysis option}$$

the Newton iteration reads

$$\rho^{n+1} = \rho^n - \frac{G^n}{G'^n} \rho_0 \quad (2.4.120)$$

The function G^n is the value of G for $\rho = \rho^n$ and the jacobian G' is defined by

$$G' = (\gamma-1)(\rho/\rho_0)^{\gamma-2} - \frac{2A}{(\rho/\rho_0)^3} \quad (2.4.121)$$

As expected, the zero of the jacobian G' is obtained at the critical mass flow condition (2.4.115) but the jacobian will remain of constant sign, positive or negative for subsonic or supersonic flows respectively.

Graphically, it is easy to see that the Newton iteration will converge to the subsonic or the supersonic solution depending on the value chosen to initiate the iteration, figure 2.4.6.

If the iteration starts at A1 at a subsonic velocity, the Newton procedure will converge to S1, while starting with A2 at a supersonic point will lead to the supersonic solution S2.

On the other hand, the fixed point iteration

$$(\rho/\rho_0)^{n+1} = F(\rho^n/\rho_0) \quad (2.4.122)$$

converges always to the subsonic solution S1 as illustrated on figure 2.4.6, excepted when the initial value is left of the supersonic solution. In this case the iteration diverges.

Boundary conditions for the streamfunction equation

The boundary conditions for the solution of the streamfunction equation are easily defined and applied.

At the inlet station, the flow is assumed to be known and therefore it is easy to determine the streamfunction distribution.

For $I=1$, figure 2.4.7,

$$\psi(x_{1,j}, y_{1,j}) = \psi_{1,j} \quad (2.4.123)$$

is given for all values of j , from the inlet velocity distribution.

At the outlet station it is nearly always possible to select a station which is situated in a region of uniform meridional flow direction. Hence, if the last station is set perpendicularly to this direction, one can assume the normal derivative to be zero. That is

$$\frac{\partial \psi}{\partial n} = 0 \quad \text{at the last station } I=n \quad (2.4.124)$$

where n is the normal direction.

The hub and shroud walls can be taken as streamlines if no end wall boundary layer is to be considered. In this case one can select

$$\begin{aligned} \psi_{I,j=1} &= 0 & \text{at hub wall} & \quad j=1 \\ \psi_{I,j=M} &= \dot{m}/2\pi & \text{at shroud wall} & \quad j=M \end{aligned} \quad (2.4.125)$$

However if an end wall boundary layer computation is performed or if the wall layer thicknesses are given, one can either displace the hub and shroud wall points by an amount equal to the local displacement thickness maintaining the above boundary conditions, or one can introduce a fictive mass flux compensating for the mass flow defect due to the shear layers.

If δ_H^* and δ_I^* represent the hub and shroud displacement thicknesses with respect to the meridional velocity profiles, one can impose

$$\psi_{I,j=1} = - \frac{1}{2\pi} (\rho w_m \delta_H^*)_{I,j=1} \quad (2.4.126)$$

$$\psi_{I,j=M} = \frac{\dot{m}}{2\pi} + \frac{1}{2\pi} (\rho w_m \delta_I^*)_{I,j=M}$$

In this case the physical end walls are not streamlines anymore.

2.4.5. Finite Difference Solutions of the Streamfunction Equation

The discretization of the streamfunction with finite differences has been initially proposed by Wu (1952). The approach of Wu was closely followed and developed to practical computer programs by Marsh (1968),

Davis (1971), (1975), Katsanis and McNally (1973), (1977), Biniaris (1975), Bosman and El Shaarawi (1977).

All these authors use central difference schemes and hence the methods are limited to subsonic flow regions, either to meridional subsonic velocities for the design option, or to relative subsonic velocities in the analysis case. The densities are obtained by the fixed point iteration scheme in all the presently published methods. Of the above mentioned methods, Davis (1971) and Katsanis and McNally (1973) contain full documented codes. In particular the latter, called MERIDL, is extensively documented.

In most methods an arbitrary grid is generated, although Katsanis and McNally work with a curvilinear orthogonal grid and Biniaris uses a cartesian grid in the meridional surface (r, z). Second order central differences are applied by these two authors, while Marsh (1968) and Davis (1971) apply up to third order central difference formulas on arbitrary grids.

The algebraic matrix system is mostly solved by LU decompositions with the exception of Katsanis and McNally (1973) and Biniaris (1975) who apply successive overrelaxation techniques.

2.4.6. Finite Element Solutions of the Streamfunction Equation

Finite element solution procedures for the through-flow problem have been introduced by Adler and Krimerman (1974), Hirsch and Warzee (1974). The first authors define triangular meshes with linear elements while Hirsch and Warzee apply biquadratic elements leading to third order accuracy for the streamfunction and hence, second order accuracy for the velocities.

SUMMARY

The specific approximations introduced in order to calculate multistage turbomachinery flows, are a combination of a distributed loss model and a quasi-three-dimensional decomposition. Two approaches, the streamsurface method or the averaging technique can be applied to define the quasi-3D formulation. The latter allows a through flow definition without ambiguity or arbitrary selected streamsurface shapes. However it does not permit a reconstruction of the full three dimensional flow.

The quasi-3D approximation enables to reduce the problem to a succession of two-dimensional flows, basically of inviscid nature. The interaction between the through-flows and the blade-to-blade flows can be extended to the transfer of losses and flow angles from the blade-to-blades to the meridional flow. However, this can be replaced by empirical information, which is required in all cases if some three-dimensional effects have to be accounted for.

The specific properties and solution methodology related to through-flow computations have been presented and different resolution techniques

have been described. None of the methods described however, is able to treat correctly relative supersonic flows in the analysis mode. This would require a different simulation of the problem, see for instance Spurr (1981).

Two methods are currently applied for through-flows : streamline curvature and streamsurface methods. The latter can be discretized either by finite differences or by finite elements.

Solution techniques for blade-to-blade flows have not been discussed in this chapter since they do not require specific methods. Depending on the level of approximation, potential, Euler or Navier-Stokes models can be applied to the blade-to-blade flows following the methods presented in the corresponding chapters dealing with the discretization of these flow models. Several examples of blade-to-blade flow computations have already been shown in chapters 2 and 7 and other examples will be presented in the following chapters.

REFERENCES

- Adler, D., Krimerman, Y. (1974). "The Numerical Calculation of the Meridional Flow Field in Turbomachines using the Finite Element Method". Israel Journal of Technology, Vol 12, pp 268-274.
- Adkins, G.G., Smith, L.H. (1982). "Spanwise Mixing in Axial Flow Turbomachines". Trans. ASME, Journal of Engineering for Power, Vol 104, pp 97-110.
- Biniaris, S. (1975). "The Calculation of the Quasi-Three Dimensional Flow in Axial Gas Turbine". Trans. ASME, Journal of Engineering for Power, Vol 97, pp 283-294.
- Bosman, C., Marsh, H. (1974). "An Improved Method for Calculating the Flow in Turbomachines, including a consistent Loss Model". Journal Mechanical Engineering Science, Vol 16, pp 25-31.
- Bosman, C., El-Shaarawi, M.A.I. (1977). "Quasi Three Dimensional Numerical Solution of Flow in Turbomachines". Trans. ASME, Journal of Fluids Engineering, Vol 99, pp 132-140.
- Casey, M.V., Roth, P. (1984). "A Streamline Curvature Throughflow Method for Radial Turbocompressors". I. Mech. E. Conference Publications 1984-3, Mechanical Engineering Publ. Ltd, London.
- Davis, W.R. (1971). "A Matrix Method Applied to the Analysis of the Flow in Turbomachinery". Report ME/A 71-6, Carleton University, Canada.
- Davis, W.R. (1975). "A General Finite Difference Technique for the Compressible Flow in the Meridional Plane of a Centrifugal Turbomachine". ASME Paper 75-GT-121.
- Davis, W.R. & Millar, D.A. (1972). "A Discussion of the Marsh Matrix Technique Applied to Fluid Flow Problems". Canadian Aeronautics and Space Journal, Vol 5, pp 64-70.
- Davis, W.R. & Millar, D. (1975). "A Comparison of the Matrix and Streamline Curvature Methods of Axial Flow Turbomachinery Analysis from a User's Point of View". Trans. ASME, Journal of Engineering for Power, Vol 97, pp 549-560.
- Davis, W.R., Millar, D.A.J. (1976). "Through Flow Calculations Based on Matrix Inversion", in Through-Flow Calculations in Axial Turbomachinery, AGARD Conf. Proceedings -CP-195.
- Denton, J. (1978). "Through Flow Calculations for Transonic Axial Flow Turbines". Trans. ASME, Journal of Engineering for Power, Vol 100, pp 212-218.
- De Ruyck, J., Hirsch, Ch., Kool, P. (1979). "An Axial Compressor End Wall Boundary Layer Calculation Method". Trans. ASME, Journal of Engineering for Power, Vol 101, pp 233-249.
- De Ruyck, J., Hirsch, Ch. (1981). "Investigations of an Axial Compressor End-Wall Boundary Layer Prediction Method". Trans. ASME, Journal of Engineering for Power, Vol 103, pp 20-33.

- De Ruyck, J., Hirsch, Ch. (1983). "End Wall Boundary Layer Calculations in Multistage Axial Compressors", in Viscous Effects in Turbomachines, AGARD Conf. Proceedings CP-351.
- Dring, R.P., Joslyn, H.D., Hardin, L.W. (1982). "An Investigation of Compressor Rotor Aerodynamics". Transaction ASME, Journal of Engineering for Power, Vol 104, pp 84-96.
- Frost, D.H. (1970). "A Streamline Curvature Through-Flow Computer Program for Analysing the Flow through Axial Flow Turbomachines". National Gas Turbine Establishment, Reports and Memoranda No 3687.
- Hawthorne, W.R. (1955). "Rotational Flow Through Cascades". Quarterly Journal Mech. and Applied Math., Vol VIII, pp 266-279.
- Hearsey, R.M. (1975). "A Revised Computer Program for Axial Compressor Design", Vol I. Report ARL TR 75-001 - Aerospace Research Laboratories Wright-Patterson Air Force Base, Dayton, Ohio.
- Hirsch, Ch. (1974). "End Wall Boundary Layers in Axial Compressors". Trans. ASME, Journal of Engineering for Power, Vol 96, pp 413-426.
- Hirsch, Ch. (1975). "Unsteady Contributions to Steady Radial Equilibrium Flow Equations", in Unsteady Phenomena in Turbomachines, AGARD Conf. Proceedings - CP195.
- Hirsch, Ch., Denton, J. (1981), Eds. Through Flow Calculations in Axial Turbomachines. AGARD AR 175.
- Hirsch, Ch., Warzee, G. (1974). "A Finite Element Method for Flow Calculations in Turbomachines". Vrije Universiteit Brussel, Dept. Fluid Mechanics, Report VUB-STR-5.
- Hirsch, Ch., Warzee, G. (1976). "A Finite Element Method for Through-Flow Calculations in Turbomachines". Trans. ASME, Journal of Fluids Engineering, Vol 98, pp 403-421.
- Hirsch, Ch., Warzee, G. (1979). "An Integrated Quasi Three Dimensional Finite Element Calculation Program for Turbomachinery Flows". Trans. ASME, Journal of Engineering for Power, Vol 101, pp 141-148.
- Horlock, J.H., Marsh, H. (1971). "Flow Models for Turbomachines". Journal of Mechanical Engineering Science, Vol 13, pp 358-368.
- Horlock, J.H., Lakshminarayana, B. (1973). "Secondary Flows Theory, Experiment and Application in Turbomachinery Aerodynamics". Annual Review of Fluid Mechanics, Vol 5, pp 247-280.
- Horlock, J.H., Perkins, H.J. (1974). Annulus Wall Boundary Layers in Turbomachines. AGARD Report AG 185.
- Horlock, J.H. (1978). Actuator Disk Theory. Mc Graw Hill, C^o, New York.
- Japikse, D. (1976). "Review-Progress in Numerical Turbomachinery Analysis". Trans. ASME, Journal of Fluids Engineering, Vol 98, pp 592-606.
- Jansen, W., Moffatt, W.C. (1967). "The Off-Design of Axial-Flow Compressors". Trans. ASME, Journal of Engineering for Power, Vol 89, pp

453-463.

- Jennions, K., Stow, P. (1984). "A Quasi-Three-Dimensional Blade Design System": ASME Papers 84-GT-26 and 84-GT-27.
- Katsanis, T. (1964). "Use of Arbitrary Quasi-Orthogonals for Calculating Flow Distributions in the Meridional Plane of a Turbomachine". NASA TN D-2546.
- Katsanis, T. (1966). "Use of Arbitrary Quasi-Orthogonals for Calculating Flow Distribution in a Turbomachine". Trans. ASME, Journal of Engineering for Power, Vol 88, pp 197-202.
- Katsanis, T., Mc Nally, W.D. (1973). "Fortran Program for Calculating Velocities and Streamlines on the Hub-Shroud Mid-Channel Flow Surface of an Axial- or Mixed-Flow Turbomachine", Vol I & II. NASA Technical Note TN-D-7343 and 7344 - superseded by NASA TN-D 8430 (1977) and TN-D 8431-(1977).
- Marsh, H. (1968). "A Digital Computer Program for the Through-Flow Fluid Mechanics in an Arbitrary Turbomachine Using a Matrix Method". Aeronautical Research Council R & M No 3509.
- Mc Nally, W.D., Sockol, P.M. (1981). "Computational Methods for Internal Flows with Emphasis on Turbomachinery". NASA TM 82764 in ASME Symposium on Computers in Flow Predictions and Fluid Dynamics Experiments. ASME Winter Annual Meeting.
- Mellor, G. & Wood, G. (1971). "An Axial Compressor End-Wall Boundary Layer Theory". Trans. ASME, Journal of Basic Engineering, Vol 93D, pp 300-316.
- Moore J. and Moore, J. (1980). "Three-Dimensional, Viscous Flow Calculations for Assessing the Thermodynamic Performance of Centrifugal Compressors". AGARD CP 282 on Centrifugal Compressors, Flow Phenomena and Performance.
- Novak, R.A. (1967). "Streamline Curvature Computing Procedures for Fluid Flow Problems". Trans. ASME, Journal of Engineering for Power, Vol 89, pp 478-490.
- Novak, R.A. (1976). "Flow Field and Performance Map Computation for Axial-Flow Compressors and Turbines", in "Modern Prediction Methods for Turbomachine Performance". AGARD-LS-83-1976.
- Novak, R.A., Hearsey, R.M. (1977). "A nearly Three Dimensional Intrablade Computing System for Turbomachinery". Trans. ASME, Journal of Engineering for Power, Vol 99, pp 154-166.
- Schulz, H.D., Neuhoﬀ, F., Hirsch, Ch. and Shreeve, R.P. "Application of Finite Element Code Q3DFLO-81 to Turbomachinery Flow Fields", Naval Postgraduate School Technical Report NP567-84-005PR, Dec 84.
- Sehra, A.K. (1979). "The Effect of Blade to Blade Flow Variations on the Mean Flow Field of a Transonic Compressor". Ph-D Thesis, MIT, Dept. Aeronautics and Astronautics, see also AFAPL-TR-79-2010.
- Sehra, A.K., Kerrebroek (1981). "Blade to Blade Effects on Mean Flow in Transonic Compressors". AIAA Journal, Vol 19, pp 476-483.

- Senoo, Y, Nakase, Y. (1972). "An Analysis of Flow through a Mixed Flow Impeller". Trans. ASME, Journal of Engineering for Power, Vol 94, pp 43-50.
- Smith, L.H. (1955). "Secondary Flows in Axial Flow Turbomachines". Trans. ASME, Journal of Engineering for Power, Vol 77, pp 1065-1076.
- Smith, L.H. Jr (1966). "The Radial Equilibrium Equation of Turbomachinery". Trans. ASME, Journal of Engineering for Power, Vol 88A, pp 1-13.
- Smith, L.H. Jr (1969). "Casing Boundary Layers in Multistage Axial Flow Compressors", in "Flow Research in Blading". Elsevier, Holland.
- Spura, A. (1981). "The Prediction of 3D Transonic Flow in Turbomachinery Using a Combined Through Flow and Blade-to-Blade Time Marching Method". International Journal of Heat and Fluid Flow, Vol 2, pp 189-199.
- Wennerstrom, A.J. (1974). "On the Treatment of Body Forces in the Radial Equilibrium Equation of Turbomachinery". ARL 74-0150, Aerospace Research Laboratories, Wright-Patterson Air Force Base, Ohio. Also in "Traupel-Festschrift", Juris-Verlag, Zurich, pp 351-367.
- Wilkinson, D.H. (1970). "Stability, Convergence and Accuracy of Two-Dimensional Streamline Curvature Methods using Quasi-Orthogonals". Proc. Inst. Mech. Eng., Vol 184, 108.
- Wu, C.H. (1952). "A General Theory of Three-Dimensional Flow in Subsonic and Supersonic Turbomachine of Axial-, Radial- and Mixed Flow Type". NACA TN 2604.
- Wu, C.H. (1976). "Three-Dimensional Turbomachine Flow Equations Expressed with Respect to Non-Orthogonal Curvilinear Coordinates and Methods of Solution". Proc. 3rd Int. Symp. on Air Breathing Engines (ISABE), Munich.

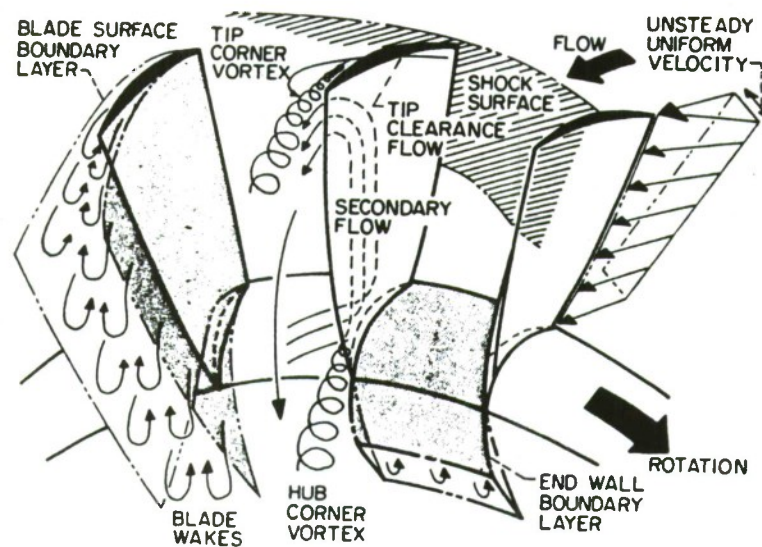


Figure 2.I.1. : Complex Flow Phenomena in compressor rotor blade row.



: Flow visualization with standard smoke-wire technique - smoke wire inside endwall boundary layer.

Figure 2.I.2. : Flow visualization of horseshoe vortex in the leading edge region of a turbine cascade. Courtesy, C. Sieverding, Von Karman Institute, Belgium.

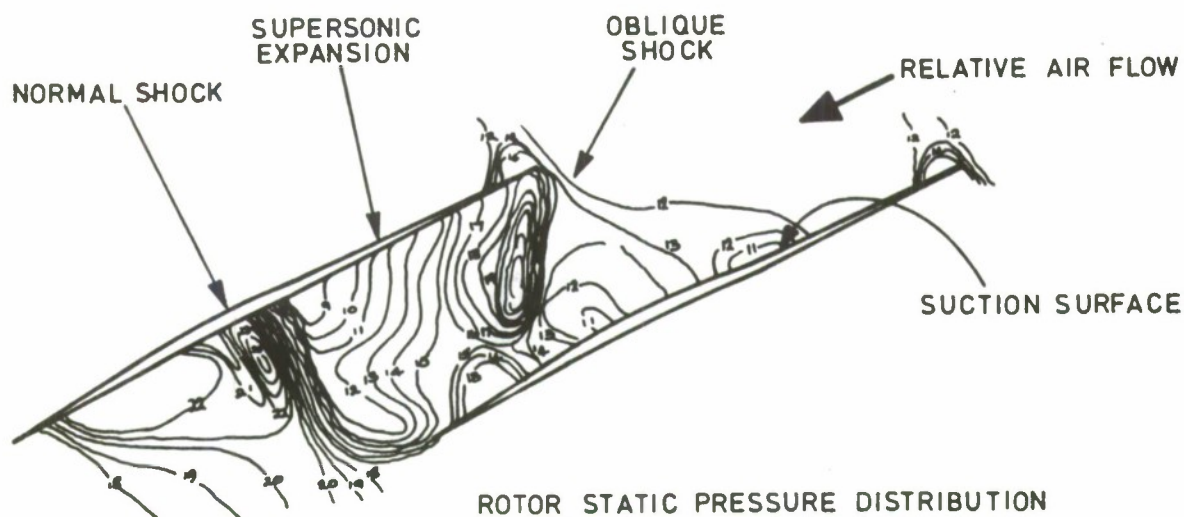


Figure 2.I.3. : Transonic pressure field in a compressor cascade. From AGARD LS 83.

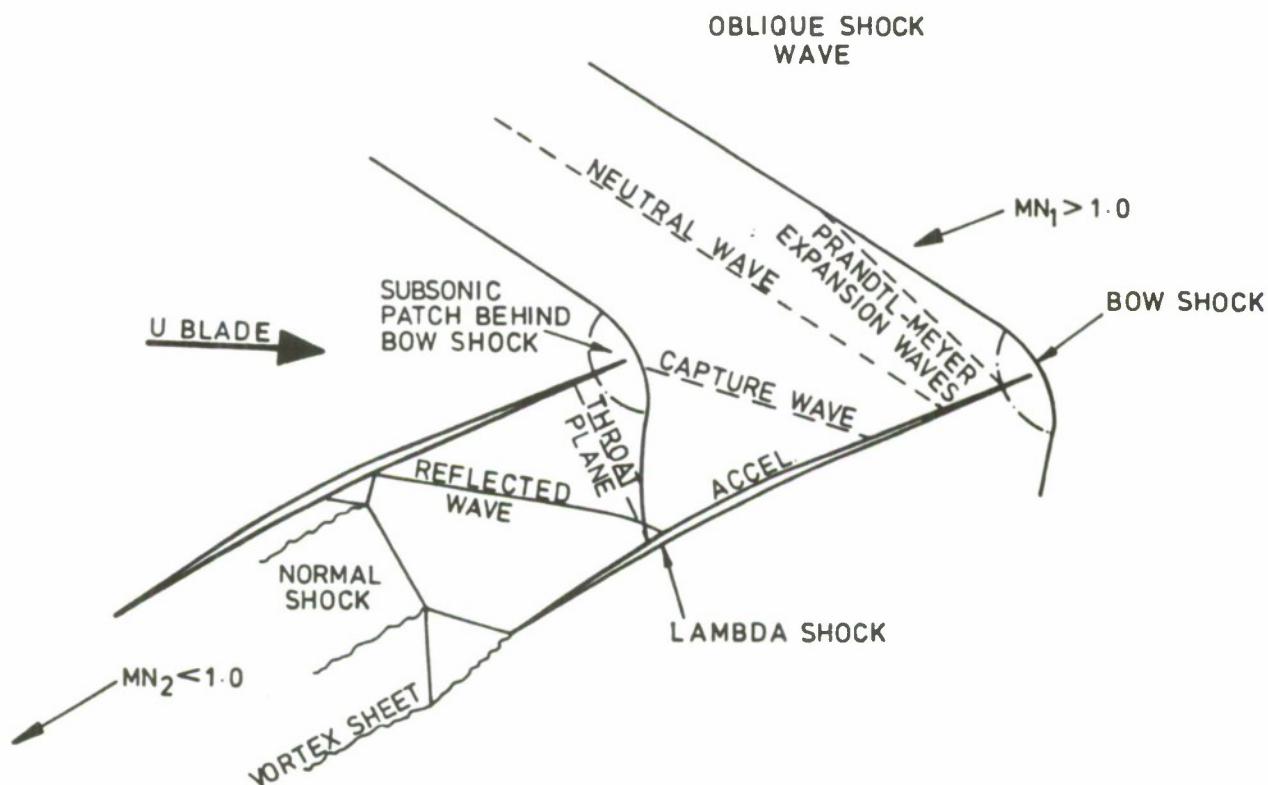


Figure 2.I.4. : Transonic flow shock model associated to figure 2.3. From AGARD LS 83

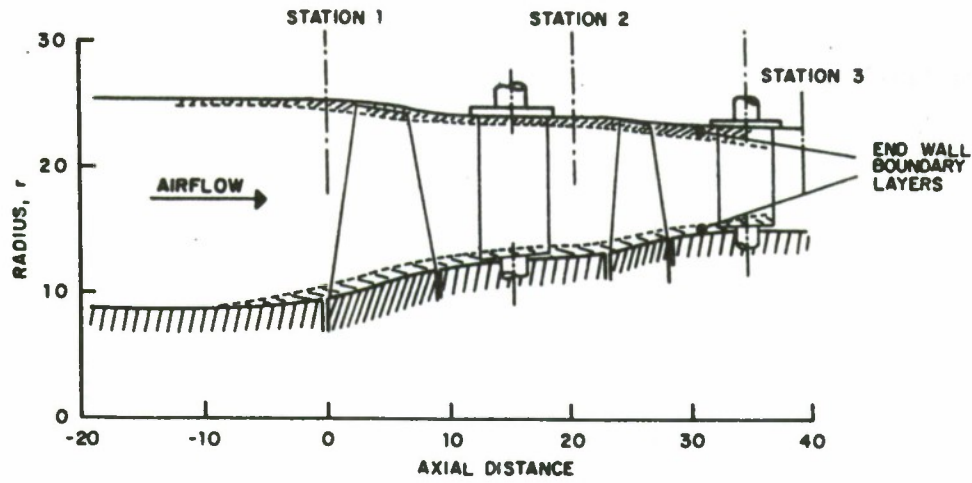


Figure 2.I.5. : Meridional section of a two-stage compressor.

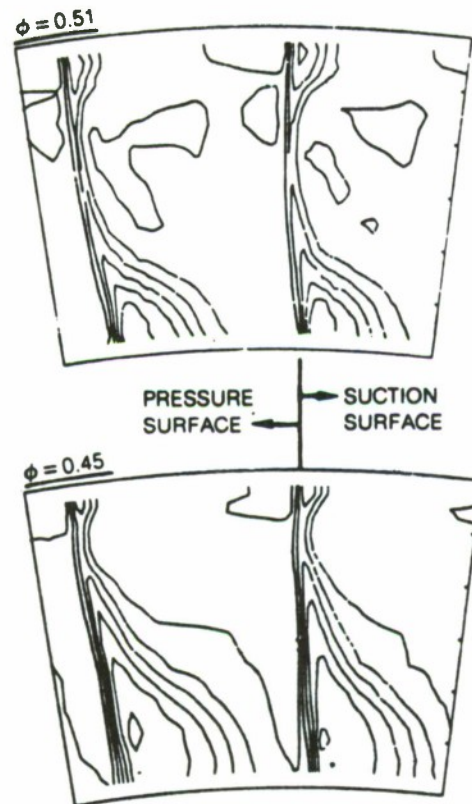


Fig. 4 Second stage stator exit total pressure contours, $\Delta CPT = 0.1$

Figure 2.I.6. : Stagnation pressure distribution at outlet of the stator of the second stage of an axial compressor. Courtesy R. Dring, United Technology Research Center, USA.

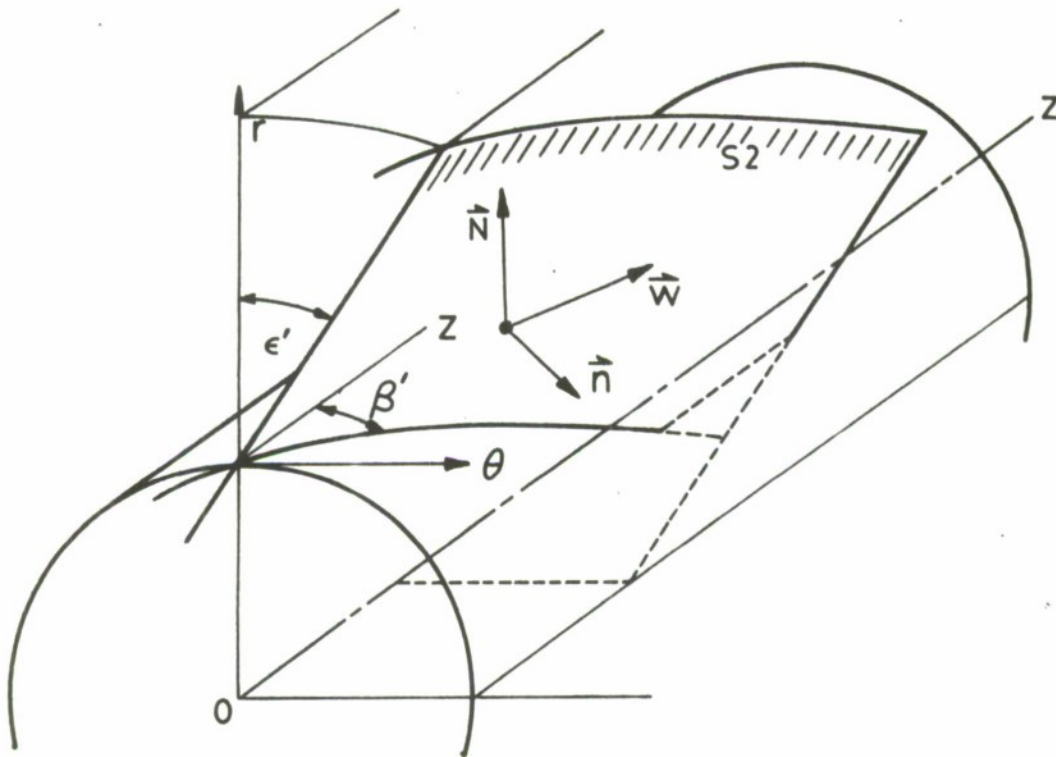


Figure 2.2.1. : Angles of S2 surface with cylindrical coordinates (r, θ, z) .

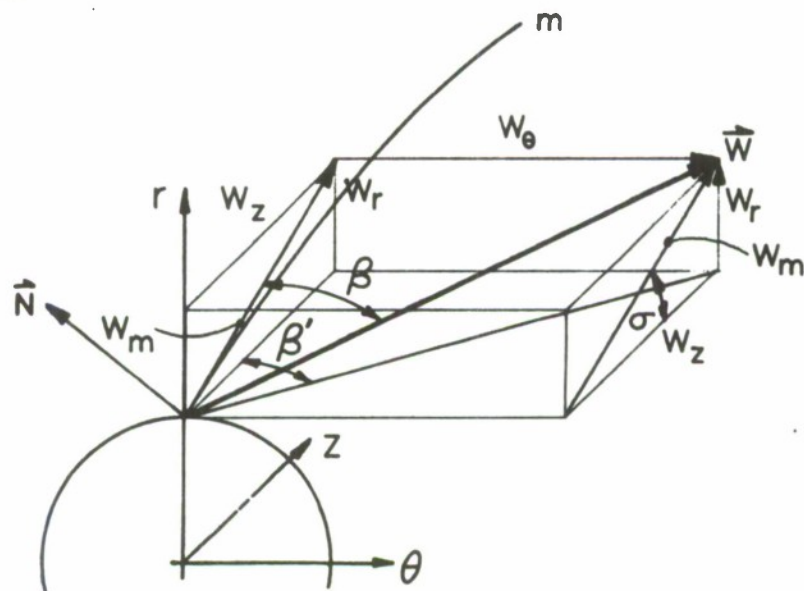


Figure 2.2.2. : Definition of flow angles and velocity components.

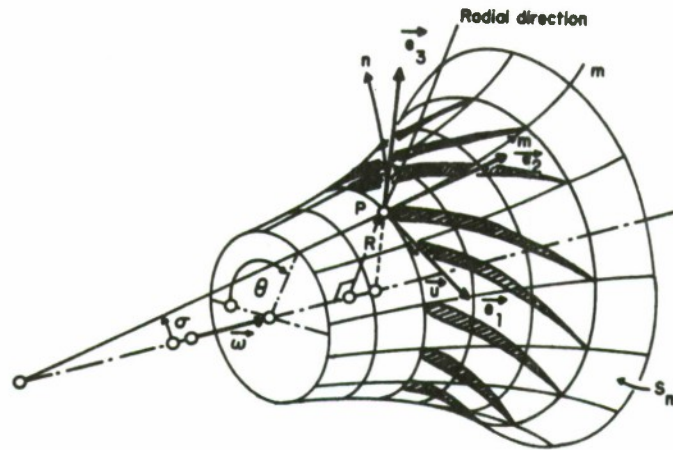
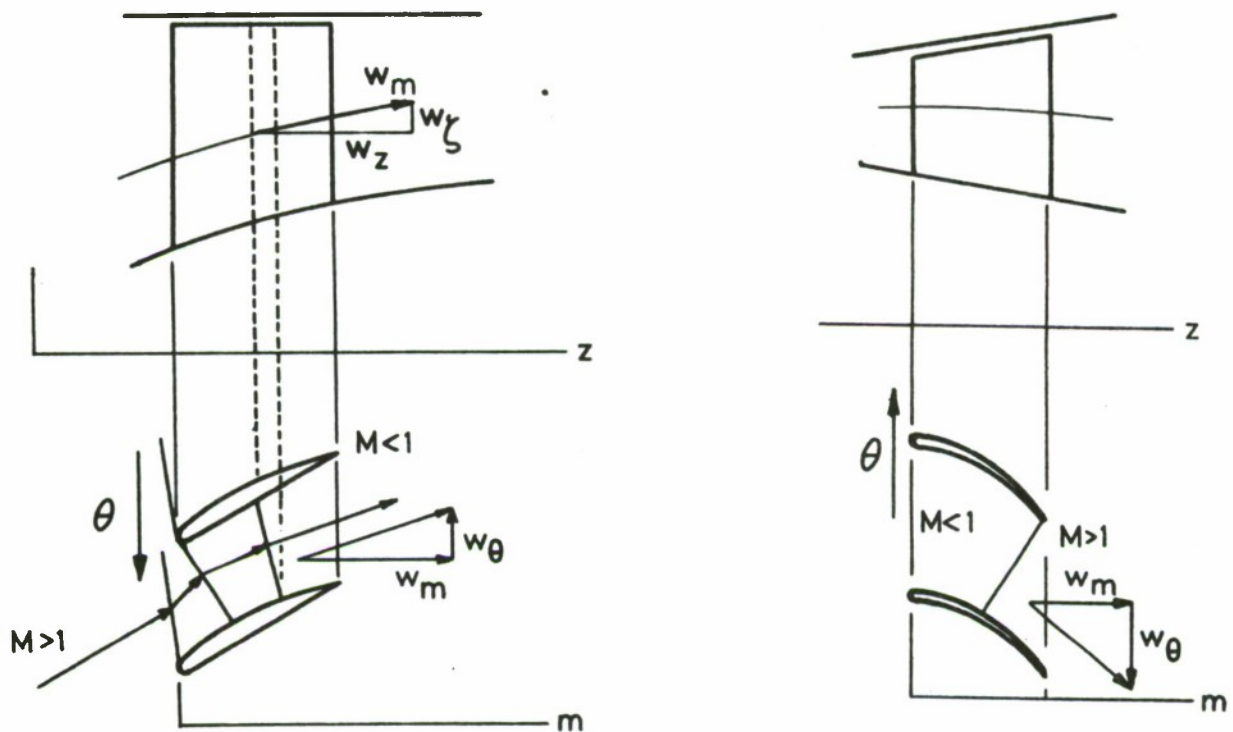


Figure 2.2.3. : Cross section of a blade row by an axisymmetric surface



Figures 2.2.4. and 2.2.5. : Through flow interaction with blade to blade flow for choked compressor and turbine configurations

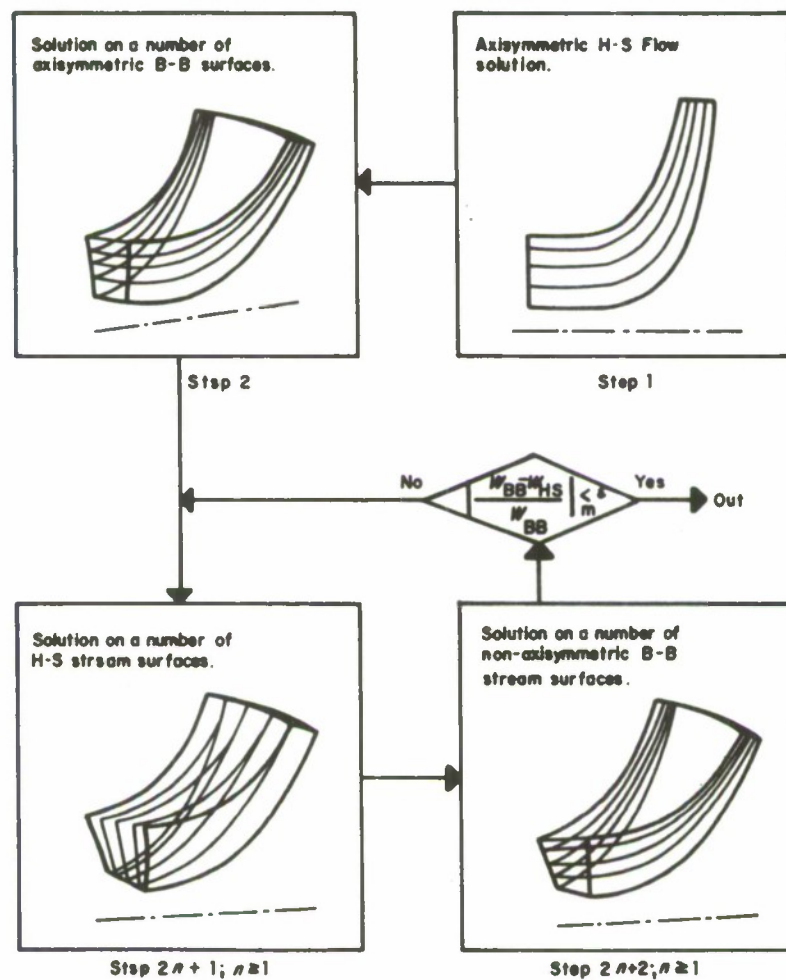


Figure 2.2.6. :Scheme of three dimensional flow computation with the streamsurface formulation, from Adler and Krimmerman (1978).

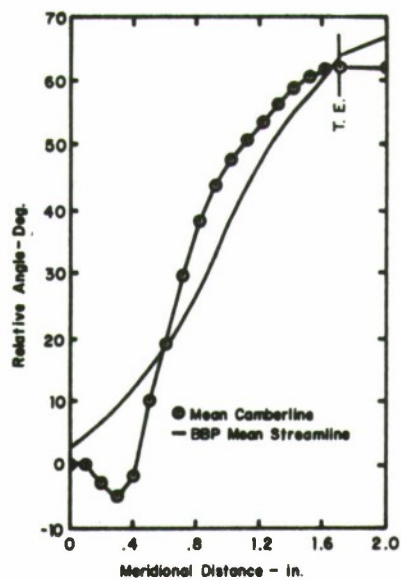


Figure 2.2.7. :Comparison of $\psi = 0.5$, mean streamline angles with mean camberline angles, from Novak and Hearsey (1977)

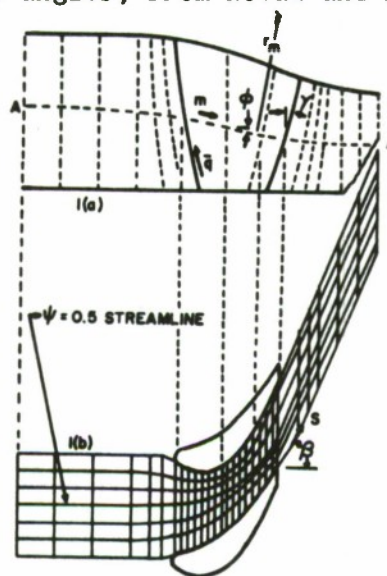


Figure 2.2.8. :Meridional and blade to blade cross section of contoured turbine nozzle, from Novak and Hearsey (1977)

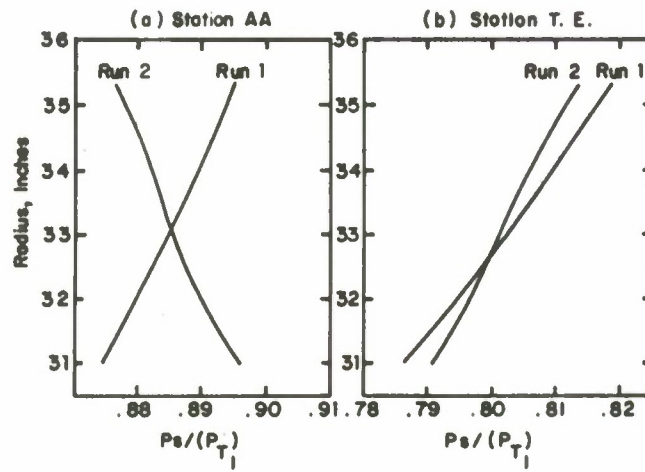


Figure 2.2.9. :Radial static pressure variation for leaned and unleaned annular turbine nozzle, from Novak and Hearsey (1977)

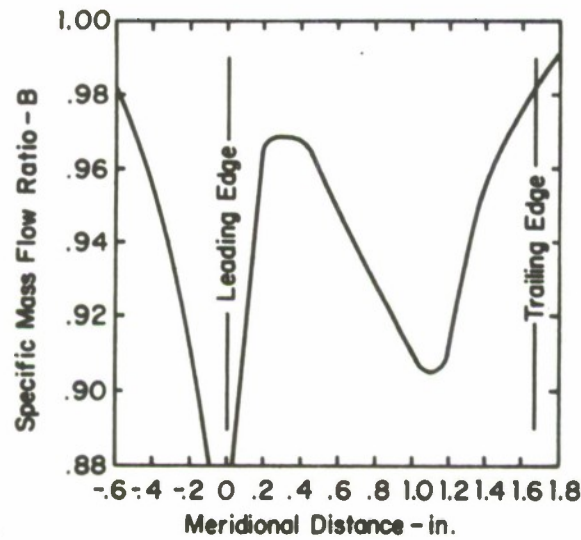
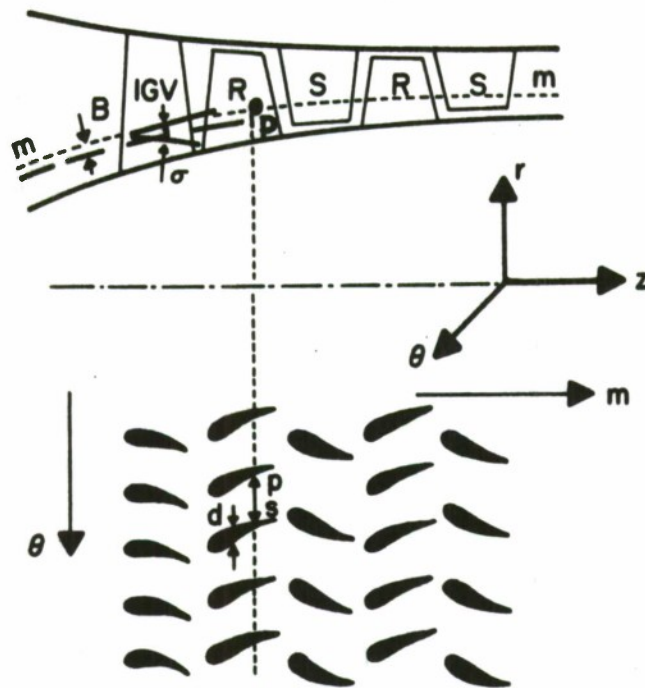


Figure 2.2.10. :Meridional distribution of B_2 or specific mass flow ratio distribution for turbine nozzle, from Novak and Hearsey (1977)



developed section through axisymmetric surface
generated by m .

Figure 2.3.1. : Meridional and blade to blade sections of a multistage axial flow turbomachine.

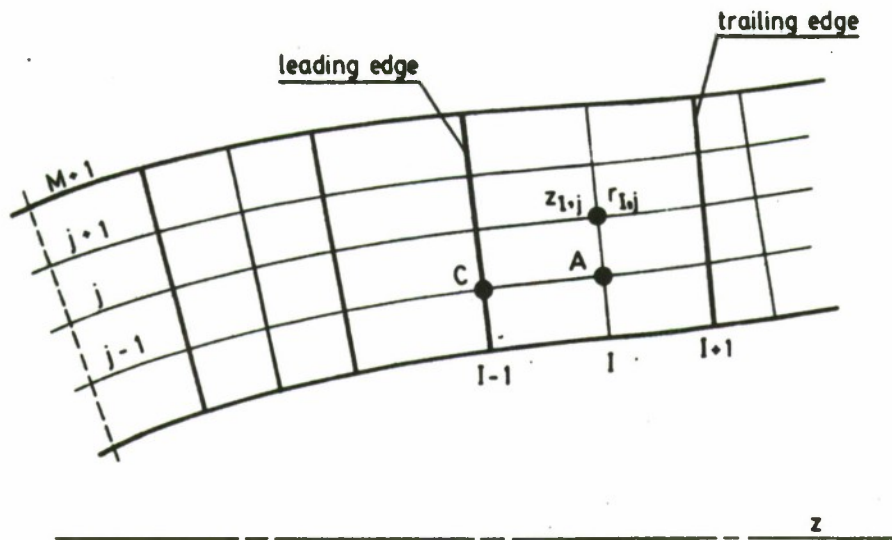


Figure 2.4.3. : Typical lay-out for streamline curvature methods
I indicates the station number, j the streamline number.

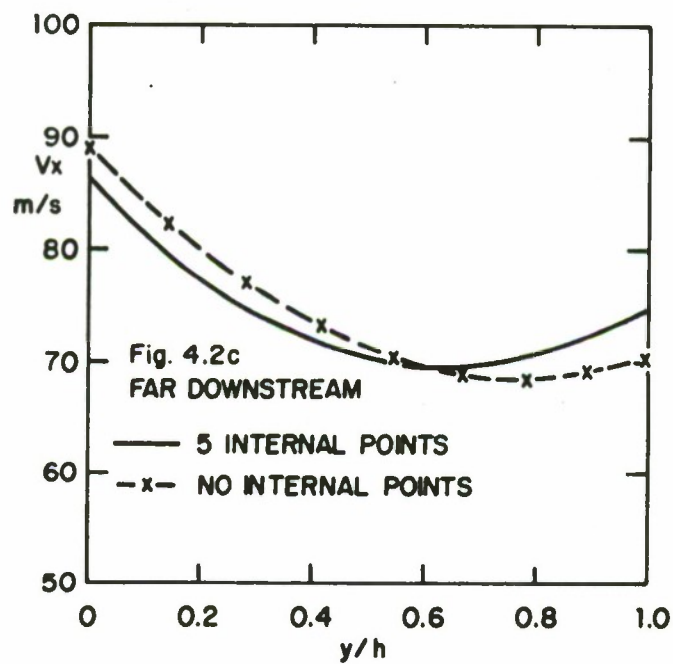


Figure 2.4.4 : Influence of curvature estimation on meridional velocity distribution in Denton's model problem; from AGARD AR175, (1981).

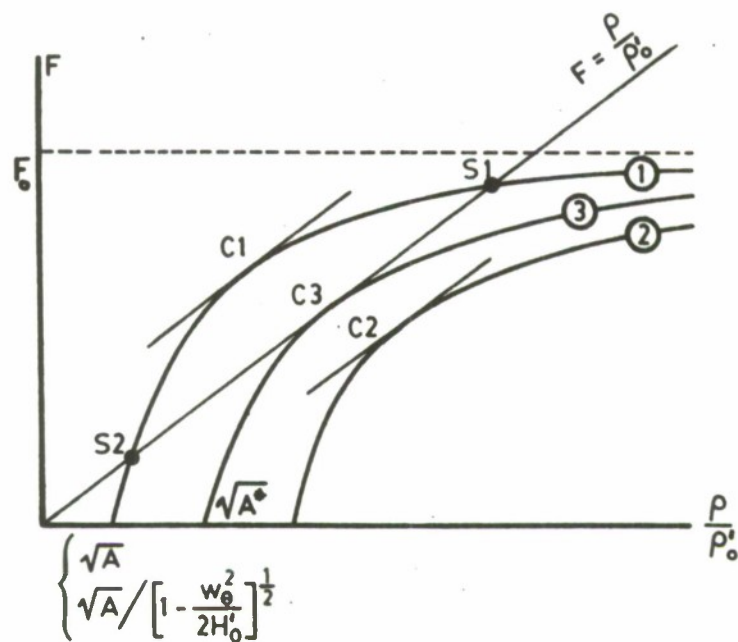


Figure 2.4.5. : Relation between density and streamfunction gradients.

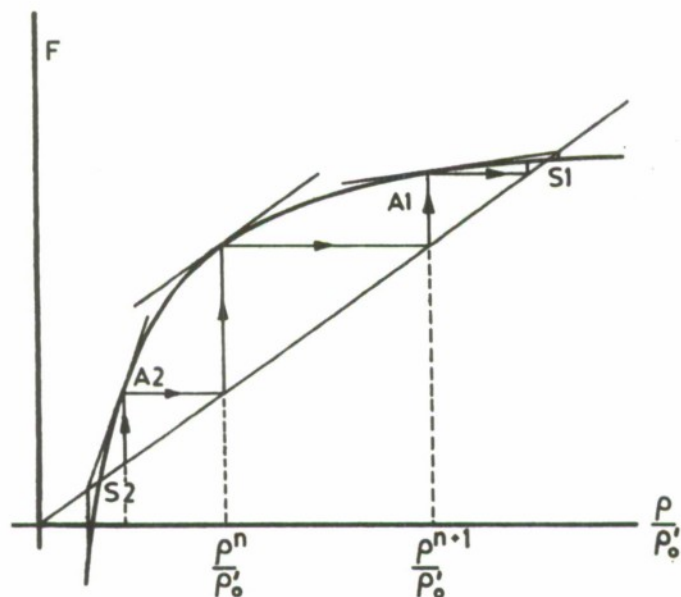


Figure 2.4.6. : Iterative solution procedure for the density equation (2.4.118), in function of streamfunction gradients.

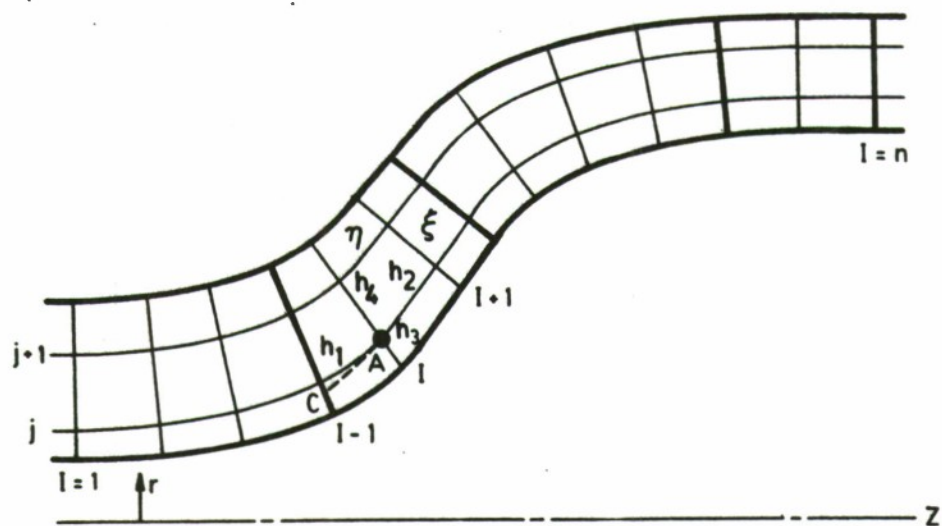


Figure 2.4.7. : Meridional section of mixed flow machine and grid layout.

INITIAL DISTRIBUTION LIST

1. Commander
Naval Air Systems Command
Washington, DC 20361
Attention: Code AIR 931 1
Code AIR 931E 1
Code AIR 932D 1
Code AIR 530 1
Code AIR 536 1
Code AIR 00D 14
Code AIR 93D 1
2. Office of Naval Research
800 N. Quincy Street
Arlington, VA 22217
Attention: Dr. A. D. Wood 1
Dr. S. Lekoudis 1
3. Commanding Officer
Naval Air Propulsion Center
Trenton, NJ 08628
Attention: G. Mangano, PE-31 1
4. Commanding Officer 1
Naval Air Development Center
Warminster, PA 19112
Attention: AVTD
5. Library 1
Army Aviation Material Laboratories
Department of the Army
Fort Eustis, VA 23604
6. Dr. Arthur J. Wennerstrom 1
AFWAL/POTX
Wright-Patterson AFB
Dayton, OH 45433
7. Air Force Office of Scientific Research 1
AFOSR/NA
Bolling Air Force Base
Washington, DC 20332
Attention: Mr. James Wilson

8. National Aeronautics & Space Administration
Lewis Research Center
21000 Brookpark Road
Cleveland, OH 44135
Attention: Chief, Internal Fluid Mechanics Division 3
Dr. J. Adamczyk, MS 5-9 1
Library 1

9. Dr. Bao B. Hwang 1
Propulsion and Auxiliary Department
David Taylor Naval Ship
Research and Development Center
Annapolis, MD 21402

10. Library 1
General Electric Company
Aircraft Engine Technology Division
DTO Mail Drop H43
Cincinnati, OH 45215

11. Library 1
Pratt & Whitney Aircraft Group
Post Office Box 109600
West Palm Beach, FL 33410-9600

12. Library 1
Pratt-Whitney Aircraft Group
East Hartford, CT 06108

13. Library 1
Curtis Wright Corporation
Woodridge, NJ 07075

14. Library 1
AVCO/Lycoming
550 S. Main Street
Stratford, CT 06497

15. Library 1
Teledyne CAE, Turbine Engines
1330 Laskey Road
Toledo, OH 43612

16. Library 1
Williams International
P. O. Box 200
Walled Lake, MI 48088

17. Library 1
Detroit Diesel Allison Division G.M.C.
P. O. Box 894
Indianapolis, IN 46202

18. Library 1
Garrett Turbine Engine Company
111 S. 34th Street
P. O. Box 5217
Phoenix, AZ 85010
19. Professor J. P. Gostelow 1
School of Mechanical Engineering
The New South Wales Institute of Technology
New South Wales
AUSTRALIA
20. Dr. G. J. Walker 1
Civil and Mechanical Engineering
Department
The University of Tasmania
Box 252C
GPO Hobart, Tasmania 7110
AUSTRALIA
21. Professor F. A. E. Breugelmans 1
Institut von Karman de la Dynamique
des Fluides
72 Chaussee de Waterloo
1640 Rhode-St. Genese
BELGIUM
22. Professor Ch. Hirsch 2
Vrije Universiteit Brussel
Pleinlaan 2
1050 Brussels
BELGIUM
23. Director 1
Gas Turbine Establishment
P. O. Box 305
Jiangyou County
Sichuan Province
CHINA
24. Professor C. H. Wu 1
P. O. Box 2706
Beijing 100080
CHINA
25. Director, Whittle Laboratory 1
Department of Engineering
Cambridge University
ENGLAND

26. Professor Jacques Chauvin 1
Universite d'Aix-Marseille
1 Rue Honnorat
Marseille
FRANCE
27. Mr. Jean Fabri 1
ONERA
29, Ave. de la Division Leclerc
92 Chatillon
FRANCE
28. Professor D. Adler 1
Technion Israel Institute of Technology
Department of Mechanical Engineering
Haifa 32000
ISRAEL
29. Dr. P. A. Paranjpe 1
Head, Propulsion Division
National Aeronautics Laboratory
Post Bag 1700
Bangalore - 17
INDIA
30. Dr. W. Schlachter 1
Brown, Boveri Company Ltd.
Dept. T-T
P. O. Box CH-5401 Baden
SWITZERLAND
31. Professor Leonhard Fottner 1
Department of Aeronautics and Astronautics
German Armed Forces University
Hochschule des Bundeswehr
Werner Heisenbergweg 39
8014 Neubiberg near Munich
WEST GERMANY
32. Professor Dr. Ing. Heinz E. Gallus 1
Lehrstuhl und Institut fuer Strahlantriebe
und Turbourbeitsmashinen
Rhein.-Westf. Techn. Hochschule Aachen
Templergraben 55
5100 Aachen
WEST GERMANY
33. Dr. Ing. Hans-J. Heinemann 1
DFVLR-AVA
Bunsenstrasse 10
3400 Geottingen
WEST GERMANY

34. Dr. H. Weyer 1
DFVLR
Linder Hohe
505 Porz-Wahn
WEST GERMANY

35. Dr. Robert P. Dring 1
United Technologies Research Center
East Hartford, CT 06108

36. Chairman 1
Aeronautics and Astronautics Department
31-265 Massachusetts Institute of Technology
Cambridge, Massachusetts 02139

37. Dr. B. Lakshminarayana 1
Professor of Aerospace Engineering
The Pennsylvania State University
233 Hammond Building
University Park, Pennsylvania 16802

38. Dr. Steven Shamroth 1
Scientific Research Associates, Inc.
PO Box 498
Glastonbury, CT 06033

39. Professor Alan H. Epstein 1
Gas Turbine Laboratory
Massachusetts Institute
of Technology
Cambridge, MA 02139

40. Mechanical Engineering Department
Virginia Polytechnic Institute and
State University
Blacksburg, VA 24061
Attn: Professor W. O'Brian 1
Professor H. Moses 1

41. Professor T. H. Okiishi 1
Professor of Mechanical Engineering
208 Mechanical Engineering Building
Iowa State University
Ames, Iowa 50011

42. Dr. Fernando Sisto 1
Professor and Head of Mechanical
Engineering Department
Stevens Institute of Technology
Castle Point
Hoboken, NJ 07030

- | | | |
|-----|--|---------|
| 43. | Dr. Leroy H. Smith, Jr.
Manager, Compressor and Fan
Technology Operation
General Electric Company
Aircraft Engine Technology Division
DTO Mail Drop H43
Cincinnati, OH 45215 | 1 |
| 44. | Dr. W. Tabakoff
Professor, Department of Aerospace
Engineering
University of Cincinnati
Cincinnati, OH 45221 | 1 |
| 45. | Mr. P. Tramm
Manager, Research Labs
Detroit Diesel Allison Division
General Motors
P. O. Box 894
Indianapolis, IN 46206 | 1 |
| 46. | Professor Frank Moore
Sibley School of Mechanical &
Aerospace Engineering
291 Gramman Hall
Cornell University
Ithaca, NY 14853 | 1 |
| 47. | Mr. P. F. Yaggy
Director
U. S. Army Aeronautical Research Laboratory
AMES Research Center
Moffett Field, CA 94035 | 1 |
| 48. | Library
Code 1424
Naval Postgraduate School
Monterey, CA 93943 | 2 |
| 49. | Office of Research Administration
Code 012
Naval Postgraduate School
Monterey, CA 93943 | 1 |
| 50. | Defense Technical Information Center
Cameron Station
Alexandria, VA 22314 | 2 |
| 51. | Naval Postgraduate School
Monterey, CA 93943
Attn: Professor M. F. Platzter (67PL)
Turbopropulsion Laboratory (67Sf) | 1
20 |